

**UNIVERSITY OF ALBERTA**

**IN-USE VEHICLE FUEL CONSUMPTION & EMISSIONS FUNCTIONS MEASUREMENT**

BY

YUTONG GAO



A THESIS SUBMITTED TO THE FACULTY OF GRADUATE STUDIES AND RESEARCH  
IN PARTIAL FULFILLMENT OF THE REQUIREMENTS FOR THE DEGREE OF

MASTER OF SCIENCE

DEPARTMENT OF MECHANICAL ENGINEERING

EDMONTON, ALBERTA

FALL 2006



Library and  
Archives Canada

Bibliothèque et  
Archives Canada

Published Heritage  
Branch

Direction du  
Patrimoine de l'édition

395 Wellington Street  
Ottawa ON K1A 0N4  
Canada

395, rue Wellington  
Ottawa ON K1A 0N4  
Canada

*Your file* *Votre référence*  
*ISBN: 978-0-494-22268-3*  
*Our file* *Notre référence*  
*ISBN: 978-0-494-22268-3*

#### NOTICE:

The author has granted a non-exclusive license allowing Library and Archives Canada to reproduce, publish, archive, preserve, conserve, communicate to the public by telecommunication or on the Internet, loan, distribute and sell theses worldwide, for commercial or non-commercial purposes, in microform, paper, electronic and/or any other formats.

The author retains copyright ownership and moral rights in this thesis. Neither the thesis nor substantial extracts from it may be printed or otherwise reproduced without the author's permission.

#### AVIS:

L'auteur a accordé une licence non exclusive permettant à la Bibliothèque et Archives Canada de reproduire, publier, archiver, sauvegarder, conserver, transmettre au public par télécommunication ou par l'Internet, prêter, distribuer et vendre des thèses partout dans le monde, à des fins commerciales ou autres, sur support microforme, papier, électronique et/ou autres formats.

L'auteur conserve la propriété du droit d'auteur et des droits moraux qui protègent cette thèse. Ni la thèse ni des extraits substantiels de celle-ci ne doivent être imprimés ou autrement reproduits sans son autorisation.

---

In compliance with the Canadian Privacy Act some supporting forms may have been removed from this thesis.

Conformément à la loi canadienne sur la protection de la vie privée, quelques formulaires secondaires ont été enlevés de cette thèse.

While these forms may be included in the document page count, their removal does not represent any loss of content from the thesis.

Bien que ces formulaires aient inclus dans la pagination, il n'y aura aucun contenu manquant.

  
**Canada**

## **ABSTRACT**

Fundamental accomplishment was achieved by development of an on-board & in-use fuel consumption and emissions measurement system adapted for easy transition from vehicle to vehicle. Instantaneous mass flow rates of fuel and emissions were measured and recorded by an ECM OBD-II scanner, a mass air flow meter, two emissions analyzers and a laptop computer on five typical mid-life vehicles representative of a significant fraction of the on-road fleet. From repeated tests in urban, highway and aggressive driving situations, on-road fuel consumption functions were developed to quantify the fuel economy and greenhouse gas CO<sub>2</sub> emission impact of vehicle, road and traffic control changes. Comprehensive emission factors analysis for HC, CO and NO<sub>x</sub> was also illustrated to highlight that vehicle power-based emission factor could represent the influences from wide varieties of vehicle power demand and acceleration driving profiles. A basic in-use power-based model was developed for use in estimating cumulative fuel consumption and tailpipe emissions for vehicles experiencing real-world driving conditions with significant differences from the standard test sequences.

## **ACKNOWLEDGMENTS**

I would like to take this opportunity to acknowledge and express my appreciation to the following people for their support and help:

Dr. M David Checkel for giving me the special opportunity to pursue my M.Sc. Degree in the University of Alberta as well as providing me with professional training and financial support.

Roger Marchand, Bernie Faulkner, Terry Nord, Alan Wilson, Wayne Pittman, Jonathan Clark, Gail Anderson and other Mechanical Engineering staff for their technical assistance and instructive guidance.

The entire Combustion and Environment Research group for their friendship in addition to valuable suggestion and advice.

Province of Alberta and Lehigh Inland Cement Limited for their financial assistance.

My wife Xianghong Tang, my parents and parents in-law for their support and encouragement throughout all my graduate studies.

# TABLE OF CONTENTS

<b>CHAPTER 1</b>	<b>INTRODUCTION TO IN-USE VEHICLE FUEL CONSUMPTION AND EMISSIONS FUNCTIONS MEASUREMENT .....</b>	<b>1</b>
1.0	INTRODUCTION.....	2
	REFERENCES.....	6
<b>CHAPTER 2</b>	<b>REVIEW OF CURRENT EMISSION REGULATIONS, EMISSION MEASUREMENT SYSTEMS AND EMISSION INVENTORIES PREDICTION PROGRAM .....</b>	<b>7</b>
2.0	INTRODUCTION.....	8
2.1	CURRENT EMISSION REGULATIONS.....	8
2.2	CURRENT EMISSION MEASUREMENT SYSTEMS .....	10
2.2.1	DYNAMOMETER TEST METHOD .....	10
2.2.2	REMOTE SENSING METHOD.....	13
2.2.3	ON-BOARD AND REAL-TIME EMISSIONS MEASUREMENT SYSTEM..	15
2.3	EMISSION INVENTORIES PREDICTION MODEL .....	22
2.4	CONCLUSION .....	23
	REFERENCES.....	29
<b>CHAPTER 3</b>	<b>EXPERIMENTAL SYSTEM AND PROCEDURES.....</b>	<b>32</b>
3.0	INTRODUCTION.....	33
3.1	EXPERIMENTAL APPARATUS DETAILS.....	34
3.1.1	VETRONIX FIVE-GAS ANALYZER .....	34
3.1.2	HORIBA MEXA-720 NO <sub>x</sub> ANALYZER .....	35
3.1.3	ECM OBD-II PORT SCANNER .....	36
3.1.4	MASS AIR FLOW METER.....	36
3.1.5	TEMPERATURE SENSOR.....	36
3.1.6	DATA ACQUISITION SYSTEM.....	37
3.1.7	DATA ANALYSIS SOFTWARE.....	38
3.2	TEST VEHICLES .....	38
3.3	EXPERIMENTAL PROCEDURE.....	40
3.4	DRIVING ROUTES.....	41
3.5	RESULTS ANALYSIS .....	42
3.6	MEASUREMENT UNCERTAINTY ANALYSIS.....	44
3.7	CONCLUSION .....	46
	REFERENCES.....	53
<b>CHAPTER 4</b>	<b>EXPERIMENTAL MEASUREMENT OF ON-ROAD CO<sub>2</sub> EMISSION AND FUEL CONSUMPTION FUNCTIONS .....</b>	<b>54</b>
4.0	INTRODUCTION.....	55
4.1	EXPERIMENTAL CONFIGURATION.....	56
4.2	TEST VEHICLES .....	59
4.3	DRIVING ROUTES.....	60

4.4	RESULTS AND DISCUSSIONS .....	61
4.4.1	FUEL EFFICIENCY ANALYSIS .....	61
4.4.2	FUEL ECONOMY COMPARISON AMONG THE DIFFERENT TESTING PATTERNS .....	63
4.4.3	RELATIONSHIP BETWEEN CO <sub>2</sub> EMISSION AND FUEL CONSUMPTION .....	64
4.4.4	FUEL CONSUMPTION FUNCTION DEVELOPMENT .....	66
4.5	MODELING RESULTS VALIDATION.....	69
4.6	CONCLUSION .....	70
4.7	FUTURE WORK .....	71
	REFERENCE.....	83
<b>CHAPTER 5</b>	<b>EMISSION FACTORS ANALYSIS FOR MULTIPLE VEHICLES USING AN ON-BOARD AND IN-USE EMISSIONS MEASUREMENT SYSTEM.....</b>	<b>84</b>
5.0	INTRODUCTION.....	85
5.1	EXPERIMENTAL CONFIGURATION.....	86
5.2	TEST VEHICLES .....	90
5.3	DRIVING ROUTES.....	90
5.4	RESULTS AND ANALYSIS .....	92
5.4.1	INSTANTANEOUS EMISSION TRACES.....	92
5.4.2	CUMULATIVE EMISSIONS.....	93
5.4.3	INFLUENCES FROM THREE TYPICAL DRIVING PATTERNS ON EMISSION FACTORS .....	95
5.4.4	COMPREHENSIVE EMISSIONS FUNCTIONS DEVELOPMENT.....	96
5.4.5	DESCRIPTION OF THE EMISSION MODEL ESTABLISHMENT.....	102
5.4.6	COMPARISON WITH AVAILABLE MODEL.....	103
5.5	CONCLUSION .....	105
5.6	FUTURE WORK .....	107
	REFERENCE.....	140
<b>CHAPTER 6</b>	<b>CONCLUSIONS .....</b>	<b>143</b>
<b>APPENDIX A</b>	<b>VEHICLE DYNAMIC MODEL AND UNCERTAINTY ANALYSIS .....</b>	<b>147</b>
<b>APPENDIX B</b>	<b>MASS EMISSIONS AND FUEL CONSUMPTION CALCULATIONS AND UNCERTAINTY ANALYSIS .....</b>	<b>158</b>
<b>APPENDIX C</b>	<b>SENSOR CALIBRATIONS .....</b>	<b>163</b>
<b>APPENDIX D</b>	<b>MATLAB PROCESSING PROGRAM .....</b>	<b>174</b>

## LIST OF TABLES

Table 3-1	Instrument Specification.....	35
Table 3-2	Vehicle Specifications .....	40
Table 3-3	Driving Routes Comparison .....	41
Table 3-4	Difference Average Value and Uncertainty From Different Trips.....	45
Table 3-5	Average NO <sub>x</sub> (g/gFuel) Value From All Tested Vehicles .....	45
Table 4-1	Instrument Specification.....	57
Table 4-2	Vehicle Features .....	59
Table 4-3	Definitions of The Four Modal Analysis Variables .....	61
Table 4-4	Comparison Between the Experiment Results and Modeling Results .	69
Table 5-1	Instrument Specification.....	86
Table 5-2	Vehicle Features .....	90
Table 5-3	Definitions of The Four Modal Analysis Variables .....	91
Table 5-4	Vehicle Catalyst Light-Off Change-Over Point .....	101
Table 5-5	Idle Emission Rates For Five Vehicles.....	103
Table 5-6	Vehicle Fuel-Based Emission Factor From Urban Tests .....	105
Table A-1	The Coefficients of Drag and Rolling For Five Tested Vehicles.....	152

## LIST OF FIGURES

Figure 2-1	FTP-72 Driving Cycle .....	25
Figure 2-2	FTP-75 Driving Cycle .....	25
Figure 2-3	SFTP US06 Driving Cycle .....	26
Figure 2-4	SFTP SC03 Driving Cycle .....	26
Figure 2-5	EPA Highway Fuel Economy (HWFET) Driving Cycle .....	27
Figure 2-6	New European Driving Cycle [NEDC] .....	27
Figure 2-7	Japanese 10-15 Mode Driving Cycle For the Light Duty Vehicles .....	28
Figure 2-8	Illustration of Emission Factors Used By MOBILE5 and 6 .....	28
Figure 3-1	Schematic of Test Instruments .....	47
Figure 3-2	Instantaneous Trace of Emissions, Mass Fuel Flow, .....	48
Figure 3-3	Effect of Vehicle Power and Acceleration on Tailpipe Emissions .....	49
Figure 3-4	Vehicle Bin Average Speed Development (Using Chevrolet Silverado) .....	50
Figure 3-5	Vehicle Bin Average Power Development (Using Chevrolet Silverado) .....	51
Figure 3-6	System Uncertainty Reduction Using Average Data .....	52
Figure 4-1	Schematic of Test Instruments and Calculations .....	72
Figure 4-2	Urban Test Route Speed Trace and Modal Fraction .....	72
Figure 4-3	US06 Test Route Speed Trace and Modal Fraction .....	73
Figure 4-4	Highway Test Route Speed Trace and Modal Fraction .....	73
Figure 4-5	Vehicle Fuel Efficiency and Tractive Power .....	74
Figure 4-6	Fuel Consumption and Tractive Energy: Audi Quattro .....	75
Figure 4-7	Fuel Consumption and Tractive Energy: Pontiac Vibe .....	75
Figure 4-8	Fuel Consumption and Tractive Energy: Chevrolet Cavalier .....	76
Figure 4-9	Fuel Consumption and Tractive Energy: Chevrolet Silverado .....	76
Figure 4-10	Fuel Consumption and Tractive Energy: GMC Savana .....	77
Figure 4-11	Vehicle Fuel Economies Comparison to Three Driving Patterns .....	77
Figure 4-12	Relationship Between Instantaneous CO <sub>2</sub> and Fuel Consumption of Chevrolet Silverado .....	78

Figure 4-13	General Relationship Function Between CO <sub>2</sub> and Fuel Consumption.....	78
Figure 4-14	Vehicle Speed and Fuel Flow Rate Time Trace.....	79
Figure 4-15	Cumulative Fuel Consumption Trend Against Vehicle Work .....	80
Figure 4-16	Vehicle Idle Fuel Flow Rate.....	80
Figure 4-17	Relationships Between Vehicle Fuel Consumption Factor and Power .....	81
Figure 4-18	General Fuel Consumption Function.....	81
Figure 4-19	Average Ratio of Vehicle Original Value against Average Trend Value.....	82
Figure 5-1	Schematic of Test Instruments and Calculations.....	108
Figure 5-2	Urban Test Route Speed Trace and Modal Fraction .....	108
Figure 5-3	US06 Test Route Speed Trace and Modal Fraction .....	109
Figure 5-4	Highway Test Route Speed Trace and Modal Fraction.....	109
Figure 5-5	Instantaneous Emission Traces Obtained From Chevrolet Cavalier..	110
Figure 5-6	Trends Of Cumulative Emissions With Driving Distance .....	111
Figure 5-7	Trends Of Cumulative Emissions With Work/Fuel Consumption.....	112
Figure 5-8	Emission Factors of Congested Driving Pattern From Truncated Data (Using Chevrolet Cavalier) .....	113
Figure 5-9	Emission Factors of Free Flow Driving Pattern From Truncated Data (Using Chevrolet Cavalier) .....	114
Figure 5-10	The Comparison of g/kW.h Among Different Driving Patterns .....	115
Figure 5-11	The Comparison of g/km Among Different Driving Patterns.....	116
Figure 5-12	The Comparison of g/kgFuel Among Different Driving Patterns.....	116
Figure 5-13	Correlation Of Chevrolet Cavalier Post-Catalyst Light-Off NO <sub>x</sub> Emission Factors With Bin Vehicle Power and Bin Average Speed .	117
Figure 5-14	Correlation Of Chevrolet Cavalier Post-Catalyst Light-Off CO Emission Factors With Bin Vehicle Power and Bin Average Speed .	118
Figure 5-15	Correlation Of Chevrolet Cavalier Post-Catalyst Light-Off HC Emission Factors With Bin Vehicle Power and Bin Average Speed .	119
Figure 5-16	Correlation Of Audi Quattro Post-Catalyst Light-Off Emission	

	Factors With Bin Vehicle Power .....	120
Figure 5-17	Correlation Of Pontiac Vibe Post-Catalyst Light-Off Emission Factors With Bin Vehicle Power .....	121
Figure 5-18	Correlation Of Chevrolet Silverado Post-Catalyst Light-Off Emission Factors With Bin Vehicle Power .....	122
Figure 5-19	Correlation Of GMC Savana Post-Catalyst Light-Off Emission Factors With Bin Vehicle Power .....	123
Figure 5-20	Correlation Of Audi Quattro Post-Catalyst Light-Off Emission Factors With Bin Average Vehicle Speed.....	124
Figure 5-21	Correlation Of Pontiac Vibe Post-Catalyst Light-Off Emission Factors With Bin Average Vehicle Speed.....	125
Figure 5-22	Correlation Of Chevrolet Silverado Post-Catalyst Light-Off Emission Factors With Bin Average Vehicle Speed.....	126
Figure 5-23	Correlation Of GMC Savana Post-Catalyst Light-Off Emission Factors With Bin Average Vehicle Speed.....	127
Figure 5-24	Correlation Of Audi Quattro Pre-Catalyst Light-Off Emission Factors With Bin Vehicle Power .....	128
Figure 5-25	Correlation Of Pontiac Vibe Pre-Catalyst Light-Off Emission Factors With Bin Vehicle Power .....	129
Figure 5-26	Correlation Of Chevrolet Cavalier Pre-Catalyst Light-Off Emission Factors With Bin Vehicle Power .....	130
Figure 5-27	Correlation Of Chevrolet Silverado Pre-Catalyst Light-Off Emission Factors With Bin Vehicle Power .....	131
Figure 5-28	Correlation Of GMC Savana Pre-Catalyst Light-Off Emission Factors With Bin Vehicle Power .....	132
Figure 5-29	Correlation Of Audi Quattro Pre-Catalyst Light-Off Emission Factors With Bin Average Vehicle Speed.....	133
Figure 5-30	Correlation Of Pontiac Vibe Pre-Catalyst Light-Off Emission Factors With Bin Average Vehicle Speed.....	134
Figure 5-31	Correlation Of Chevrolet Cavalier Pre-Catalyst Light-Off Emission Factors With Bin Average Vehicle Speed.....	135

Figure 5-32	Correlation Of Chevrolet Silverado Pre-Catalyst Light-Off Emission Factors With Bin Average Vehicle Speed.....	136
Figure 5-33	Correlation Of GMC Savana Pre-Catalyst Light-Off Emission Factors With Bin Average Vehicle Speed.....	137
Figure 5-34	Basic Power-Based In-Use Emissions Prediction Model.....	138
Figure 5-35	Emissions Values Comparison Among the Experiment, In-use Model, Fuel Based Calculation and MOBILE6 .....	139
Figure A-0	Schematic of Dynamic Vehicle Resistances.....	148
Figure A-1	Overall Instrument Uncertainty Against Power.....	155
Figure A-2	Ratio of Uncertainty From Instrument Against Tractive Power ( $\varepsilon_p / P$ ).....	155
Figure A-3	Bin Values of Overall Instrument Uncertainty in Tractive Power.....	156
Figure C-1	Mass Air Flow Meter Calibration Experimental Setup.....	172
Figure C-2	Mass Air Flow Meter 1 Calibration Curve.....	172
Figure C-3	Mass Air Flow Meter 1 Calibration Curve.....	173
Figure C-4	Ambient Temperature Sensor Calibration Curve.....	173

## NOMENCLATURE

a	Instantaneous Vehicle Acceleration [m/s <sup>2</sup> ]
AFR	Air to Fuel ratio
ASME	The American Society of Mechanical Engineers
C <sub>6</sub> H <sub>14</sub>	Hexane
C <sub>8</sub> H <sub>18</sub>	Iso-Octane
C <sub>d</sub>	Drag Coefficient
C <sub>r</sub>	Rolling Resistance Coefficient
CARB	California Air Resources Board
CDT	Coast Down Test
CNC	Condensation Nucleus Counter
CO	Carbon Monoxide
CO <sub>2</sub>	Carbon Dioxide
CPC	Optical Particle Counter
CVS	Constant Volume Sample
DAQ	Data Acquisition
DEC	Department of Environmental Conservation
ECM	Engine Control Module
EDC	European Driving Cycle
EF	Emission Factor
EPA	Environmental Protection Agency

EUDC	Extra Urban Driving Cycle
FA	Frontal Area of the Vehicle [m <sup>2</sup> ]
F <sub>aero</sub>	Aerodynamic Resistance [N]
F <sub>inertial</sub>	Inertial Resistance [N]
F <sub>rolling</sub>	Rolling Resistance [N]
FE	Fuel Economy
FID	Flame Ionization Detection
FTP	Federal Test Program
FTIR	Fourier Transform Infrared
g	Gravitational Acceleration Constant [m/s <sup>2</sup> ]
GUI	Graphical User Interface
GVWR	Gross Vehicle Weight Rating
HC	Hydrocarbons
H/C	Hydrogen to Carbon Ratio
I/M	Inspection and Maintenance
IR	Infrared
LHV	Lower Heating Value
m	Vehicle mass [kg]
MAF	Mass Air Flow [g/s]
MCT	Mercury Cadmium Telluride
MPG	Miles Per Gallon
MW <sub>air</sub>	Molecular Weight of Ambient Air [kg/kmol]

MW <sub>i</sub>	Molecular Weight of the i <sup>th</sup> Emission Species [kg i/kmol i]
MW <sub>exh</sub>	Molecular Weight of the Exhaust Components [kg/kmol]
NDIR	Non-Dispersive Infrared
NDUV	Non-Dispersive Ultraviolet
NI	National Instruments
NMHC	Non-Methane Hydrocarbons
NO <sub>x</sub>	Oxides of Nitrogen
O <sub>2</sub>	Oxygen
OBD	On-Board Diagnostics
OBD I	On-Board Diagnostics (Generation 1)
OBD II	On-Board Diagnostics (Generation 2)
OEM	Original Equipment Manufacturer
P	Total Vehicle Tractive Power [kW]
PM	Particulate Matter
RAVEM	Ride Along Vehicle Emission Measurement
RPM	Revolutions per Minute
R <sub>u</sub>	Universal Gas Constant [kJ/(kmol-K)] = 8.3143
SAE	Society of Automotive Engineers
t	Time [sec]
T <sub>amb</sub>	Ambient Air Temperature [K]
TILDAS	Tunable Infrared Laser Differential Absorption Spectroscopy
US 06	U.S. EPA Supplemental Federal Test Procedure Driving Cycle
UV	Ultraviolet

V	Vehicle velocity [m/s]
WOT	Wide Open Throttle
$\eta$	Fuel Efficiency [percent/100%]
$\rho_{air}$	Density of Air [kg/m <sup>3</sup> ]
$\rho_{air}^o$	Density of Air [=1.205 kg/m <sup>3</sup> ], at T = 293.15 [K], P = 101.3 [kPa]
$\theta$	Road Grade (defined as positive uphill) [rad]
$\lambda$	Excess Air Ratio
$\bar{X}$	Sample Mean Value
$s$	Standard deviation of population about $\bar{X}$
$s_{\bar{x}}$	Standard deviation of sample mean values
$N$	Sample size

# **CHAPTER 1**

## **Introduction to In-Use Vehicle Fuel Consumption and Emissions Functions Measurement**

*Chapter 1 illustrates the motivation for studies on motor vehicle related fuel consumption and emissions measurement, highlights the objectives of this research and outlines the contents of the following chapters.*

## 1.0 INTRODUCTION

Motorized transport has been a key element to global economic success since improvements in road construction and vehicular technology allowed an ever-increasing number of vehicles on the road. However, considering the depletion of energy resources and the aggravation of pollutant emissions issues, it is critical to improve vehicle fuel consumption and control tailpipe emissions.<sup>[1][2]</sup> These demands as well as the more stringent environmental regulations are increasing the impetus for not only developing cleaner automobiles, but also more advanced fuel consumption and emissions measurement systems representing the real-world driving conditions.<sup>[3][4]</sup>

As the most repeatable method for confirming emission compliance, the traditional chassis dynamometer tests are still widely utilized by most laboratories and emissions legislation bodies.<sup>[5]</sup> In order to obtain fuel consumption and emissions measurement, the tested vehicle must be mounted on a test bed and driven through certified driving cycles simulating certain vehicle on-road operations. However, many concerns have been raised about the extent to which emissions produced or fuel consumed by on-road vehicles can be represented using these standard test procedures.<sup>[6]</sup>

On-board emissions measurements have emerged as a promising new approach for obtaining representative real-world tailpipe emissions data based upon actual on-road driving at any location and in any weather.<sup>[7]</sup> This remedies many of the shortcomings of laboratory-based methods and of field-based methods such as remote sensing and tunnel studies, which are limited in sites. The increasing availability of instrumentation for performing on-road emissions studies, the development of data collection and analysis protocols, and the increasing availability of example on-board studies suggest that on-board data collection is a potentially practical and useful source of data for the fuel consumption and emission inventories estimation.<sup>[8][9]</sup>

This thesis describes a measurement system and method to quantify real-time, on-road vehicle fuel consumption and emissions. The objectives of the research presented here are:

1. To rebuild a fuel consumption and emissions measurement system adapted for easy transition from vehicle to vehicle permitting testing of a number of different light-duty gasoline vehicle classes.
2. To generate suggestions for fuel saving strategies through on-road fuel efficiency analysis.
3. To develop a general vehicle work-based fuel consumption function and build a basic prediction model to estimate the cumulative fuel consumption and greenhouse gas CO<sub>2</sub> emission for the test vehicles.
4. To study three emission factors (g/kW.h, g/km, g/kgFuel) for HC, CO and NO<sub>x</sub>. A basic model established by the practical emission functions will predict complete emission profiling of the test vehicles for any given simulation vehicle speed trace.

Most current emission factors used in emission inventories are determined from chassis dynamometer testing procedures facing the criticism of poorly representing the actual on-road driving conditions. The reason for this study was to provide the methodologies of developing in-use fuel consumption and emissions functions, improve the relevance of the emission factors and improve the accuracy of emission inventories. The project objectives were totally achieved after the completion of this thesis research.

The literature review presented in Chapter 2 illustrates the need for an in-use measurement system by comparing the advantages and disadvantages among the current emission measuring techniques. Chapter 2 also briefly introduces current emission regulations governing the sale of vehicles in North America, Europe and Japan as well as the associated certified driving cycles. The history of OBD (On Board Diagnostic System) and the emission inventories estimation model developed by U.S. EPA helps understand of the measurement system setup and the development of the in-use fuel consumption and emissions prediction models.

Chapter 3 details an on-board & in-use emissions and fuel consumption system by introducing all experimental apparatus and test procedures. The background and specifications of five typical mid-life vehicles with engine displacement varying from 1.8 L to 5.7 L are described, highlighting the on-board & in-use measurement system's adaptability and stability.

The next section, presented as a stand alone SAE technical paper (Chapter 4), focuses on the fuel efficiency analysis and fuel consumption functions development. The relationship between CO<sub>2</sub> emission and gasoline fuel consumption from the experimental results is proven reasonably accurate by comparing with the theoretical carbon balancing method. The specific fuel consumption rates and vehicle tractive energy demands are correlated with the vehicle tractive power and average speed respectively giving the potential to indicate the vehicle power/speed range where vehicles have the higher fuel efficiency and to build a fuel consumption estimation model based on the fuel consumption functions.

Comprehensive analysis of the emission factors expressed in terms of g/kW.h, g/km and g/kgFuel for HC, CO and NO<sub>x</sub> is illustrated in Chapter 5 which is also presented as a stand alone SAE technical paper. The idle emission rates with cold-start or warmed-up start as well as the emission functions both in the pre-catalyst light-off region and post-catalyst light-off region are measured and developed to build a basic in-use emission inventories model for test vehicles.

The last chapter of this thesis summarizes the conclusions presented in the previous chapters. The research provides the foundations and general methodologies for developing the fuel consumption and emissions functions and the associated prediction models utilized in the future on-road vehicle tests.

Four appendices provide fundamental support for the fuel consumption and emissions behaviors analysis for the test vehicles. Appendix A details the vehicle dynamic model method and coast down test procedures used to determine the coefficient of rolling

resistance ( $C_r$ ) and coefficient of drag ( $C_d$ ) as well as the vehicle tractive power. Appendix B demonstrates how to calculate fuel consumption and emission factors in addition to the instantaneous mass flow rates of fuel and emissions. Appendix C describes the sensor calibration procedures performed on the Vetronix 5- Gas Analyzer, Horiba Mexa-720 NO<sub>x</sub> Sensor, Mass Air Flow Sensor and Ambient Temperature Sensor. Appendix D illustrates the Matlab program written to process the data and provide all calculations used for any data analysis.

## REFERENCES

1. Yutong Gao, M. David Checkel. "Experimental Measurement of On-Road Fuel Consumption Functions", Combustion Institute/Canadian Section, in Waterloo, Ontario, Spring Technical Meeting 2006.
2. Kurt Engeljehringer. "Trends of Future Emission Legislation and its Measurement Requirements", SAE Paper 2004-01-3291, Society of Automotive Engineers, 2004.
3. M. D. Checkel, A. Brownlee, L. Doblanko. "Optimizing Vehicle Fuel Consumption and Emissions Through Traffic Optimization Using Vehicle and Traffic Forecasting Models", Combustion Canada 99 Technical Paper H 1.4, 1999.
4. J. R. Wootton, A. Garcia-Ortiz, S. M. Amin. "Intelligent Transportation Systems: A Global Perspective", Mathl. Comput. Modelling Vol. 22, No. 4-7, pp. 259-268, 1995.
5. Basil Daham, Gordon Andrews, Hu Li. "Application of a Portable FTIR for Measuring On-road Emissions", SAE Paper 2005-01-0676, Society of Automotive Engineers, 2005.
6. M. Gautam, G.Thompson, D. Carder, N.Clark. "Measurement of In-Use, On-Board Emissions from Heavy-Duty Diesel Vehicles: Mobile Emissions Measurement System", SAE Paper 2001-01-3643, Society of Automotive Engineers, 2001.
7. H. Christopher Frey, Alper Unal, Jianjun Chen. "Recommended Strategy For On-Board Emission Data Analysis and Collection For The New Generation Model", Prepared for: Office of Transportation and Air Quality U.S. Environmental Protection Agency, Ann Arbor, MI. February 4<sup>th</sup>, 2002. Department of Civil Engineering, North Carolina State University, Raleigh, NC.
8. J. D. Hawirko. "Modeling Vehicle Emission Factors Determined with an In-Use & Real-Time Emissions Measurement System", Master of Science Thesis, Department of Mechanical Engineering, University of Alberta, 2003.
9. Travis B. Manchur. "Accuracy Of On-Board Vehicle Emission Measurements", Master of Science Thesis, Department of Mechanical Engineering, University of Alberta, 2005.

## **CHAPTER 2**

### **Review of Current Emission Regulations, Emission Measurement Systems and Emission Inventories Prediction Program**

*The purpose of the literature review is to present the background of the current vehicle tailpipe emission regulations, research on different emission measurement systems and emission inventory estimation models. The requirement of the advanced emission measurement system representing the real-world & in-use driving conditions will be highlighted in Chapter 2 by comparing the emission testing procedures and testing requirements among the traditional chassis dynamometer system, remote sensing system and in-vehicle measurement system.*

## **2.0 INTRODUCTION**

Besides Carbon Dioxide (CO<sub>2</sub>), the major greenhouse gas blamed for global warming, any fossil fuel combustion also produces minor emissions of Carbon Monoxide (CO), Hydrocarbon (HC) and Nitrogen Oxides (NO<sub>x</sub>), all of which are poisonous gases or significantly contribute to air pollution problems such as the smog, acid rain, etc. Since motorized transport has become an essential part of our world economic system, motor vehicle emissions have become the major source of air pollution problems in most urban areas. <sup>[1][2]</sup>

The first section of this literature review briefly introduces current emission regulations governing the sale of vehicles in North America, Europe and Japan. The trend towards more stringent emissions standards for the vehicles is also emphasized in this section.

The second section of the literature review discusses the advantages and disadvantages of traditional chassis dynamometer measurement, remote sensing measurement and on-board & in-use measurement. In addition, it briefly introduces the most-used driving cycles developed to certify that vehicles meet the emissions standards implemented officially in all developed countries and most of the developing countries. <sup>[3]</sup>

The last part of the literature review briefly introduces the background of the MOBILE6 emission prediction model developed by U.S. EPA (U.S. Environmental Protection Agency) as well as the methodology used to achieve regional emission inventory estimates and its limitation of representing real-world driving conditions.

## **2.1 CURRENT EMISSION REGULATIONS**

In order to make improvements in air quality, the amount of pollutants being emitted into the air must be measured and reduced. The Emissions Measurement Center develops standards and evaluates testing methods so that regulations can be developed and enforced. <sup>[3]</sup> USA, Europe and Japan were the pioneers in defining and

implementing emissions legislation including the vehicle test cycle, the test procedure and the tailpipe emissions limits. The test cycle should represent the usual operation of a vehicle or an engine. For light duty vehicles the test cycle simulates the actual driving on the road and represents the driving pattern for such vehicles and drivers by defining a vehicle velocity profile over the test time. For the heavy duty and off road engines, the test cycle defines a speed and torque profile over the test time. The test procedure illustrates the details of how the test is executed, which test systems have to be used as well as the test conditions and the measurement specifications. The emissions limits expressed in mass per driving distance (g/km) or mass per work (g/kW.h) vary according to vehicle weight class and specify the maximum accepted emissions of the regulated components in the engine exhaust. <sup>[3]</sup>

USA, Europe and Japan developed their own emission regulations with different test cycles and limits, but with similar test procedures. The core of all procedures is the measurement methods formulated by the U.S. EPA. Many countries follow the European or American emission standards, but only a few have adopted Japanese standards. Since 1988, Environment Canada has followed the regulations developed by U.S. EPA to harmonize the manufacturing of vehicles between the two very integrated countries. The On-Road Vehicle and Engine Emission Regulations (SOR2003-2) introduce more stringent national emission standards for on-road vehicles and engines and a new regulatory framework under the Canadian Environmental Protection Act, 1999 (CEPA, 1999). These Regulations for controlling emissions from on-road vehicles and engines came into effect on January 1, 2004. <sup>[3][4][5]</sup> Future emissions standards will likely continue to impose more stringent control on toxic emissions from passenger vehicles, light-duty and heavy-duty trucks to limit the impact on the environment from the increasing numbers of on road vehicles.

## **2.2 CURRENT EMISSION MEASUREMENT SYSTEMS**

The measurement equipment and methods used for measuring vehicle emissions vary widely, from the lab-based Constant Volume Sampler (CVS) system utilized to pass environmental legislation certification, to road-side remote sensing systems, to portable on-board measurement systems examining the emissions while the vehicle is in real service. The following is a description of these systems.

### **2.2.1 DYNAMOMETER TEST METHOD**

The traditional vehicle emissions measurement is the chassis dynamometer test with the vehicle or engine running on a dynamometer under fully controlled laboratory driving conditions. In addition to tailpipe emissions testing, this method is also able to conduct fuel consumption testing and engine mapping (such as power, torque, etc) during a designed driving cycle. The driving cycle is composed of a unique profile of starts, constant speed cruises, accelerations, decelerations and stops and is typically characterized by an overall time-weighted average speed. The emissions testing equipment used to pass environmental legislation certification is known as the CVS system. In order to ensure that the emission composition is stabilized and measure exhaust mass flow accurately, the vehicle exhaust is drawn into a dilution wind tunnel, which handles a fixed mass of total flow. The dilution cools the exhaust rapidly, ensuring that composition is stabilized. If there is very little exhaust coming from the car, it will show a very low concentration of pollutants. If the car is running at high power and producing a large exhaust flow, the amount of dilution air is reduced, resulting in a higher pollutant concentration. During the test, a small fraction of the mixed components is extracted and stored in a non-reactive plastic bag for later analysis. The components in the plastic bag include hydrocarbon, carbon monoxide, carbon dioxide, oxygen and nitrogen oxides, etc. Therefore, the contents of the bag are a representative sample for the vehicle exhaust.<sup>[1]</sup> To determine the vehicle emissions, different analyzers are utilized according to the demands. Usually, an NDIR analyzer is used to measure CO and CO<sub>2</sub>, a chemiluminescent analyzer is used to measure NO<sub>x</sub>,

and an FID analyzer is used to measure HC. Dynamometer tests are widely used in regulatory procedures to check compliance of new vehicles with emission standards or to inspect in-use vehicles.<sup>[4]</sup>

Traditional dynamometer test typically suffers from a major shortcoming that the actual driving conditions are not represented. As all vehicles are tested on the dynamometer in the laboratory, the driving conditions are idealized and fully controlled, failing to represent the real-world influences from factors like different driver behaviors, severe weather, heavy loads, and Wide-Open Throttle (WOT) acceleration on the vehicle emissions. The actual factors mentioned above cause higher emission levels than that measured by CVS measurement system conducted in the laboratory, and this is partly due to higher fuel consumption, partly because gasoline engines operate fuel-rich at WOT and partly because of higher combustion chamber temperatures under such conditions.<sup>[6]</sup> The limitations of testing with lab dynamometer lead to an interest in using advanced measure techniques (remote emissions sensing technology and on-board emissions measurement) to study behavior of vehicle emissions under real world driving conditions.

#### 2.2.1.1 Driving Cycles

All developed countries and most of the developing countries today have emission regulations implemented. The test cycle comprising a certain distance and varying speed profiles are designed to certify the different country's emission standards. The driving cycles have two main objectives: (a) to provide a representative indicator of vehicle emissions and energy consumption at the local and national level. (b) to function as a control instrument in connection with certification or Inspection and Maintenance (I/M). The main driving test cycles accepted by Canadian and USA vehicle emission standards are FTP72, FTP75, SC03, US06 and Highway Fuel Economy Test (HWFET) driving cycles.<sup>[7]</sup> The New European Driving Cycle (NEDC) and 10-15 Mode Cycle are the main test cycles for light duty vehicles in Europe and Japan respectively.<sup>[8]</sup>

The U.S. FTP-72 cycle is also called Urban Dynamometer Driving Schedule (UDDS) or LA-4 cycle. The same engine driving cycle is known in Sweden as A10 or CVS cycle and in Australia as the ADR 27 (Australian Design Rules) cycle. The specified cycle simulates an urban route of 12.07 km with frequent stops as shown in Figure 2-1. The maximum speed is 91.2 km/h and the average speed is 31.5 km/h. The cycle consists of two phases: (1) 505 seconds driving period, 5.78 km distance at 41.2 km/h average speed with cold start. (2) 864 seconds driving period with 6.3 km distance at 26.2 km/h average speed. Emissions are expressed in g/km. <sup>[7]</sup>

The FTP-75 cycle shown in Figure 2-2 is derived from the FTP-72 cycle by adding 10 minutes soak time and a third phase of 505s, identical to the first phase of FTP-72 but with a hot start. The purpose of the FTP75 cycle is to measure urban driving tail pipe exhaust emissions and evaporative emissions. <sup>[8]</sup> This cycle has three separate phases: a cold-start (505 seconds) phase known as Bag 1, a hot-transient (870 seconds) phase known as Bag 2, and a hot-start (505 seconds) phase known as Bag 3. The three test phases are referred to as Bag 1, Bag 2, and Bag 3 because exhaust samples are collected in separate Tedlar bags during each phase. During a 10-minute cool-down between the second and third phase, the engine is turned off. The total test time for the FTP-75 is 2,457 seconds (40.95 minutes), the maximum speed is 91.2 km/h, and the average speed is 34.1 km/h. The distance driven is approximately 17.86 km. The emissions from each phase are analyzed and expressed in g/km. <sup>[7]</sup>

The US06 Supplemental Federal Test Procedure (SFTP) shown in Figure 2-3 is developed to address the shortcomings with the FTP-75 test cycle in the representation of aggressive driving behavior, high speed and high acceleration. The cycle represents a 12.8 km route with an average speed of 77.9 km/h, maximum speed of 129.2 km/h, and a duration of 596 seconds. <sup>[7][9][10]</sup>

The SC03 Supplemental Federal Test Procedure (SFTP) shown in Figure 2-4 has been introduced to represent the engine load and emissions associated with the use of air

conditioning units in vehicles certified over the FTP-75 test cycle. The cycle represents a 5.8 km route with an average speed of 34.8 km/h, maximum speed of 88.2 km/h, and a duration of 596 seconds. <sup>[7][10]</sup>

The HWFET cycle illustrated in Figure 2-5 is another chassis dynamometer driving schedule, developed by the U.S. EPA for the determination of fuel economy of light duty vehicles. The cycle represents a 16.45 km route with an average speed of 77.7 km/h, maximum speed of 96.4 km/h, and a duration of 765 seconds. <sup>[7][10]</sup>

A combined chassis dynamometer test used for emission testing and certification in Europe is shown in Figure 2-6. It is composed of four ECE Urban Driving Cycles, simulating city driving, and one Extra Urban Driving Cycle (EUDC), simulating highway driving conditions. The cold-start version of the test, introduced in 2000, is also referred to as the New European Driving Cycle (NEDC). The cycle represents a 11 km route with an average speed of 33.6 km/h, maximum speed of 120 km/h and a duration of 1180 seconds. <sup>[9][10]</sup>

The 10-15 Mode cycle shown in Figure 2-7 is currently used in Japan for emission certification and fuel economy for light duty vehicles. It is derived from the 10 Mode cycle by adding another 15 Mode segment with a maximum speed of 70 km/h. The whole cycle is 4.16 km distance with 660 seconds driving duration at 22.7 km/h average vehicle speed. Emissions are expressed in g/km. <sup>[9][10]</sup>

It should be stated that the vehicles are calibrated using the certified dynamometer cycles so it can be expected that off-cycle conditions will be less well calibrated and lead to higher emissions.

## 2.2.2 REMOTE SENSING METHOD

Typically, an on-road remote emissions sensing system comprises an infrared (IR) source, an IR detector module, an ultraviolet (UV) source, an UV detector module and

a video camera. The criteria of site selection is based on the road type, number of lanes, traffic volume and vehicle mix, traffic speed and acceleration mode, road grade, traffic signal location, geographical distribution and representation. In 2002, Chan carried out an experiment and measured the concentrations of HC, CO, CO<sub>2</sub>, NO<sub>x</sub> in real time simultaneously using a remote sensing vehicle exhaust emissions testing system (ESP Accuscan RSD3000).<sup>[11]</sup> A device including an emitter bar and a detector bar was used to measure the speed and acceleration/deceleration of vehicles driving past the remote sensor. A color video camera system was utilized in the experiment to record the vehicle license plate so that the vehicle information could be obtained at a later stage.

In 1997, a sampling site was set up in the Caldecott Tunnel, located east of San Francisco Bay on highway 24 by Kirchstetter et al (1999).<sup>[12]</sup> Background pollutant concentrations were measured at the fresh air intake ventilation fans. CO and CO<sub>2</sub> concentrations were quantified using gas filter correlation spectrometers, and NO<sub>x</sub> was measured with chemiluminescent analyzer (Thermo environmental Instruments model 42). The pollutant concentrations inside the tunnel were measured by CO and NO<sub>x</sub> analyzers located in the fan room. An approximately fifty meters Teflon sample line was used to draw air samples directly from the traffic tube. Particle concentrations in the tunnel were measured continuously by a Condensation Nucleus Counter (CNC), an Optical Particle Counter (CPC) and an aethalometer. The experimental results clearly indicated that the stability of NO<sub>x</sub> emission factors when expressed on a fuel consumed basis supported their use in the development of fuel-based emission inventories.

Remote sensing of passenger car emissions was pioneered by Donald Stedman and Gary Bishop of the University of Denver using Non-dispersive Infrared and Ultraviolet (NDIR-NDUV) techniques for measuring NO<sub>x</sub> emissions. However, NDIR based instruments can operate with very limited cross-road path lengths due to the angular dispersion of their non-laser light. The longest path lengths reported with this type of instrument are 12-15 m, so this system only operated well on a single lane road. However, Tunable Infrared Laser Differential Absorption Spectroscopy (TILDAS) remote sensor used by Jimenez et al (2000). was quite sensitive on-road remote sensing

technique for NO<sub>x</sub> measurement, and could operate with an optical path length of 88 m or more than five times that of NDIR-NDUV instrument. <sup>[13]</sup> TILDAS technique is suitable for the emissions measurements made across a four-lane highway.

In comparison with the traditional in-laboratory emission testing, the remote emission sensing system can collect emission data that naturally reflects the on-road vehicle fleet combinations and current vehicle technologies. The major advantage is that it is possible to measure a large number of on-road vehicles. In contrast, the disadvantage is that it only gives an instantaneous estimate of emissions at a specific location. The remote sensing system neither measures the mass of emissions due to the shortage of detailed vehicle information, (i.e. vehicle exhaust mass flow rate, engine speed, power, torque, etc.) nor tells which vehicle is under good condition and which vehicle needs repairs urgently based on the 'snapshot' emissions at a specific spot.

### 2.2.3 ON-BOARD AND REAL-TIME EMISSIONS MEASUREMENT SYSTEM

Engine emissions vary a lot depending on operation mode, particularly for vehicle where the engine must produce a very wide range of power from idle to cruise to maximum power as well as negative power during engine braking. As the engine shifts operation modes, both the concentration of exhaust pollutants and mass rate of exhaust production vary widely and rapidly. This makes it difficult to actually measure the pollutant production on a mass basis. But the mass of pollutant put into the atmosphere is normally the critical value which must be controlled. To achieve a reasonable mass emission measurement, it is necessary to carefully control the vehicle operation conditions and to measure the pollutant in a way that accounts for the variable concentration and variable exhaust flow rate. Therefore, until the late of 1990s, the on-board & in-vehicle emission measurement was not widely used because it would have been prohibitively expensive to overcome the challenges mentioned above. However, in the last few years, in-use emission measurement methods have been developed dramatically, partially because of recent improvements in emissions equipment size, portability, and affordability, and partially because of the increased regulatory

emphasis on air pollution from vehicles leading to an increasing amount of research on portable emission measurement systems. The following is a brief review of the on-board systems that have been proposed and used for measuring the real-world vehicle tailpipe emissions.

A low-cost portable on-board emission measurement system, capable of measuring five exhaust gases (CO, CO<sub>2</sub>, O<sub>2</sub>, HC, NO<sub>x</sub>) from in-use vehicles, was developed by Vojtisek-Lom and Cobb of the University of Pittsburgh in 1997. The system required no modification to the vehicle and used a five-gas RG240 Digital Gas Analyzer made by OTC SPX, a Snap-On MT-2500 engine diagnostic scanner and a laptop computer. Repeated tests were carried out on a designed Pittsburgh Campus Test Route using twenty compressed natural gas vans. The test results showed that significant variance existed among the tests and vehicles, especially for HC and NO<sub>x</sub> emissions, but the CO<sub>2</sub> mass emissions had reasonable accuracy. Nevertheless, this on-board emission measurement system provided an alternative to research vehicles on which instruments were permanently mounted. <sup>[6]</sup>

OEM-2100<sup>TM</sup> The concepts employed by Vojtisek-Lom and Cobb were commercialized by Clean Air Technologies International, Inc., which marketed the OEM-2100<sup>TM</sup> portable emissions measurement system. Comprised of a five-gas analyzer, an engine diagnostic scanner and an on-board computer, this system can be installed in approximately fifteen minutes in a light duty vehicle. The equipment has a width of 53 cm, a height of 41 cm, a depth of 31 cm and weighs approximately 30 Kg. <sup>[14][15]</sup> OEM-2100<sup>TM</sup> not only measures on-road tailpipe emissions of CO, CO<sub>2</sub>, O<sub>2</sub>, NO<sub>x</sub>, HC on a second-by-second basis during actual driving, but also records eight On-Board Diagnostics (OBD) port parameters, such as vehicle speed, engine speed, engine coolant temperature, intake air temperature, manifold absolute pressure, percent of wide open throttle, and open loop/ closed loop flag. There are three interfaces with a vehicle: (1) tailpipe exhaust gas if sampled, (2) engine data were downloaded via diagnostic link, (3) system electrical power supplied via the cigarette lighter, power

port, or via direct connection to the vehicle's battery. All the connections are fully reversible and do not require any modifications to the vehicles. The accuracy of the OEM-2100™ was tested by the New York Department of Environmental Conservation (DEC) and at the U.S. EPA's National Fuels and Vehicle Emissions Laboratory. By using FTP, US06, FWY-HI driving cycles, the three vehicles emissions were measured simultaneously by the dynamometer equipment and the OEM-2100™. The test results pointed out that the OEM-2100™ had good precision with low standard error (less than ten percent of the mean emissions for all of the pollutants).

Frey et al. (2000) examined eleven different vehicles using OEM-2100™ and demonstrated that the emissions during some modes (i.e., idling) are generally low compared to emissions during other modes (i.e. acceleration), the highway vehicle air quality management strategies should focus on how vehicles were driven, and not necessarily regarding how far they were driven. <sup>[15]</sup> However, the slow response emission analyzer had limited ability to catch the emission spikes caused by aggressive drives in the real-world driving conditions. The vehicle tractive power, one of the most important vehicle parameters, could not be calculated accurately due to the lack of the instantaneous ambient temperature records.

RAVEM SYSTEM Ride Along Vehicle Emission Measurement (RAVEM) was among the first on-board emission measurement systems developed, and remains one of the very few that can measure emissions of particulate matter (PM) accurately. RAVEM system is based on proportional partial-flow constant volume sampling (CVS). The key advantage of the CVS principle for vehicle emission measurements is that the pollutant mass flow rate in the vehicle exhaust and pollutant concentrations can be measured readily, while exhaust mass flow rates are difficult and expensive to measure accurately, especially under transient conditions. <sup>[16][17]</sup>

RAVEM has been applied to a wide variety of emission measurements. The range of pollutants that can be measured has been expanded and now includes carbonyls, air toxics, N<sub>2</sub>O, and ammonia as well as NO<sub>x</sub>, CO, CO<sub>2</sub>, and PM. The principle

contributor to error in the emission results is inaccuracy in determining the CVS flow rate. Leaks in the tubing and valves that conduct the gas sample to the analyzers are another potential source of error.

FTIR SYSTEM In the early 1990s, a Fourier Transform Infrared (FTIR) system was installed on a 1992 Aerostar Minivan by Ford Motor Co., Dearborn, Mi. Chemistry Dept. FTIR is capable of acquiring time-resolved emissions of thirty exhaust components including CO, CO<sub>2</sub> and NO.<sup>[18]</sup> Basically, this on-board multi-component exhaust gas measurement system was composed of three major components. (1) The FTIR spectrometer equipped with a water cooled glow bar source and a MCT detector. When the vehicle was mobile, nitrogen gas was used to purge the spectrometer and circulated water was used to cool the infrared (IR) source. (2) The FTIR Data Acquisition System, which was controlled by a PC compatible computer. (3) Exhaust Gas Heated Sampling and Dilution System. A constant flow of nitrogen gas was mixed with the exhaust in the dilution chamber.<sup>[19]</sup>

At the turn of the century, another FTIR system was developed by University of California and Honda R&D Americas Inc. This new system was designed to simultaneously measure vehicle exhaust and ambient roadway pollutant concentrations. It was capable of accurately measuring Non-Methane Hydrocarbons (NMHC), CO and NO at the low concentrations encountered in ambient (roadway) air and vehicle exhaust. Sampling probes were installed in the vehicle's front grill, and 40 cm into the tailpipe. The sampling measurement systems were identical for each sample, with the exception of a heated line to keep the exhaust sample above dew-point temperatures. FTIR signals were processed with a Pentium-400 computer, permitting real-time display of NMHC, CO, NO, CO<sub>2</sub> concentration data with an update time of less than two seconds.<sup>[20]</sup> In infrared gas analysis, IR light was passed through a sample in a gas cell. Some of the infrared light was absorbed by the sample and some passed through. The measurement of these absorbed and transmitted wavelengths of infrared light constituted an infrared spectrum. Since no two chemical species had the same infrared

spectrum, the spectrum served as a fingerprint for identifying different gas components in the sample. The intensity of the infrared absorption indicated the quantity of the component in the sample. Truex et al. (2000) conducted a series of the validation experiments, which proved that their FTIR system had good accuracy and sensitivity to measure the very low NMHC, CO and NO concentrations. <sup>[21]</sup> However, they failed to work out a method for time alignment of the on-road data.

Daham et al. (2005) <sup>[22]</sup> developed an on-road emissions measurement system utilizing a commercial, portable FTIR Spectrometer capable of measuring up to 51 different compounds and measuring concentrations as low as 0.5-3 ppm. The whole system also included a fuel flow meter, a throttle position sensor, an air flow meter, a vehicle speed sensor, multiple temperature sensors, two laptop computers and two backup batteries. The major advantage of this measurement system was its ability to differentiate between various hydrocarbon species (toluene, formaldehyde, acetaldehyde, butadiene, benzene, etc) in gaseous mixture. Another useful application was the speciation of nitrogen-containing compounds such as NH<sub>3</sub>, NO<sub>2</sub>, NO and N<sub>2</sub>O. On the other hand, the major shortcoming was that the whole system weighed 180 kg, which caused an increase in emissions as it was equivalent to carrying at least two passengers.

ON-BOARD SYSTEM DEVELOPED IN UNIVERSITY OF ALBERTA Hawirko and Checkel (2003) developed an on-board emission measurement system using a Vetronix PXA-1100 five-gas analyzer, an ECM AFRecorder 2400E, a Siemens mass air flow meter, and three AD590 temperature probes for coolant water, ambient air and intake air temperatures. The five-gas analyzer could measure HC, CO, CO<sub>2</sub>, O<sub>2</sub> and NO<sub>x</sub> concentrations in the exhaust. Communication with all of the instruments and sensors was conducted through a Fujitsu laptop computer running Labview 6i. All data were synchronized by a dedicated Matlab process program for the further analysis in the laboratory. A 1990 GMC three-quarter ton regular cab pickup was tested on a repeated 17.4 km urban/suburban route with one driver and one vehicle over a one-year period. Their research mainly focused on the driving behavior and ambient temperature influences on the mass emissions rate. <sup>[23]</sup>

Based on Hawirko and Checkel's emission measurement system protocol, Manchur adopted a fast response Horiba Mexa-720 NO<sub>x</sub> analyzer and an Engine Control Module (ECM) data scanner (Autotap).<sup>[4]</sup> A Horiba zirconia ceramic NO<sub>x</sub> sensor was mounted on the exhaust pipe downstream of the catalytic converter of a 1999 Chevrolet Silverado Extended Cab pickup, and the ECM scanner connected with the vehicle OBDII port connector under the driver side dashboard could read the vehicle sensors data. Manchur's research results provided a comprehensive evaluation of the differences between the slow response gas analyzer and the fast response in-line sensor as well as the differences between the manually installed sensors and the ECM sensors. His on-board emission measurement system was also limited to one-vehicle and one-driver tests. In order to generate the general in-use emissions functions and fuel consumption functions, it is critical to develop a portable, low weight fuel consumption and emission measurement system adapting for multiple vehicles.

ON-BOARD DIAGNOSTIC SYSTEM (OBD) With the development of the automotive industry, the vehicle electronic control system has been evolving rapidly. The electronic control system, commonly defined as the ECM, was used to control fuel injection system, ignition system, transmission system, emissions control system, etc. This computer based electronic control system poses significant challenges for repair technicians. This is particularly challenging in areas where the I/M programs are in place, because component problems could frequently lead to high emissions without adversely affecting vehicle drivability. In this case, the On-Board Diagnostic program is then added to the ECM, which could help to indicate the emission-related malfunctions.<sup>[24]</sup>

In 1970, the American Congress passed the Clean Air Act and established the Environmental Protection Agency (EPA). This started a series of graduated emission standards and requirements for maintenance of vehicles for extended periods of time. To meet these standards, OBD-I (the first generation of On-Board Diagnostic system) was proposed and then adopted by California Air Resources Board (CARB) in April 1988.<sup>[24]</sup> The OBD-I requirements applied to new light-duty vehicles beginning with

the 1988 model year and continued to apply to some vehicles through the 1996 model year. The OBD-I system was greatly helpful for the service technicians to diagnose and repair the parts/components leading to the vehicle emissions failure. However, the OBD-I system was limited in that it did not monitor all emission control system components. As a result, it still remained difficult for the repair technicians to identify and repair malfunctions associated with unmonitored components. Moreover, the OBD-I system connector location and the fault codes used to identify specific malfunctions varied from manufacture to manufacture, and sometimes within a manufacture.

In 1988, the Society of Automotive Engineers (SAE) developed a standard that used a standard sixteen-pin connector plug and a set of diagnostic test signals. Therefore, OBD-II (the second generation of On-Board Diagnostic system) was an expanded set of standards and practices developed by SAE and adopted by the EPA and CARB for implementation by January 1, 1996. The OBD-II link of all car models is located under the dashboard of the vehicle. In contrast to the OBD-I regulations, where monitoring of only a limited number of components was required, the current OBD-II regulations require a system to detect the failure of any component which can affect emissions. In other words, OBD-II system is capable of monitoring the following: catalyst system, engine misfire, evaporative emission control system, oxygen sensors, exhaust gas recirculation system, positive crankcase ventilation system, engine cooling system, cold start emission reduction strategy, air conditioning system, variable valve timing system, direct ozone reduction system and diesel particulate trap. Due to the problems associated with multiple protocols, the new OBD regulations require that all 2008 and subsequent model year vehicles use one protocol, a Controller Area Network (CAN) protocol, which is the leading network in power-train and body electronic applications. The high speed CAN network is well accepted by European carmakers and it is also becoming the leading network in America and the Far East. <sup>[24][25][26]</sup>

Connected with OBD-II port plug, a diagnostic scanner can be used to read different vehicle operation parameters (vehicle speed, engine speed, intake air temperature,

coolant temperature, ambient pressure, etc.) as well as the vehicle emission control sensor data (EGR, TPS, O<sub>2</sub>, etc). At present, many kinds of OBD-II port scanners produced by many manufactures such as B&B electronics, AUTOXRAY, Snap-On, NGK, etc, are widely used in the automotive service shops as well as in research institutions.

### **2.3 EMISSION INVENTORIES PREDICTION MODEL**

Emission inventory is used to estimate and predict the amount of pollution that automobiles release into the atmosphere. This is an important tool for city planners in managing traffic problems associated with the fast urban growth and increased use of motor vehicles.

Developed by U.S. EPA, MOBILE5, an emission inventory prediction program developed in the 1990s, was able to estimate emissions of hydrocarbons, carbon monoxide, and oxides of nitrogen for cities or regions. MOBILE5 distributes the on-road vehicle fleet into eight main weight different categories. The vehicle composite emissions factor (g/km) was essentially based on the vehicle accumulative mass of the pollutant divided by the driving distance illustrated by the solid line in Figure 2-8 which shows an example of a HC cumulative emission trace with a cold start. This single emission factor calculated by MOBILE5 had good accuracy only for the simulation trip distance near 20 km. The emissions were under-estimated when the simulation distance was less than 20 km and over estimated when the distance was more than 20 km. Since the release of MOBILE5 on December 4<sup>th</sup>, 1992, MOBILE5 had been found to contain a number of minor errors that can affect the emission factors calculated by the model under certain conditions. For this reason, the Office of Mobile Sources had developed two corrected versions, which were called MOBILE5a (March 26<sup>th</sup>, 1993) and MOBILE5b (October, 1996). However, the inaccurate single emission factor development method was still adopted by the above new versions. <sup>[23][27]</sup>

MOBILE6 was developed to overcome many of the MOBILE5 problems and is capable of predicting gram per km emissions of HC, CO, NO<sub>x</sub>, CO<sub>2</sub> and Particulate Matter (PM) from cars, trucks, and motorcycles under various conditions. MOBILE6 further expands the previous eight vehicle categories into twenty-eight vehicle weight sections. The basic emission rates are derived from emissions tests conducted under standard conditions such as temperature, fuel, and driving cycle. Emission rates further assume a pattern of deterioration in emission performance over time, again based on results of standardized emission tests. MOBILE6 calculates adjustments to basic emission rates for conditions that differ from typical standard testing. Adjustments are used both to reflect how an in-use vehicle population is different from the tested samples and for conditions different from those used in the testing program. <sup>[28]</sup>

For the cumulative emission calculation for each pollutant, MOBILE6 uses two emission values. The first value is called starting emission value shown as the intercept between the Y axis and the dashed line in Figure 2-8. The second value describes the running emission factor shown as the slope of the dashed line. The total mass emission can be calculated by adding the starting emission value with running emission factor multiplied by driving distance. Obviously, the MOBILE6 model will estimate the vehicle emissions better than MOBILE5.

Because the data obtained from driving cycles is typically reported only a trip average basis, it is not possible to estimate emissions at smaller time or spatial scales. Thus, typical driving cycle data cannot be used to evaluate microscale vehicle emissions. The emission factor (g/km) used by the MOBILE series of models is also based on standard dynamometer testing and may not represent the vehicle emission rates at the high power demand, high acceleration with low vehicle speed driving situations.

## **2.4 CONCLUSION**

As a consequence of urban growth and increasing traffic levels, many cities experience serious air pollution problems. More stringent emission regulations are moving forward

innovation of the exhaust after treatment technologies and the development of the advanced tailpipe emission measurement representing the actual on-road driving conditions. Computerized emission inventories models make it possible to estimate the regional emissions both in the past and in the future supplying good guides for urban planners in managing traffic pollution problems. To improve the accuracy of those air pollution prediction models, it is preferable to develop on-road fuel consumption and emission functions instead of deriving them from the legislated drive cycle data tested on the chassis dynamometer which may not be representative of real-world traffic conditions. <sup>[22][29]</sup>

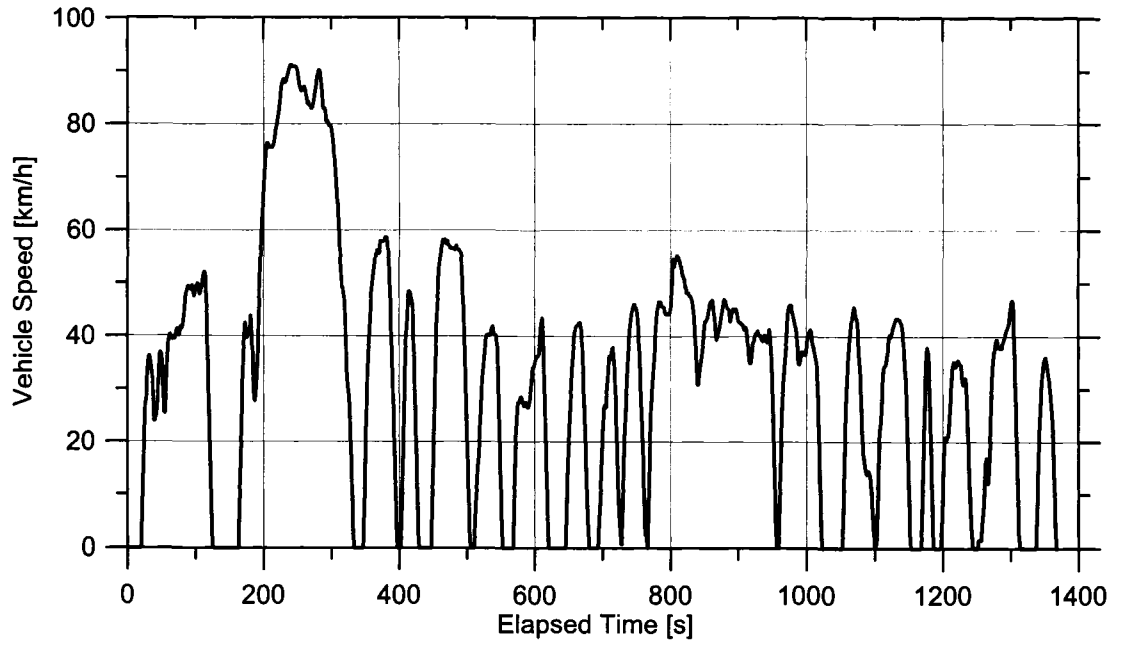


**Figure 2-1** FTP-72 Driving Cycle

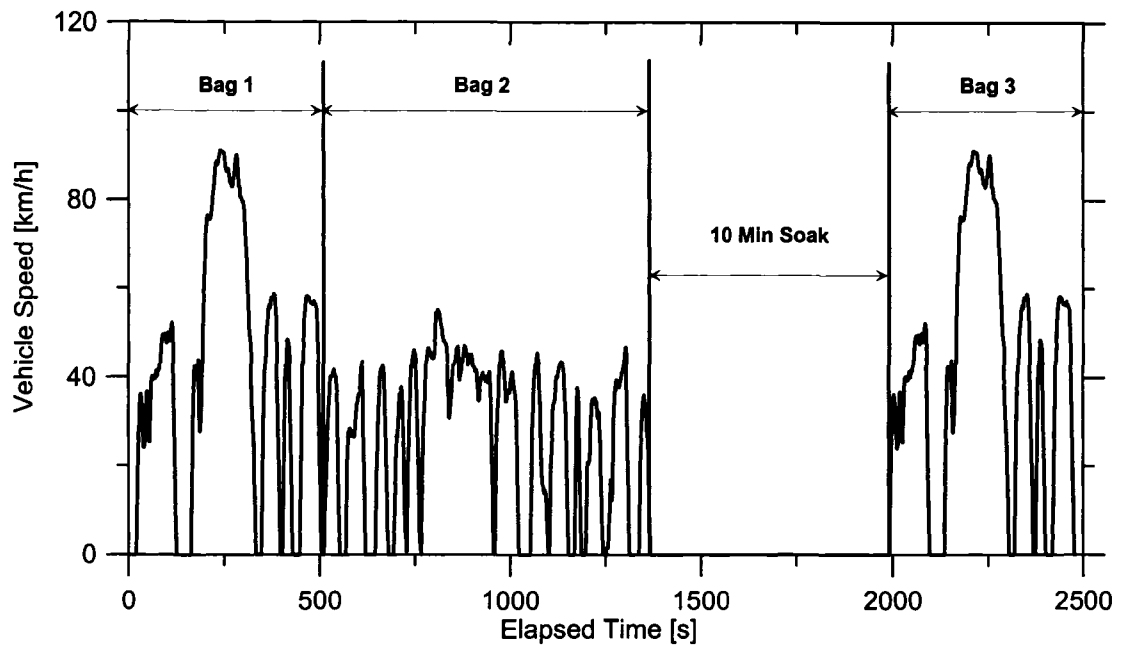


**Figure 2-2** FTP-75 Driving Cycle

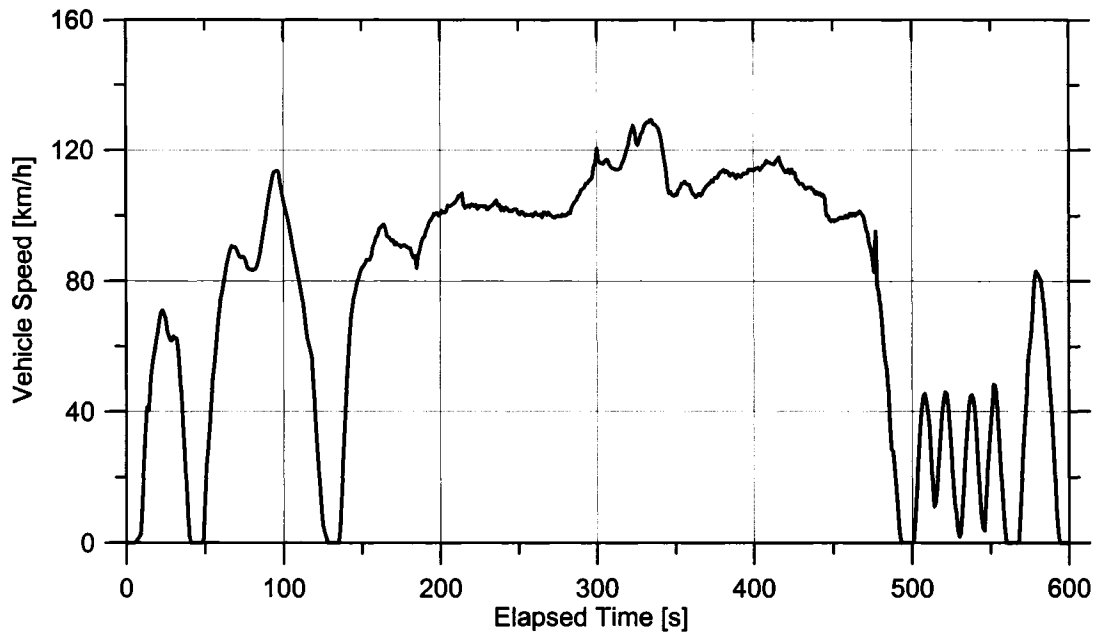


**Figure 2-3** SFTP US06 Driving Cycle

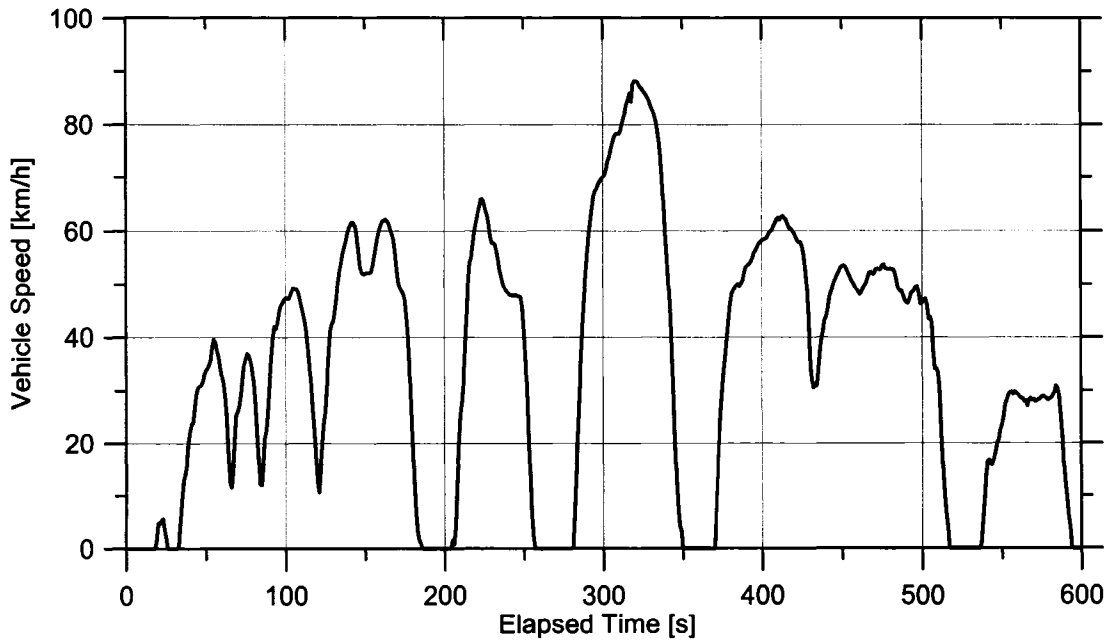


**Figure 2-4** SFTP SC03 Driving Cycle

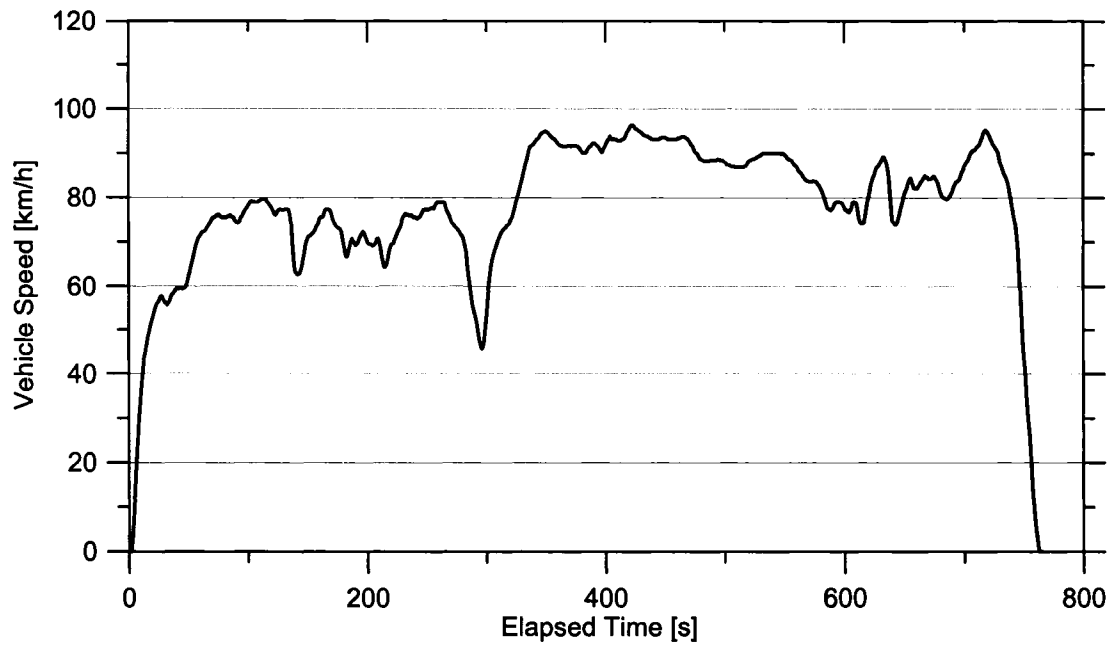


**Figure 2-5** EPA Highway Fuel Economy (HWFET) Driving Cycle

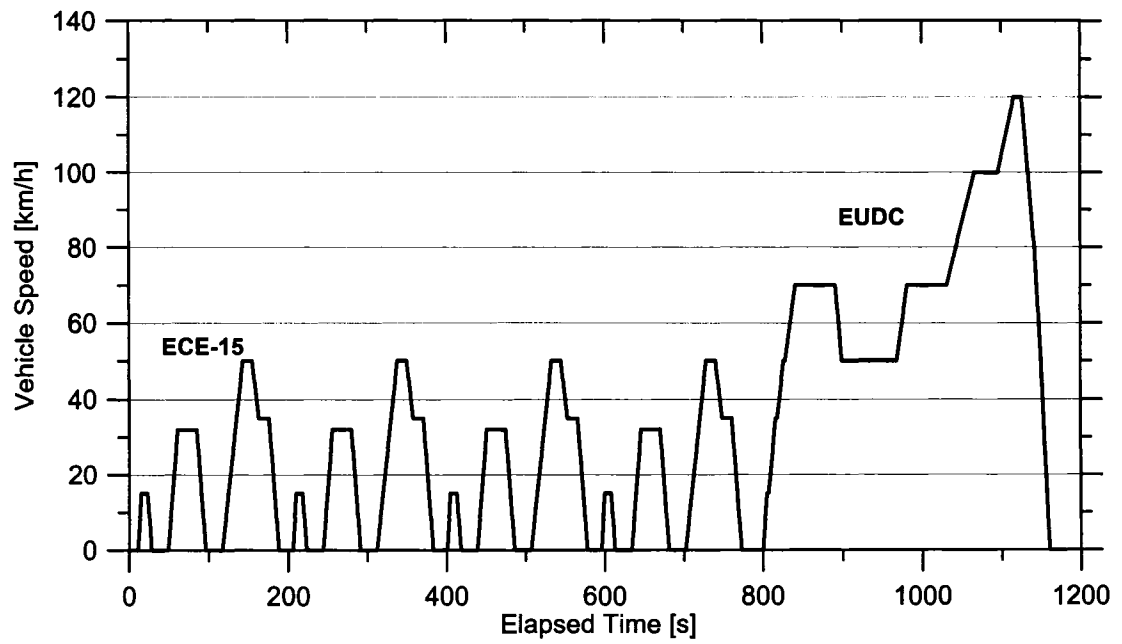


**Figure 2-6** New European Driving Cycle [NEDC]

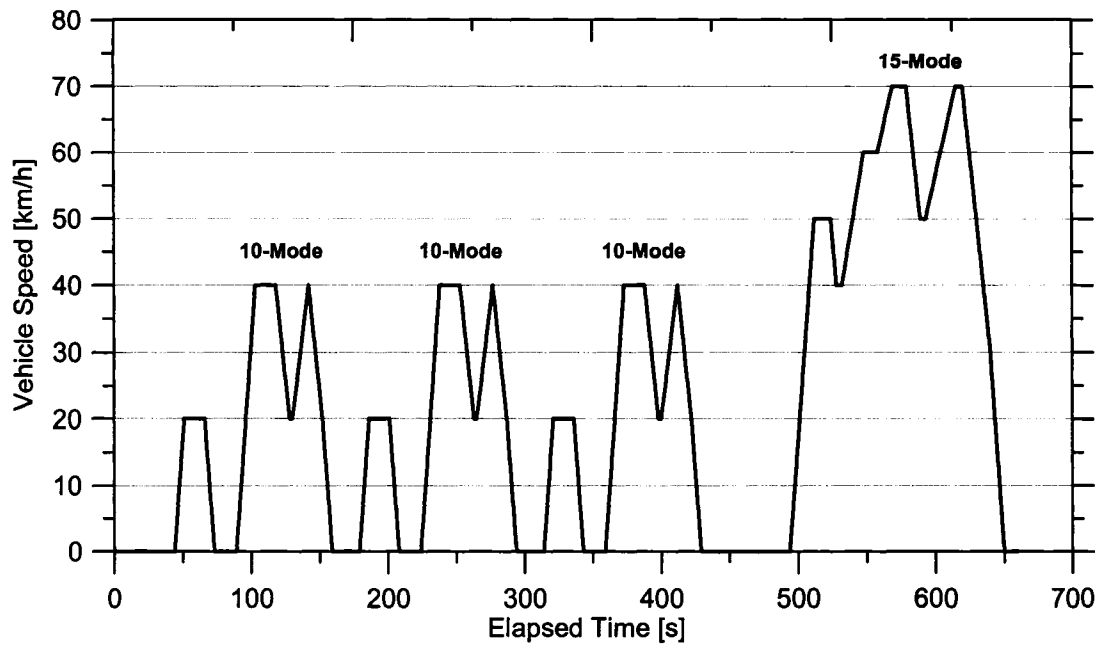


**Figure 2-7** Japanese 10-15 Mode Driving Cycle For the Light Duty Vehicles

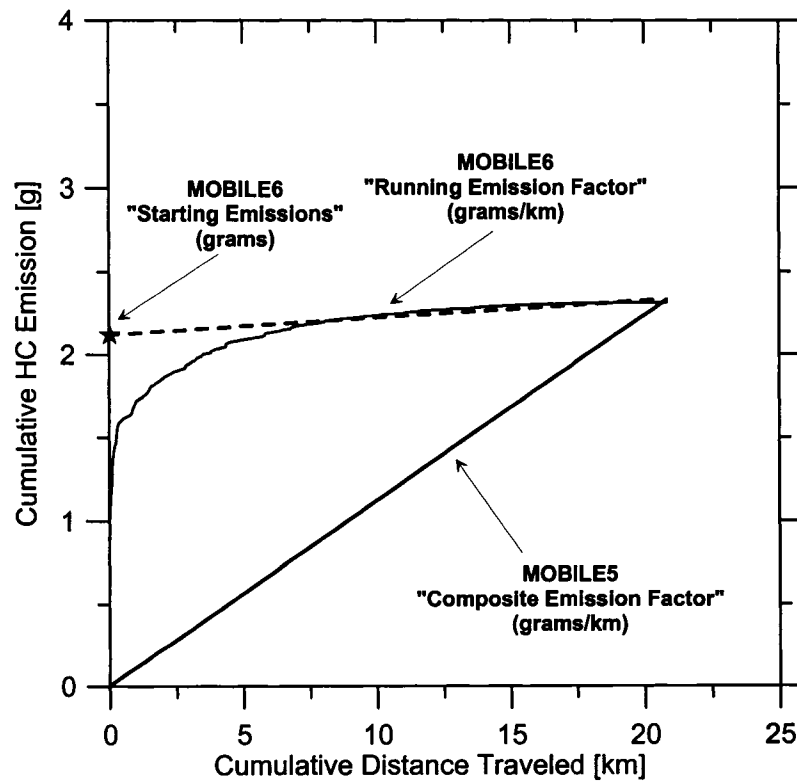


**Figure 2-8** Illustration of Emission Factors Used By MOBILE5 and 6

## REFERENCES

1. M. D. Checkel. "MecE 541 Combustion Engines Lecture Notes", University of Alberta. Sept 2004.
2. Yutong Gao, M. Dave Checkel. "Experimental Measurement of On-Road Fuel Consumption Functions", Combustion Institute/Canadian Section, in Waterloo, Ontario, Spring Technical Meeting 2006.
3. Kurt Engeljehringer. "Trends of Future Emission Legislation and its Measurement Requirements", SAE Paper 2004-01-3291, Society of Automotive Engineers, 2004.
4. Travis B. Manchur. "Accuracy Of On-Board Vehicle Emission Measurements", Master of Science Thesis, Department of Mechanical Engineering, University of Alberta, 2005.
5. Website: <http://www.ec.gc.ca/CEPARRegistry/regulations>
6. Michal Vojtisek-Lom; James T. Cobb, Jr. "Vehicle Mass Emissions Measurements Using a Portable 5-gas Exhaust Analyzer and Engine Computer Data", In proceedings- Emissions Inventory, Planning for the Future, Air & Waste Management Association; Pittsburgh, PA, 1997.
7. Website: <http://www.epa.gov/otaq/sftp.htm#cycles>
8. SAE Information Report. "Emission Test Driving Schedules", SAE J1506 Apr 1993.
9. S Samuel, L Austin, D Morrey. "Automotive Test Drive Cycles for Emission Measurement and Real-World Emission Levels-A Review", ISSN: 0954-4070, Proc Instn Mech Engrs Vol 216, PP. 555-564 (2002), Part D: J Automobile Engineering.
10. Website: <http://www.dieselnet.com/standards>
11. Chan, T L; Ning, Z; Leung, C W; Cheung, C S; Hung, W T; Dong, G. "On-Road Remote Sensing Of Petrol Vehicle Emissions Measurement And Emission Factors Estimation In Hong Kong". IRN 10520739, ISSN 1352-2310, CISTI. 26 January 2004.
12. Kirchstetter, T W; Harley, R A; Kreisberg, N M; Stolzenburg, M R; Hering, S V. "On-Road Measurement Of Fine Particle And Nitrogen Oxide Emissions From Light-And Heavy-Duty Motor Vehicles", IRN 10520739, 989118729, CISTI. 8 January 1999.

13. Jose L. Jimenez, Gregory J. Mcrae, Dacid D. Nelson, Mark s. Zahniser, and Charles E. Kolb. "Remote Sensing of NO and NO<sub>2</sub> Emissions from Heavy-Duty Diesel Trucks Using Tunable Diode Lasers", Environmental Science and Technology, Vol.34, No.12, 2000.
14. H. Christopher Frey, Nagui M. Roupail, A. Unal, and James D. Colyar. "Measurement of On-Road Tailpipe CO, NO, and Hydrocarbon Emissions Using a Portable Instrument", In proceedings, Annual Meeting of the Air & Waste Management Association, held in Orlando, Florida, and published by A & WMA, Pittsburgh, PA, June 24-28, 2001.
15. H. Christopher Frey, Nagui Roupail, Alper Unal, and James Colyar. "Emissions And Traffic Control: An Empirical Approach", Proceedings, CRC On-Road Vehicle Emissions Workshop, held in San Diego, CA, March 2000.
16. Christopher S. Weaver and Marco V. Balam-Almanza. "Development of the 'RAVEM' Ride-Along Vehicle Emission Measurement System for Gaseous and Particulate Emissions", SAE Paper 2001-01-3644, Society of Automotive Engineers, 2001.
17. Christopher S. Weaver and Lawrence E. Petty. "Reproducibility and Accuracy of On-Board Emission Measurements Using the RAVEM<sup>TM</sup> System", SAE Paper 2004-01-0965, Society of Automotive Engineers, 2004.
18. Ford Mortor Co., Dearborn, Mi. Chemistry Dept. "On-Road NO<sub>x</sub> Emissions Intercomparison Of On-Board Measurements And Remote Sensing". Final Report, Feb, 1994.
19. Christine A. Gierczak, Gerald Jesion, John W. Piatak, J.W.Butler; Ford Research Laboratory; Ford Motor Company. "On-Board Vehicle Emissions Measurement Program", Final Report, CRC Report No, VE-11-1, April 1994.
20. Jeff Jetter; Shinji Maeshiro; Seiji Hatcho; Robert Klebba. "Development of an On-Board Analyzer for Use on Advanced Low Emission Vehicles", SAE Paper 2000-01-1140, Society of Automotive Engineers, 2000.
21. Timothy J. Truex ; John F. Collins; Jeff J. Jetter; Benjamin Knight; Tadayoshi Hayashi; Noriyuki Kishi and Norio Suzuki. "Measurement of Ambient Roadway and Vehicle Exhaust Emissions-An Assessment of Instrument Capability and Initial On-Road Test Results with an Advanced Low Emission Vehicle", SAE Paper 2000-01-1142, Society of Automotive Engineers, 2000.

22. Basil Daham, Gordon Andrews, Hu Li. "Application of a Portable FTIR for Measuring On-road Emissions", SAE Paper 2005-01-0676, Society of Automotive Engineers, 2005.
23. Jason D. Hawirko, M. David Checkel. "Quantifying Vehicle Emission Factors for Various Ambient Conditions using an On-Road, Real-Time Emissions System", SAE Paper 2003-01-0301, Society of Automotive Engineers, 2003.
24. Paul Baltusis. "On Board Vehicle Diagnostics", SAE Paper 2004-21-0009, Society of Automotive Engineers, 2004.
25. Website: <http://www.obdii.com>
26. Website: <http://www.can-cia.org/can/protocol>
27. Website: <http://www.epa.gov/otaq/m5.htm>
28. Website: <http://www.epa.gov/otaq/models/mobile6/r02035.pdf>
29. M. D. Checkel, A. Brownlee, L. Doblanko. "Optimizing Vehicle Fuel Consumption and Emissions Through Traffic Optimization Using Vehicle and Traffic Forecasting Models", Combustion Canada 99 Technical Paper H 1.4, 1999.

## **CHAPTER 3**

### **Experimental System and Procedures**

*Chapter 3 introduces an on-board & in-use emission and fuel consumption measurement system by describing the experimental system setup and procedures. The aim of this section is to demonstrate that this in-use system is portable, practical and capable of accurately measuring the instantaneous mass flow rates of fuel and emissions as well as several operation parameters such as tractive power while the tested vehicle is in real service.*

### 3.0 INTRODUCTION

Understanding the role of real-world mobile source emission on air quality is moving us to develop new exhaust after treatment technologies as well as to design advanced emission measurement systems to evaluate on-road emissions from motor vehicles. <sup>[1]</sup> The most common method for measuring vehicle emissions and fuel consumption has been the use of chassis dynamometer tests in a laboratory test facility. Unlike the laboratory, where factors such as temperature and humidity can be controlled to within a specification, and where a vehicle can be operated on a standard speed or engine load trace, the on-road or in-field operation of a vehicle is subject to uncontrollable variability of ambient conditions and, in the case of on-road vehicles, of traffic conditions. Thus, the scheduling of data collection in an on-board study is more critical than it would be in the laboratory. <sup>[2]</sup> The opportunities for collecting data under desired conditions of ambient temperature, traffic flow, and other ambient or external uncontrollable factors are limited. It is therefore the challenge to develop a portable, fast installation in-use emission and fuel consumption measurement system with minimal impact on vehicle normal operations. <sup>[3]</sup>

This chapter focuses on a description of the experimental design and the test procedures employed in measuring real-world vehicle mass fuel consumption and emissions with an on-board & in-use measurement system adapted for multiple light-duty gasoline vehicles. Section 3.1 summarizes six individual subsystems of the experimental apparatus and one data processing program (Vetronix 5-Gas Analyzer, Horiba 720 NOx Analyzer, OBD-II Port Scanner, MAF Meter, Ambient Temperature Sensor, Data Acquisition System and Matlab program). The detail specifications of five test vehicles are summarized in Section 3.2. An overview of the experimental procedures used in conducting this study, driving routes designed and a typical start-stop test analysis are given in Section 3.3, Section 3.4 and Section 3.5 respectively. Section 3.6 details the measurement uncertainty analysis using the statistical method.

### 3.1 EXPERIMENTAL APPARATUS DETAILS

Figure 3-1 provides a schematic of the emission analyzers, sensors and data acquisition system used as an on-board & in-use measurement system. Vehicle speed, mass flow rate (g/s) of fuel and exhaust emissions (NO<sub>x</sub>, CO, CO<sub>2</sub>, HC, O<sub>2</sub>) are achieved using an ECM OBD-II scanner (Autotap), a Mass Air Flow sensor (Siemens), and two emissions analyzers (Horiba and Vetronix) with the rated resolution and accuracy listed in Table 1. All measurements are coordinated and recorded using a Dell laptop computer. The following sub-sections describe the components of this measurement system.

#### 3.1.1 VETRONIX FIVE-GAS ANALYZER

The Vetronix PXA-1100, a self-contained device which operates from vehicle electrical power (12v), is a portable, light weight (13 lbs) diagnostic exhaust gas analyzer. It is equipped with quick connect/disconnect hoses, which include one sampling line, two exhaust lines and one drainage line with a check valve. A flexible probe assembly at the end of the sampling hose is designed to insert into the vehicle tailpipe and secured by a chain during road tests. The emission samples are pumped into the Five Gas Analyzer through the sample line by the built-in vacuum pump. The mole fraction of C<sub>6</sub>H<sub>14</sub>, CO, CO<sub>2</sub>, O<sub>2</sub> and NO<sub>x</sub> can be measured and displayed on the analyzer screen. These emission gases are analyzed by two different methods: NDIR for HC, CO and CO<sub>2</sub> composition and two electro-chemical detectors for O<sub>2</sub> and NO<sub>x</sub> detection. The PXA-1100 is also equipped with a 22- key keypad which allows the user to make selections or input data needed to operate the gas analyzer. Before conducting the experimental test, the gas analyzer takes approximately 15 minutes from the time it is powered up for the internal, infrared gas detectors and sample chamber to complete the warm-up cycle. 'Zero Gas Data' is one of the steps after the analyzer warms up. Zeroing the gas analyzer adjusts the internal bench (HC, CO, CO<sub>2</sub> Detector Bench) and NO<sub>x</sub> sensor to read zero relative to the ambient air. Therefore, it is critical to locate the analyzer in a place with ventilated fresh air. In order to ensure the measurement accuracy, calibration was conducted every two weeks using a premixed blend <sup>[4][5]</sup>. In

order to record the emissions data continuously, the PXA-1100 can transmit the instantaneous data into a Dell Inspiron-1100 laptop computer through a RS-232 interface cable at 1.7 Hz sampling frequency.

**Table 3-1 Instrument Specification**

Value	Range	Resolution	Sensitivity	Accuracy (Rated)
5 Gas HC	0-20,000 ppm	1 ppm	N/A	5% of reading
5 Gas CO	0-10%	0.01%	N/A	5% of reading
5 Gas CO <sub>2</sub>	0-20%	0.10%	N/A	5% of reading
5 Gas O <sub>2</sub>	0-25%	0.01%	N/A	5% of reading
5 Gas NOx	0-4000 ppm	1 ppm	N/A	32 ppm at 0-1000 ppm 60 ppm at 1001-2000 ppm 120 ppm at 2001-4000 ppm
Horiba NOx	0-3000 ppm	1 ppm	N/A	30 ppm at 0-1000 ppm 3% at 1001-2000 ppm 5% at 2001-3000 ppm
Horiba A/F	3.99-500	0.01 A/F	N/A	0.35 A/F at 9.5-Stoich 0.15 A/F at Stoich 0.40 A/F at Stoich-20.00 A/F 0.90 A/F at 20.01-30.00 A/F 1.70 A/F at 30.01-40.00 A/F 2.60 A/F at 40.01-50.00 A/F 3.70 A/F at 50.01-60.00 A/F 0.5 vol% O <sub>2</sub> at >=60.01 A/F
Siemens HFM 62B	2-153 g/s	27.72 mg/s	22.72 (g/s) / V	1.0 g/s
AD 590	-55 -- 150 °C	0.12 °C	1000 °C / V	0.5 °C

### 3.1.2 HORIBA MEXA-720 NO<sub>x</sub> ANALYZER

Mexa-720 NO<sub>x</sub> analyzer is a low weight (1 kg), compact (130×75×200 mm), multi-function portable NO<sub>x</sub> emissions analyzer using a zirconia-ceramic sensor. The unit provides fast-response measurements of NO<sub>x</sub> concentrations from diesel or gasoline engines and simultaneously measures O<sub>2</sub>, Air/Fuel Ratio (AFR), and Excess Air Ratio ( $\lambda$ ). The sensor can be directly inserted into the vehicle downstream exhaust flow, eliminating the need for a sample-handling unit. This feature minimizes measurement time delays due to dead-volume sampling. The Mexa-720 NO<sub>x</sub> analyzer operates on vehicle electrical power (12v) and needs approximately three minutes warm-up time. Recommended calibration consists of measuring four points (Zero, Middle, Span, High

NO<sub>x</sub>). Calibration was conducted for this zirconia-ceramic NO<sub>x</sub> sensor once a month. The values of NO<sub>x</sub> and AFR can be read by the data acquisition system and recorded in the Dell laptop computer at 10 Hz sampling frequency. <sup>[6]</sup>

### 3.1.3 ECM OBD-II PORT SCANNER

An Auto Tap OBD-II Diagnostic Scanner is used to read the ECM sensor data in real time from any domestic and imported OBD-II vehicles after 1996. The vehicle parameters such as vehicle speed, engine speed, coolant temperature, intake air temperature, etc are available to be chosen and displayed in table, graph, meter or gauge displays. Those visual displays are convenient for the user to monitor and test the vehicle performance. All selected vehicle parameters can be recorded in the Dell laptop computer via USB connector. With a greater number of parameters being recorded, the OBD-II Scanner updates the instantaneous data values at a slower rate. Sampling frequency of about 3 Hz was for all tested vehicles during the experiments. <sup>[7]</sup>

### 3.1.4 MASS AIR FLOW METER

Vehicle intake mass air flow rate is measured by a Siemens HFM 62B MAF meter mounted in the vehicle air intake system manually before conducting the road tests. This MAF meter is a compact, light weight (160g) device operating on the vehicle electrical power (12v), with a mass air flow range from 2 g/s to 153 g/s. The HFM 62B was calibrated every three months in order to ensure the accuracy and stability. Like other equipment, this MAF meter also needs to warm up around fifteen minutes before the road tests. The device produces an analog output voltage, which can be converted into the mass air flow rate (g/s) using a calibration curve derived from comparison with an ASME standard nozzle per SAE standard J244. The mass air flow rate is recorded at frequency of 10 Hz by the Dell laptop computer in the same spread sheet as the Horiba NO<sub>x</sub> and AFR values.

### 3.1.5 TEMPERATURE SENSOR

The ambient temperature is measured by AD590, which is an integrated-circuit temperature transducer capable of producing an output current proportional to absolute temperature. The ambient air temperature sensor was mounted on the radio antenna of the vehicles where it could be exposed to the ambient air and would not be affected by the heat under the hood. This sensor is also powered by the vehicle electrical power (12v) and produces a linear current output ( $1 \mu A / K$ ) between  $-55^{\circ}C$  and  $150^{\circ}C$ . The calibration curve can be developed by a three points calibration method, which was actually conducted every three months as requirement. Like the HFM 62B MAF meter, the converting process of voltage to Celsius degree for AD590 can be achieved by the data acquisition system. The ambient temperature values in term of Celsius degree are recorded in the Dell laptop computer at a frequency of 10 Hz along with Horiba NOx, AFR and MAF data.

### 3.1.6 DATA ACQUISITION SYSTEM

The data acquisition system includes a Dell Inspiron-1100 laptop computer, a National Instruments AL-16E-4 PCMCIA Data Acquisition Card (DAQ) and two Labview 6i programs. The DAQ Card is capable of monitoring eight differential channels of analog input with twelve bit resolution and selectable gains of 1, 2, 5, 10, 20, 50 and 100. The data acquisition card collects data from the HFM 62B MAF meter, AD590 ambient temperature sensor and Horiba Mexa-720 NOx. Labview 6i program codes are written to process the analog inputs from the data acquisition card as well as to communicate with PXA-1100 gas analyzer via RS-232 interface cable. The data acquisition system is able to read and record all instantaneous data from the measurement equipment into the Dell laptop computer <sup>[5]</sup>.

The whole system weighing 17 kg (38 lbs) is installed in a designed steel case to be convenient for the operator to carry from vehicle to vehicle. This on-board & in-use emission measurement system is capable of being installed easily on a wide variety of vehicles, and being used during the regular everyday duty of the vehicles. Since the light-weight system can be belted on the passenger seat and the emission sampling hose

is secured along the vehicle body, the measurement system does not pose a real or perceived danger to the vehicle drivers, passengers or the general public <sup>[8]</sup>.

### 3.1.7 DATA ANALYSIS SOFTWARE

Using a Graphical User Interface (GUI) to provide onscreen options, a dedicated MATLAB program was composed to process raw experimental data files to interpolate data values due to the different sampling frequencies, synchronize the timing of the exhaust gas composition measurements with the other measurements due to the transport delay from the tail pipe to the five gas analyzer, and calculate the instantaneous vehicle power, mass emission rate and the fuel consumption rate as well as three types of emission factors. The detailed explanation of the program routines and sub-routines is illustrated in Appendix D.

A vehicle dynamic model was established in the processing program to calculate the vehicle tractive power at each time step. Tractive power is a measure of actual power transmitted to the road by the test vehicle based on the aerodynamic drag, rolling and inertial resistance of the vehicles. The complete calculations are illustrated in Appendix A. The instantaneous emissions rates and fuel consumption rates were calculated by balancing the combustion equations as detailed in Appendix B. The fuel consumption and emissions could be calculated in various formats such as g/s, g/km, g/kW.h and g/kgFuel. These measures were used to develop fuel consumption and emissions factors playing fundamental roles for building the associated prediction models in Chapter 4 and 5.

## 3.2 TEST VEHICLES

Five typical mid-life vehicles of model year 1997 to 2004 were used for these tests. As listed in Table 3-2, these vehicles included three passenger cars, one light duty pickup truck and one cargo van. Engine displacement varied from 1.8 L to 5.7 L with four automatic transmissions and one manual transmission. Vehicle odometer reading varied from 22,000 to 442,000 km. All vehicles were in “normal” operating conditions

with no diagnostic trouble codes or obvious faults. The vehicle classes represented by these vehicles represent a significant fraction of the on-road fleet.

A 1999 Audi Quattro A4, all-wheel drive passenger car was used as one of the test vehicles for experiments. The vehicle was equipped with a 1.8 L four-cylinder gasoline fueled engine with turbo charger, and five speed manual transmission and all-wheel drive. The odometer reading was 101,000 km during the testing period. The rated peak power is 150 HP at 5700 rpm engine speed.

The 2004 Pontiac Vibe, front-wheel drive passenger car was equipped with a 1.8 L four-cylinder DOHC gasoline fueled engine and automatic transmission. The engine and ECM control system were produced by Toyota Motor Corporation. The odometer reading was 22,700 km during the testing period. The rated peak power is 130 HP at 6000 rpm engine speed.

The 1997 Chevrolet Cavalier, front-wheel drive passenger car was equipped with a 2.2 L four-cylinder DOHC gasoline fueled engine and automatic transmission. The odometer reading was 129,600 km during the testing period. The rated peak power is 120 HP at 5200 rpm engine speed.

The 1999 Chevrolet Silverado C1500, extended cab, four-wheel drive pickup was equipped with a 5.4 L V8 Vortec gasoline fueled engine and automatic transmission, which was operated in two-wheel drive mode for all tests. The odometer reading was about 122,000 km during the testing period. The rated peak power is 270 HP at 4000 rpm engine speed. The truck was originally obtained for competition in the 2000 Ethanol Vehicle Challenge sponsored by General Motors and the U.S. and Canadian governments. After the completion of the competition, the vehicle was converted back to the stock gasoline power configuration. The pickup is currently used as an emissions research test vehicles, as well as a utility vehicle for student vehicle projects at the University of Alberta. <sup>[9]</sup>

**Table 3-2 Vehicle Specifications**

Vehicle Type	LDGV	LDGV	LDGV	LDGT2	LDGT3
Vehicle Model	Audi Quattro	Pontiac Vibe	Chevrolet Cavalier	Chevrolet Silverado	GMC Savana
Vehicle Symbol	LDGVA	LDGVV	LDGVC	LDGTSP	LDGTSV
Model Year	1999	2004	1997	1999	2001
Odometer Reading	101,000 km	22,700 km	129,600 km	122,000 km	442,300 km
Engine & ECM Maker	Audi, Germany	Toyota, Japan	Chevrolet, USA	Chevrolet, USA	GMC, USA
Engine Type / Size	1.8 L L4 AWD	1.8 L L4 FWD	2.2 L L4 FWD	5.4 L V8 4WD	5.7 L V8 RWD
Supply OBDII Port Data	Yes	Yes	Yes	Yes	Yes
Real Weight During Test	1557 kg	1407 kg	1357 kg	2360 kg	2690 kg
Transmission	Manual	Automatic	Automatic	Automatic	Automatic
Length	4522 mm	4365mm	4580 mm	6261 mm	6063 mm
Width	1733 mm	1775 mm	1712 mm	1994 mm	2012 mm
Height	1418 mm	1580 mm	1392 mm	1798 mm	2096 mm

The 2001 GMC Savana 2500, rear-wheel drive cargo van was equipped with a 5.7 L V8 gasoline fueled engine and automatic transmission. The rated peak power is 290 HP at 5200 rpm engine speed. The odometer reading was 442,300 km during the testing period, which was high for its age.

In order to minimize the extra engine load from the accessories, the radio/CD player and air conditioner were turned off, but the ventilation fan was set at the lowest level during experimental tests on every vehicle.

### 3.3 EXPERIMENTAL PROCEDURE

Once all instrumentation had been calibrated and installed onto the tested vehicle, it was possible to begin the experiments. The Vetronix PXA-1100 5-gas analyzer and Horiba Mexa-720 NOx analyzer were turned on first because they have longer warm-up time. To supply power for ECM OBD-II scanner, the vehicle ignition switch was turned to the “ON” position. However the engine would not be cranked at this moment. Next step was to turn on the laptop computer and load the two Labview programs and the Auto Tap program. Once all equipment was warmed up, the user manually composed the recorded file names for each program and triggered the record buttons.

The last step was to start up the engine and make sure every experimental apparatus or program works well. The weather conditions and test route traffic conditions were recorded after each in-use test as good references for the later research analysis.

### 3.4 DRIVING ROUTES

Six urban routes were selected in Edmonton city, each of which is similar to FTP 75 urban driving cycle consisting of one fraction of the congested stop-start urban roads including one way, one lane each way, two lanes each way, and two fractions of relatively high-speed suburban roads. Those routes have an average distance of 16 km with an average vehicle speed of 30 km/h, maximum vehicle speed of around 80 km/h and a duration of 27 minutes.

**Table 3-3** Driving Routes Comparison

Item	Distance [km]	Average Speed [km/h]	Maximum Speed [km/h]	Duration [minutes]
<b>Urban Route</b>	16.0	30.0	80.0	27.0
FTP 75	17.9	34.1	91.2	31.0
<b>Aggressive Driving</b>	10.0	80.0	130.0	11.0
US 06	12.8	77.9	129.2	9.9
<b>Highway Route</b>	20.0	80.0	100.0	13.0
HWFET	16.5	77.7	96.4	12.8

Two routes were chosen along the Whitemud Freeway at the south of Edmonton to simulate the aggressive driving behaviors represented by the EPA US06 driving cycle. The driving distance was about 10 km with an average vehicle speed of 80 km/h, designed maximum vehicle speed of 130 km/h, maximum acceleration of 3.0 m/s<sup>2</sup> and a duration of 11 minutes driving time. However, not every experimental test had that high maximum vehicle speed due to the limitation of the real-world traffic conditions.

Two routes were chosen along Highway 2 between Edmonton and Leduc to simulate the Highway Fuel Economy test cycle. The driving distance is about 20 km with an average vehicle speed of 80 km/h, maximum speed of 100 km/h and a duration of 13 minutes. Table 3-3 summarizes the comparison of the designed driving routes with the corresponding certified driving cycles.

### **3.5 RESULTS ANALYSIS**

This section displays analysis of a typical start-stop driving profile to illustrate the capabilities of the in-use measurement system. Figure 3-2 shows instantaneous vehicle speed, tractive power, fuel consumption rate and mass emission traces between two full stops extracted from an urban test. The vehicle experienced two rapid accelerations and one slow acceleration with vehicle speeds varying from zero to 80 km/h. From the bottom graph in Figure 3-2, it could be stated that vehicle tractive power not only varied with vehicle speed, but also with vehicle acceleration since each peak power happened at the end of the acceleration regardless of whether the vehicle speed was high or low. On the other hand, the instantaneous fuel consumption and mass emissions rates acted in compliance with the vehicle tractive power as shown clearly in the graphs. The vehicle produced 8, 30, 10 and 9 times increase for HC, CO, NO<sub>x</sub> and mass fuel flow rate respectively with vehicle tractive power increasing from zero to 55 kW for the first acceleration period. CO emission appeared only sensitive to the higher peak power for this test vehicle since the CO emission mostly remained quite low when the vehicle power was lower than 25 kW.

Another way to evaluate the influences on the emissions from the vehicle tractive power and acceleration can be illustrated by bubble plots in Figure 3-3. All instantaneous mass emissions data of HC, CO and NO<sub>x</sub> during the 140 seconds driving period were plotted in a single graph mainly considering the basic vehicle emissions behaviors with the vehicle operational parameters. The emissions were at the clean region with low values when the vehicle experienced low acceleration, low tractive

power and all deceleration situations. With increasing vehicle power as well as acceleration, the mass emission rates started jumping out of the low emission value region to the high emission region. From this typical experimental test, it should be stated that vehicle tractive power has more direct influences on the fuel consumption and emissions rates than vehicle speed, which indicates the vehicle power based fuel consumption and emission factors will give more fuel consumption and emissions details during the transient driving pattern than vehicle speed/distance based factors.

The whole experimental test data file can be truncated in accordance with vehicle speed and tractive power to give the average value in each speed bin and tractive power bin. In this thesis, the average speed and tractive power especially used in fuel consumption and emissions functions development are defined as bin average speed and bin average tractive power respectively. For example, all data within 4 km/h and 6 km/h go with 5 km/h speed bin, and those within 7 kW and 9 kW go with 8 kW tractive power bin. Figure 3-4 shows the histogram fraction of different vehicle speed bin as well as individual distance-based fuel consumption values and average fuel consumption values located in their related road speed bins. The vehicle spent 21% of its time at idle conditions and run most of time at low vehicle speed implying the stop-start congested urban driving pattern. The individual fuel consumption data scatter a lot along the whole vehicle instantaneous speed range, but the distance-based fuel consumption trend with road speed is clearly expressed by the bin average values in the bottom graph of Figure 3-4. The similar method is also used for the bin average tractive power development shown in Figure 3-5. Again, the typical urban driving pattern is demonstrated by the tractive power histogram plot with 50 % of the driving time at less than 1 kW. In the tractive power interval of zero to 50 kW, the trend of instantaneous mass fuel flow rates increasing with vehicle tractive power is demonstrated very well by the bin average values in the bottom graph of the same figure. However, the trend becomes unclear due to the less data were collected at the high tractive power region, and the average values were biased by some individual data. Therefore, in order to reduce overall measurement uncertainty and bias, the data averaging strategy is widely used in the vehicle fuel consumption and emissions behaviors analysis in the follow

chapters. The theory of increasing and averaging the collected data to reduce overall uncertainty is detailed in the next section.

### 3.6 MEASUREMENT UNCERTAINTY ANALYSIS

As mentioned in the previous sections, this in-use fuel consumption and emission measurement system is made up of a chain of instruments, each of which is subject to individual inaccuracy as summarized in Table 3-1. The overall uncertainty of the calculated values (i.e. specific emission rate g/gFuel, g/km, g/kW.h) can be computed from the individual errors of several different equipments using the Root-Sum-Square uncertainty analysis methods as detailed in Appendix A and Appendix B. The nature of the in-use measurement system is to represent real-world driving conditions which is the major advantage over the standard chassis dynamometer. However, the repeatability of in-use measurement is low because the vehicle experiences a variety of traffic conditions, road conditions, driving behaviors, etc. The combined system uncertainty of individual measurements is dominated by the larger error from the repeatability since the instrument accuracies are satisfied by the periodic calibrations. However, the data averaging inherent in calculating specific emission rates from many individual measurements can reduce the uncertainty as indicated in Equation 1<sup>[10][11]</sup>, since the final emission rate is inherently an average of a large sample size  $N$ .

$$s_{\bar{X}} = \frac{s}{\sqrt{N-1}} \quad [1]$$

$s_{\bar{X}}$  : Standard deviation of sample mean values

$s$  : Standard deviation of population about  $\bar{X}$

$N$  : Sample size

Figure 3-6 shows the individual specific NO<sub>x</sub> emission rate (g/gFuel) from one trip using the Audi Quattro. The data are scattered along the vehicle speed axis (i.e. independent of speed) and have an average value of  $\bar{X} = 0.00279$  and standard

deviation  $s = 0.00259$  for the 2,374 individual measurements. Calculated with Equation 1, the standard deviation of mean values is  $s_{\bar{X}} = 0.0000532$ . Assuming a Gaussian distribution <sup>[11]</sup>, the 95% confidence range is  $\bar{X} \pm 1.96 \times s_{\bar{X}} = 0.00279 \pm 3.7\%$ .

**Table 3-4** Difference Average Value and Uncertainty From Different Trips

Vehicle	Trip	Average NOx (g/gFuel)	95% Confidence Uncertainty
Audi Quattro	1	0.00279	3.7%
	2	0.00201	9.6%
	3	0.00293	5.2%
	4	0.00198	9.1%
<b>Audi Average</b>		<b>0.00243</b>	<b>6.9%</b>

Table 3-4 shows the average values and corresponding uncertainties from four trips using the same vehicle. The resulting average NOx value of 0.00243 g/gFuel with 6.9% uncertainty is accurate enough to characterize this vehicle.

**Table 3-5** Average NOx (g/gFuel) Value From All Tested Vehicles

Vehicle	Average NOx (g/gFuel)
Audi Quattro	0.00243
Pontiac Vibe	0.00052
Chevrolet Cavalier	0.00140
Chevrolet Silverado	0.00408
GMC Savana	0.00355
5 Vehicle Average Value	0.00240
95% Confidence Uncertainty	60.1%

Table 3-5 shows the range of NOx emission rates developed for all 5 tested vehicles. Considering the range of vehicle values, the average specific NOx emission value of 0.0024 g/gFuel could be used to represent the whole light duty gasoline vehicle population, but with a statistical uncertainty of  $\pm 60.1\%$  at 95% confidence. This large statistical uncertainty is not surprising when considering the huge range of fleet models

and ages on the road. The uncertainty of  $\bar{X}$  is reduced as sample size  $N$  increases, therefore at least 580 vehicles in different categories should be tested in order to represent the total light duty gasoline vehicle population with 5% uncertainty.

Similar statistical analysis of data can also be used in other fuel consumption factors and emission factors calculations.

### **3.7 CONCLUSION**

While the environmental impact of the automobile has long been regarded as a relevant and important research topic, increasingly strict environmental regulations and ever-expanding automobile use are increasing the impetus of developing a portable real-time emission measurement method. Having introduced the experimental apparatus and illustrated the details of the experimental design and test procedures, this chapter described an on-board & in-use fuel consumption and emission measurement system rebuilt and adapted for multiple light-duty gasoline vehicles. The capability of this in-use measurement system to examine the real-world instantaneous mass flow rates of fuel and emissions as well as other operational parameters was demonstrated by analyzing a typical start-stop driving test. The experimental results clearly showed how the operational parameters (such as vehicle tractive power) affected vehicle pollutant emissions and fuel consumption rates. Statistical analysis clearly showed that system overall uncertainty was reduced greatly through averaging individual data and increasing sample number.

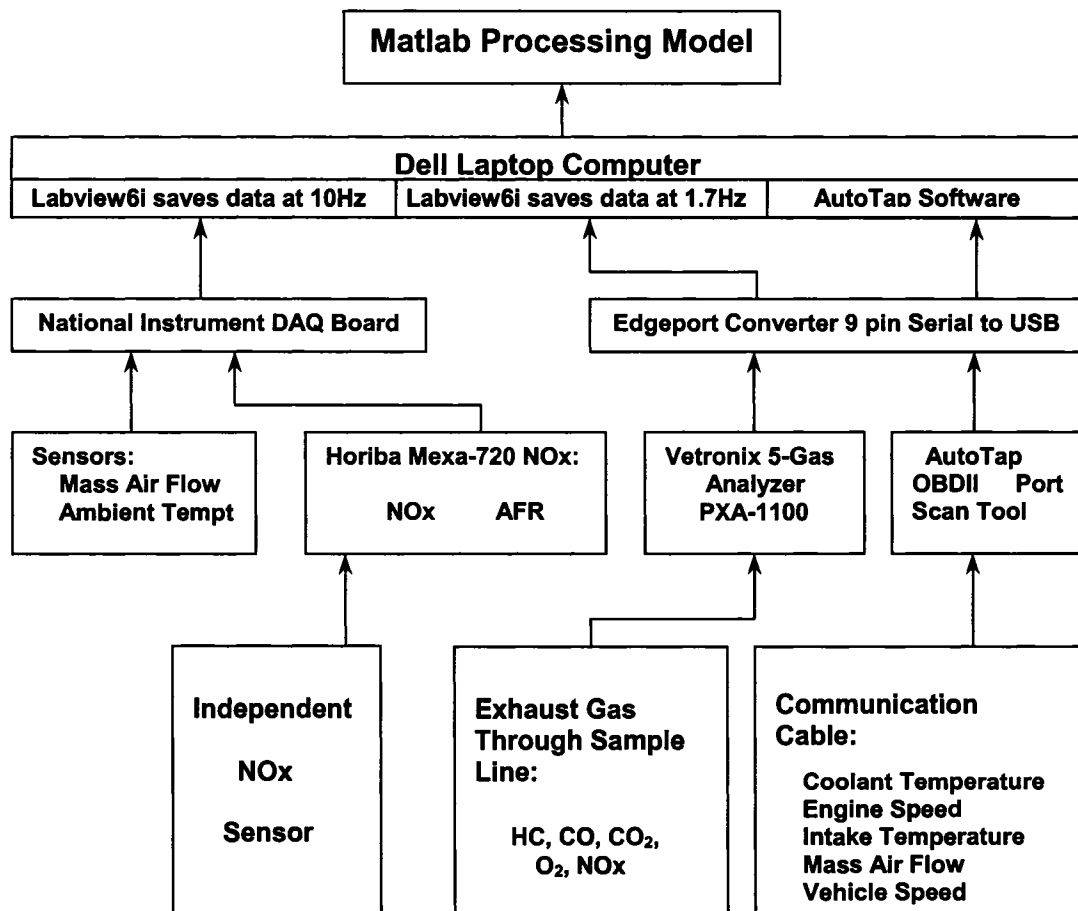


**Figure 3-1** Schematic of Test Instruments

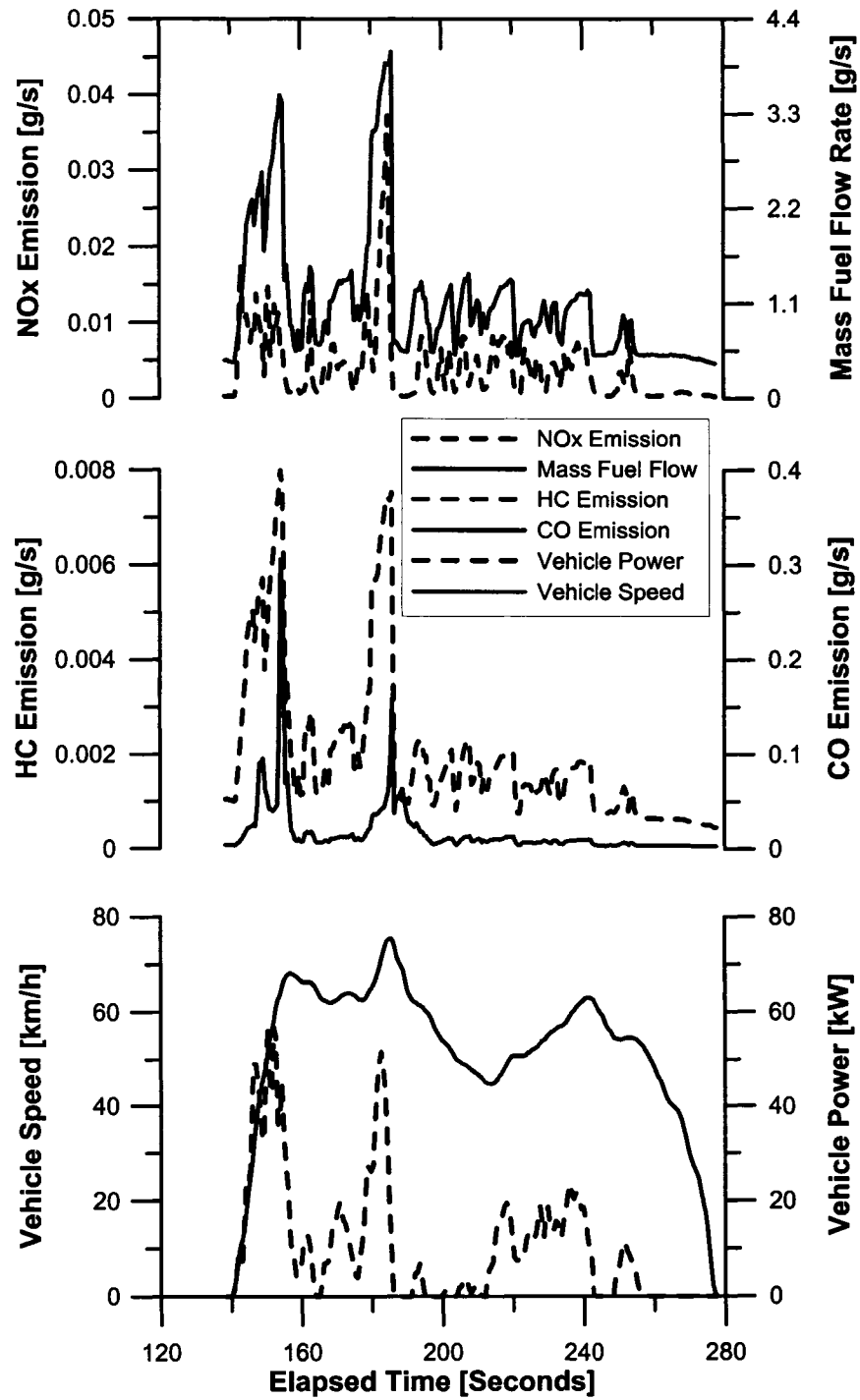


**Figure 3-2** Instantaneous Trace of Emissions, Mass Fuel Flow, Vehicle Power and Speed (Using Chevrolet Silverado)

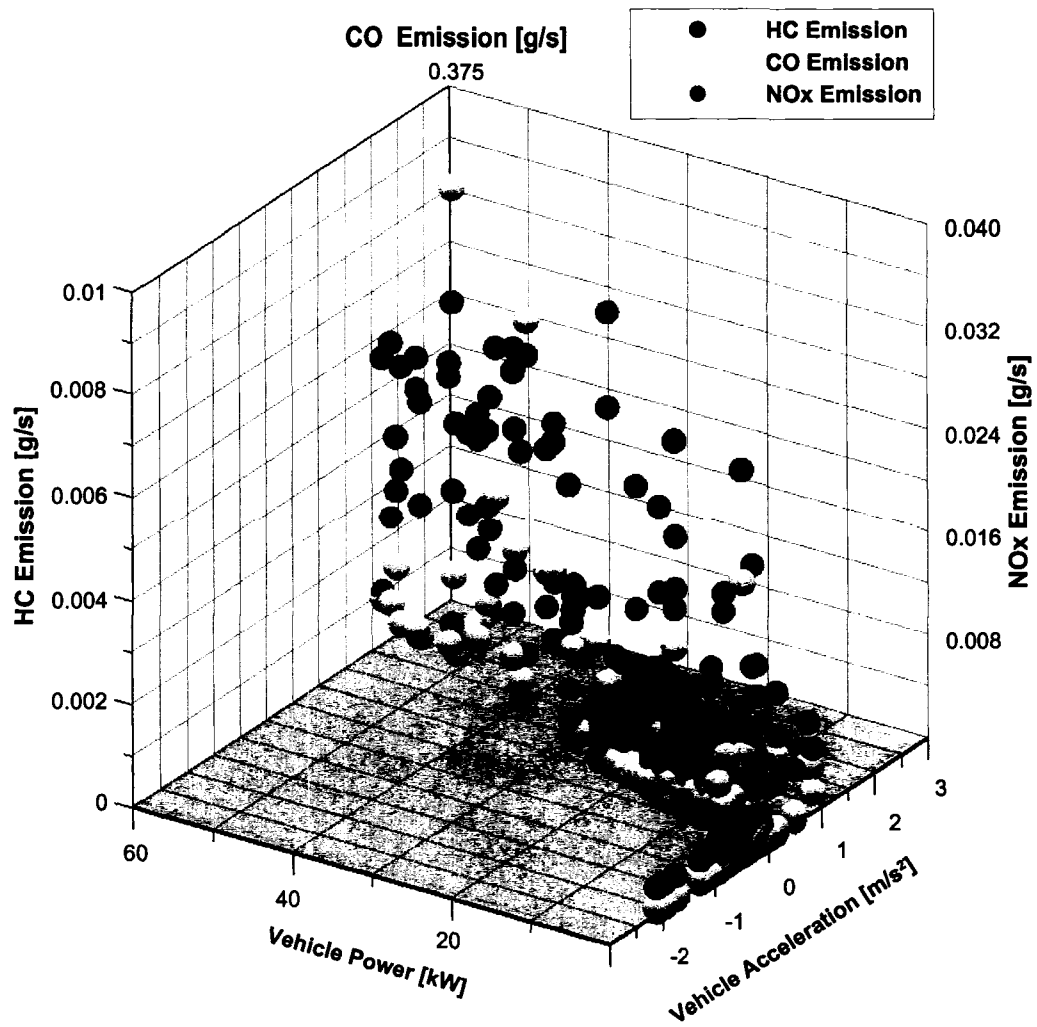


**Figure 3-3** Effect of Vehicle Power and Acceleration on Tailpipe Emissions  
(Using Chevrolet Silverado)

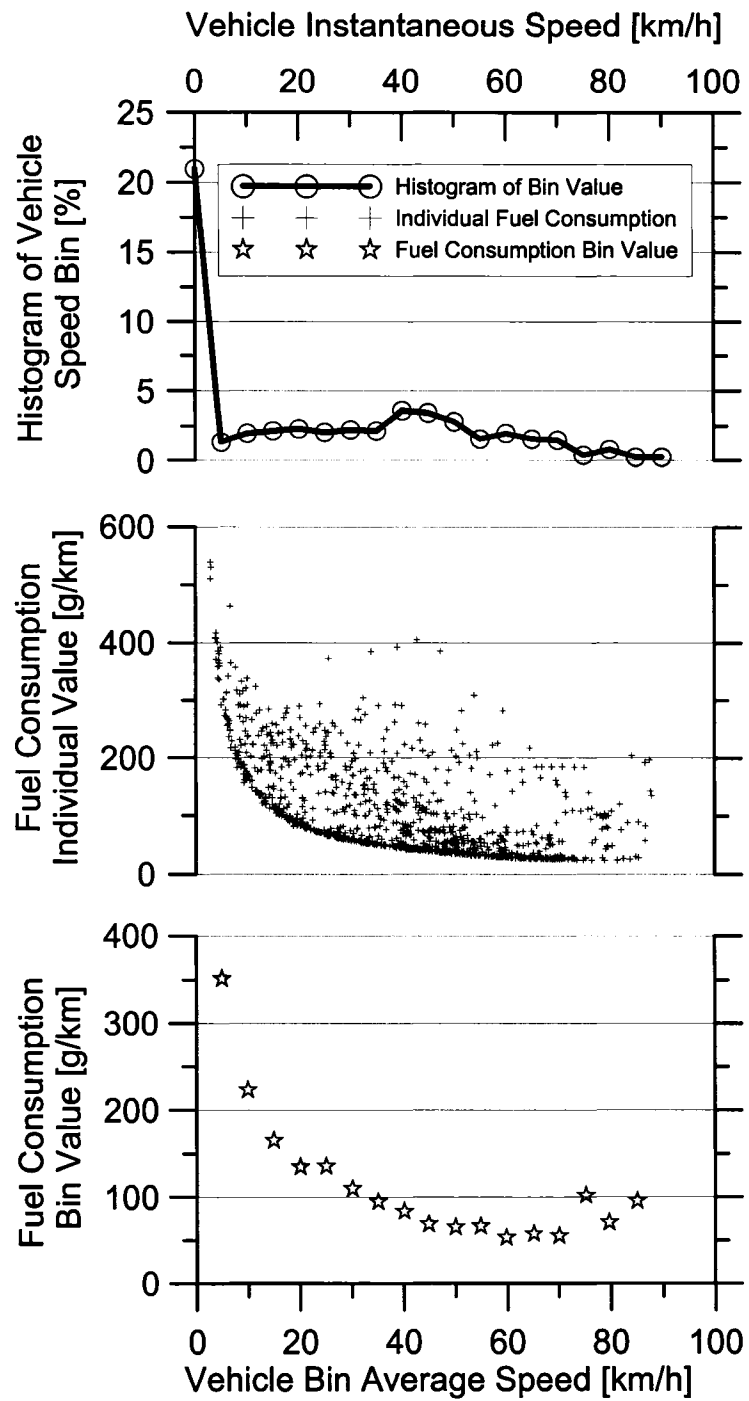


**Figure 3-4** Vehicle Bin Average Speed Development (Using Chevrolet Silverado)

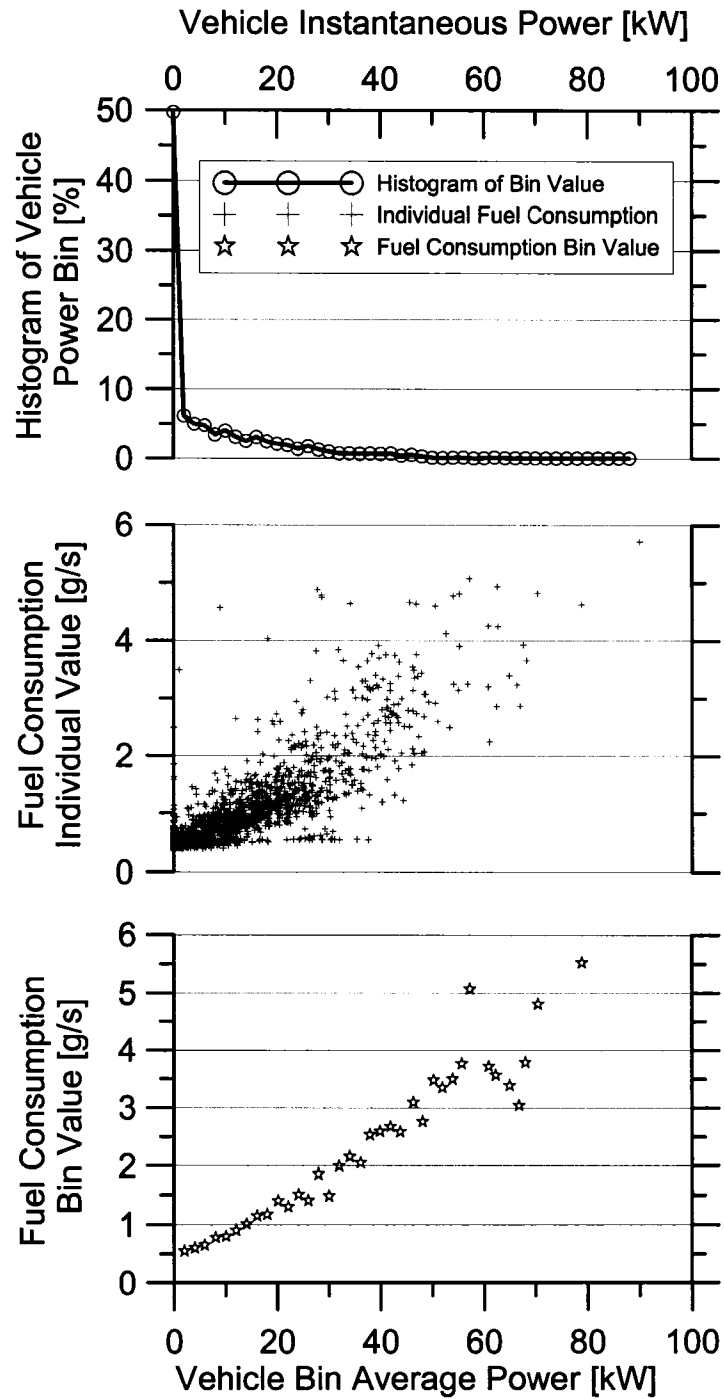


**Figure 3-5** Vehicle Bin Average Power Development (Using Chevrolet Silverado)

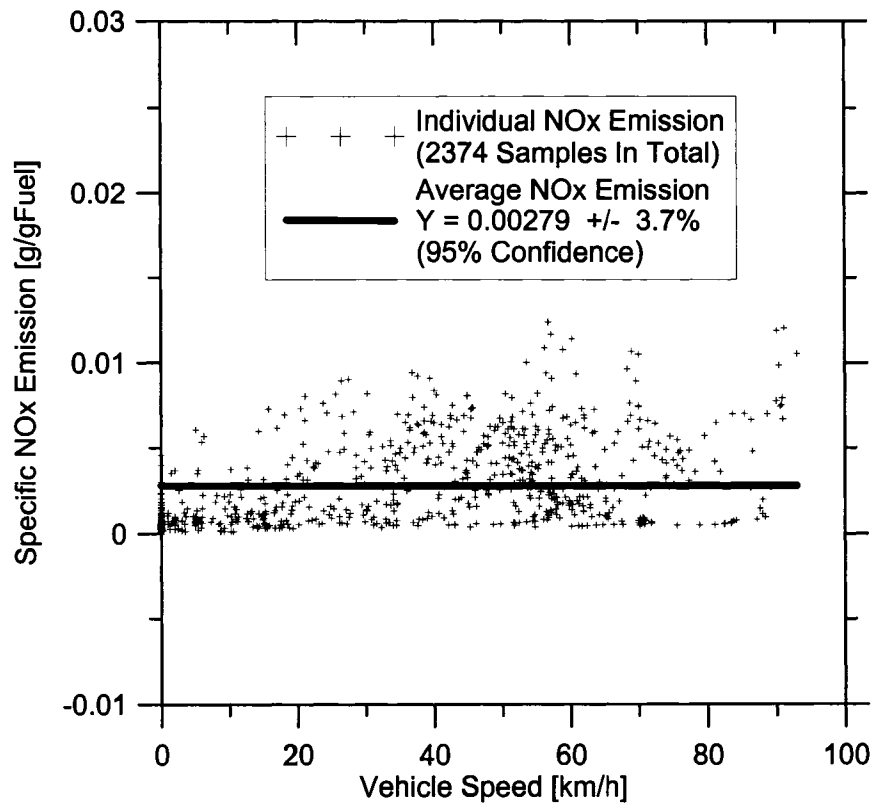


**Figure 3-6** System Uncertainty Reduction Using Average Data  
 (Assume g/gFuel is Independent of Vehicle Speed and Tractive Power)

## REFERENCES

1. Steven H. Cadle, Robert A. Gorse, Brent K. Bailey, Douglas R. Lawson. "Real-World Vehicle Emissions: A summary of the Tenth Coordination Research Council On-Road Vehicle Emissions Workshop", submitted for publication to the Journal of the Air & Waste Management Association, 2001.
2. H. Christopher Frey, Alper Unal, Jianjun Chen. "Recommended Strategy For On-Board Emission Data Analysis and Collection For The New Generation Model", Prepared for: Office of Transportation and Air Quality U.S. Environmental Protection Agency, Ann Arbor, MI. February 4<sup>th</sup>, 2002. Department of Civil Engineering, North Carolina State University, Raleigh, NC.
3. Yutong Gao, M. David Checkel. "Experimental Measurement of On-Road Fuel Consumption Functions", Combustion Institute/Canadian Section, in Waterloo, Ontario, Spring Technical Meeting 2006.
4. PXA-1100 Gas Analyzer Operator's Manual, Vetronix Corporation. Printed in USA, July 1996.
5. J. D. Hawirko. "Modeling Vehicle Emission Factors Determined with an In-Use & Real-Time Emissions Measurement System", Master of Science Thesis, Department of Mechanical Engineering, University of Alberta, 2003.
6. Horiba Mexa-720 NOx Instruction Manual, Horiba Corp. Portaiton.
7. <http://www.autotap.com/contact.html>, B & B Electronics Mfg Co.
8. Michal Vojtisek-Lom, Joseph E. Allsop. "Development Of Heavy-Duty Diesel Portable, On-Board Mass Exhaust Emissions Monitoring System With NOx, CO<sub>2</sub> And Qualitative PM Capabilities", SAE Paper 2001-01-3641, Society of Automotive Engineers, 2001.
9. Travis B. Manchur. "Accuracy Of On-Board Vehicle Emission Measurements", Master of Science Thesis, Department of Mechanical Engineering, University of Alberta, 2005.
10. Ernest O. Doebelin. "Measurement Systems Application And Design", Fourth Edition, Page 37-94. Department of Mechanical Engineering, The Ohio State University.
11. "Mechanical Measurements" Course Notes, Department of Mechanical Engineering, University of Alberta. September 1, 2002.

## CHAPTER 4

### Experimental Measurement of On-Road CO<sub>2</sub> Emission And Fuel Consumption Functions

*Motorized transport has become an essential part of our world economic system with an ever-increasing number of vehicles on the road. However, considering the depletion of energy resources and the aggravation of greenhouse gas issues, it is critical to improve vehicle fuel consumption. These demands are moving us toward advanced engine and powertrain technologies. However, understanding our progress also requires improvements in the way we measure and certify vehicle emissions and fuel economy performance.*

*This chapter describes the use of an on-board fuel consumption and emissions measurement system to develop on-road fuel consumption functions that can be used to quantify the fuel economy impact of vehicle, road and traffic control changes. The system uses an ECM OBD-II scanner, a Mass Air Flow meter and an emissions analyzer to monitor fuel and exhaust CO<sub>2</sub> mass flow rate (in g/s) as well as vehicle speed and other parameters. All measurements are coordinated and recorded using a laptop computer. Vehicle tractive power is calculated from speed measurements using vehicle dynamic models, allowing calculation of actual fuel efficiency. In the results, the measured CO<sub>2</sub> emission values correlate well with those predicted by a carbon balance from measured fuel consumption, confirming the validity of a range of measurements.*

*Chapter 4 reports on fuel consumption behaviors for five typical vehicles over seventy repeated tests in urban, highway and aggressive driving situations. Although it is well known that vehicle energy demand goes up with increasing steady speed, the results show the strong importance of fuel efficiency, vehicle accelerations and idle periods on actual on-road fuel consumption. Fuel efficiency is essentially zero at idle but rises to a high level for vehicle tractive power over 30% of the rated power. This trend indicates the potential for reduced fuel consumption through engine down-sizing and powertrain controls. For vehicles running in normal traffic situations, the fuel consumption tends to be best in the 60 km/h to 100 km/h average speed range due to the reduced severity of accelerations and lack of idling. Those results emphasize the potential for fuel savings through improvements of road structure and traffic control to reduce congestion. The test results are used to generate a fuel consumption model based on a vehicle dynamic model data and speed trace. This model can be used to quantify the fuel consumption and greenhouse gas CO<sub>2</sub> emission effect for changes in vehicle structure and on-road operating conditions.*

*This chapter is based on a technical paper submitted for publication to SAE World Congress & Exhibition 2007.*

## 4.0 INTRODUCTION

Automotive tailpipe emissions are the major source of air pollution in most urban areas. <sup>[1]</sup> Besides controlling criteria emissions, (CO, HC, NO<sub>x</sub>), reducing CO<sub>2</sub> as a green house gas is a critical world target with some countries planning to implement regulatory measures. CO<sub>2</sub> cannot be eliminated by practical exhaust after-treatment systems so the only practical approach to reducing CO<sub>2</sub> is to lower fuel consumption. <sup>[2]</sup> Fuel consumption ranks with car performance as a highly valued feature in the eyes of prospective car buyers. However, there is significant uncertainty in actual in-use fuel consumption with significant differences in actual consumption between same-model vehicles on the road and significant differences from the certification tests. Making progress on the critical demands to reduce vehicle fuel consumption and tailpipe CO<sub>2</sub> emissions not only requires advanced engine technology, but also requires improvements in the way we measure and certify vehicle emissions and fuel economy performance. <sup>[3]</sup>

On-board fuel consumption and emissions measurement is widely recognized as a desirable approach for quantifying emissions from vehicles since data is collected under real-world conditions at any location traveled by the vehicle. <sup>[4]</sup> Currently, various portable emission measurement equipment and OBD II port scanners have been developed and provide the capability to measure and record multiple vehicle operating parameters simultaneously with emissions. <sup>[5]</sup> This chapter describes the use of an on-board & in-use measurement system capable of measuring the vehicle mass emission rates and fuel consumption rate as well as vehicle speed, mass air flow rate and other operating parameters. To better understand actual fuel consumption and CO<sub>2</sub> emission, seventy repeated tests were conducted using five typical vehicle types. The objective was to generate a basic model to be capable of evaluating the fuel consumption and CO<sub>2</sub> emission of typical gasoline vehicles as a function of vehicle power demand while operating in typical traffic situations.

## 4.1 EXPERIMENTAL CONFIGURATION

Figure 4-1 provides a schematic of the emission analyzers, sensors and data acquisition system used as an on-board & in-use measurement system. Vehicle speed, operating parameters and mass flow rate (g/s) of fuel and exhaust emissions (NO<sub>x</sub>, CO, CO<sub>2</sub>, HC, O<sub>2</sub>) were all measured using an ECM OBD-II scanner (Autotap), a Mass Air Flow sensor (Siemens), and two emissions analyzers (Horiba and Vetronix) with the rated resolution and accuracy values shown in Table 4-1. All measurements were coordinated and recorded using a Dell laptop computer. The raw experimental data files were processed by a dedicated MATLAB program to calculate the vehicle power, mass emission rate, fuel consumption rate and other parameters of interest, as illustrated in more detail by Appendix A and Appendix B. Hereinafter, the equipment details will be expounded.

**VETRONIX FIVE-GAS ANALYZER:** The PXA-1100, a self-contained device which operates from vehicle electrical power (12v), is a portable, light weight (13 lbs) diagnostic exhaust gas analyzer. It is equipped with quick connect hoses, which include one sampling line, two exhaust lines and one drainage line with a check valve. A flexible probe assembly at the end of the sampling hose is designed to insert into the vehicle tailpipe and secured by a chain during road tests. The emission samples are pumped into the Five-Gas Analyzer by a built-in vacuum pump. The mole fraction of Hydrocarbon (as hexane, HC), Carbon Monoxide (CO), Carbon Dioxide (CO<sub>2</sub>), Oxygen (O<sub>2</sub>) and Oxides of Nitrogen (NO<sub>x</sub>) are measured and displayed on screen as well as being transmitted to the computer via a RS-232 serial link. These emission gases are analyzed by two different methods: non-dispersive infrared (NDIR) for HC, CO and CO<sub>2</sub> composition and two electro-chemical detectors for O<sub>2</sub> and NO<sub>x</sub> detection. The gas analyzer takes approximately 15 minutes from the time it is powered up for the internal, infrared gas detectors and sample chamber to complete the warm-up cycle. One of the start-up steps is a 'Zero Gas Data' step where the gas analyzer adjusts its readings to zero using a sample of ambient air. Therefore, it is

critical to locate the analyzer in a place with a supply of ventilated fresh air. To ensure measurement accuracy, the PXA-1100 was calibrated every two weeks using a premixed blend. <sup>[5][6]</sup>

**Table 4-1 Instrument Specification**

Value	Range	Resolution	Sensitivity	Accuracy (Rated)
5 Gas HC	0-20,000 ppm	1 ppm	N/A	5% of reading
5 Gas CO	0-10%	0.01%	N/A	5% of reading
5 Gas CO <sub>2</sub>	0-20%	0.10%	N/A	5% of reading
5 Gas O <sub>2</sub>	0-25%	0.01%	N/A	5% of reading
5 Gas NO <sub>x</sub>	0-4000 ppm	1 ppm	N/A	32 ppm at 0-1000 ppm 60 ppm at 1001-2000 ppm 120 ppm at 2001-4000 ppm
Horiba NO <sub>x</sub>	0-3000 ppm	1 ppm	N/A	30 ppm at 0-1000 ppm 3% at 1001-2000 ppm 5% at 2001-3000 ppm
Horiba A/F	3.99-500	0.01 A/F	N/A	0.35 A/F at 9.5-Stoich 0.15 A/F at Stoich 0.40 A/F at Stoich-20.00 A/F 0.90 A/F at 20.01-30.00 A/F 1.70 A/F at 30.01-40.00 A/F 2.60 A/F at 40.01-50.00 A/F 3.70 A/F at 50.01-60.00 A/F 0.5 vol% O <sub>2</sub> at >=60.01 A/F
Siemens HFM 62B	2-153 g/s	27.72 mg/s	22.72 (g/s) / V	1.0 g/s
AD 590	-55 -- 150 °C	0.12 °C	1000 °C / V	0.5 °C

**HORIBA MEXA-720 NO<sub>x</sub> ANALYZER:** The Mexa-720 NO<sub>x</sub> analyzer is a light weight (1 kg), compact (130×75×200 mm), multi-function portable Oxides of Nitrogen (NO<sub>x</sub>) emissions analyzer with zirconia-ceramic sensor. The single unit provides fast-response measurements of both Oxides of Nitrogen (NO<sub>x</sub>) and Oxygen (O<sub>2</sub>) as well as giving Air/Fuel Ratio (AFR) and Excess Air Ratio ( $\lambda$ ). The sensor was directly inserted into the vehicle exhaust flow using an exhaust gas oxygen sensor fitting added downstream of the catalytic converter. This location minimizes measurement time delays due to dead-volume sampling. The Mexa-720 NO<sub>x</sub> analyzer operated on vehicle electrical power (12v) and needed approximately three minutes warm-up time. The NO<sub>x</sub> concentration and AFR were read and recorded directly by

the data acquisition system. A monthly four-point calibration, (Zero, Middle, Span, High NO<sub>x</sub>) was conducted.

ECM OBD-II PORT SCANNER: An Auto Tap OBD-II Diagnostic Scanner was used to read the ECM sensor data, (which is available in real-time from all 1996 and later vehicles complying with OBD-II requirements). Operating parameters such as vehicle speed, engine speed, coolant temperature, intake air temperature, etc could be displayed in table, graph, meter or gauge visual displays as well as being transmitted via USB connection to the Dell laptop computer for recording.

MASS AIR FLOW METER: Vehicle intake air consumption was measured by a Siemens HFM 62B MAF meter manually mounted in the vehicle air system of each vehicle. This MAF meter is a compact, light weight (160g) device operating on the vehicle electrical power (12v). The MAF was allowed to warm up for 15 minutes prior to road testing and covered a 2 g/s to 153 g/s range with an analog voltage output. To ensure accuracy and stability, the MAF was calibrated every three months. The calibration was accomplished by measuring the flow drawn through an ASME standard nozzle as described in SAE standard J244.

TEMPERATURE SENSOR: Ambient temperature was measured with an AD590 integrated-circuit temperature transducer fastened to the vehicle radio antenna. The AD590 was powered by the vehicle electrical power (12v) and produces a linear current output ( $1 \mu A / K$ ) over the range  $-55^{\circ}C$  to  $150^{\circ}C$ . The calibration curve was developed with a three-point calibration conducted every three months. The voltage-to- $^{\circ}C$  calculation was achieved by the data acquisition program.

DATA ACQUISITION SYSTEM: The data acquisition system included a Dell Inspiron-1100 laptop computer, a National Instruments AL-16E-4 PCMCIA data acquisition card and two Labview 6i programs. The DAQ Card is capable of monitoring eight differential channels of analog input with twelve bit resolution and selectable gains of 1, 2, 5, 10, 20, 50 and 100. The data acquisition card collected data from HFM 62B MAF meter, AD590 ambient temperature sensor and Horiba Mexa-720

NOx. Labview 6i program codes are written to process the analog inputs from the data acquisition card as well as to communicate with PXA-1100 gas analyzer via RS-232 interface cable. The data acquisition system is able to read and record all instantaneous data from the measurement equipment into the Dell laptop computer. [5] All experimental data are recorded after the user manually composes the recorded files names for each program and triggers the record buttons. After conducting the experiments, the user needs to record the weather conditions, test routes number and start time as references for the later research analysis.

The whole system weighing 17 kg (38 lbs) is installed in a designed steel case to be quite convenient for the operator to carry from vehicle to vehicle. This on-board & in-use emission measurement system is capable of being installed easily on a wide variety of vehicles, being used during the regular everyday duty of the vehicle. Since the light-weight system can be belted on the passenger seat and the emission sampling hose is secured along the vehicle body, the measurement system does not pose a real or perceived danger to the vehicle drivers, passengers or the general public. [7]

**Table 4-2 Vehicle Features**

Vehicle Type	LDGV	LDGV	LDGV	LDGT2	LDGT3
Vehicle Model	Audi Quattro	Pontiac Vibe	Chevrolet Cavalier	Chevrolet Silverado	GMC Savana
Vehicle Symbol	LDGVA	LDGVV	LDGVC	LDGTSP	LDGTSV
Model Year	1999	2004	1997	1999	2001
Odometer Reading	101,000 km	22,700 km	129,600 km	122,000 km	442,300 km
Engine & ECM Maker	Audi, Germany	Toyota, Japan	Chevrolet, USA	Chevrolet, USA	GMC, USA
Engine Type / Size	1.8 L L4 AWD	1.8 L L4 FWD	2.2 L L4 FWD	5.4 L V8 4WD	5.7 L V8 RWD
Supply OBDII Port Data	Yes	Yes	Yes	Yes	Yes
Real Weight During Test	1557 kg	1407 kg	1357 kg	2360 kg	2690 kg

## 4.2 TEST VEHICLES

Five typical mid-life vehicles of model year 1997 to 2004 were used for these tests. As listed in Table 4-2, these vehicles included three passenger cars, one light duty pickup truck and one cargo van. Engine displacement varied from 1.8 L to 5.7 L with four automatic transmissions and one manual transmission. Vehicle odometer reading varied

from 22,000 to 442,000 km. All vehicles were in “normal” operating conditions with no diagnostic trouble codes or obvious faults. The vehicle classes represented by these vehicles represent a significant fraction of the on-road fleet.

In order to minimize the extra engine load from the accessories, the radio/CD player and air conditioner were turned off, but the ventilation fan was set at the lowest level during experimental tests on every vehicle.

### **4.3 DRIVING ROUTES**

Six urban routes were selected in Edmonton city, each of which is similar to FTP 75 urban driving cycle consisting of one fraction of the congested stop-start urban roads including one way, one lane each way, two lanes each way, and two fractions of relatively high-speed suburban roads. Those routes have an average distance of 16 km with an average vehicle speed of 30 km/h, maximum vehicle speed of around 80 km/h and a duration of 27 minutes. An example of vehicle speed trace and the four driving modals distribution for the experimental test is shown in Figure 4-2. The graph shows that there are 23 stops and frequent accelerations. 65% of the driving time is used on acceleration and deceleration, and idle time occupies almost one quarter of the total driving time. The definitions of idle, acceleration, deceleration and cruise modals are listed in Table 4-3.

Two routes were chosen along the Whitemud Freeway at the south of Edmonton city to simulate the aggressive driving behaviors represented by the EPA US06 driving cycle. The driving distance was about 10 km with an average vehicle speed of 80 km/h, designed maximum vehicle speed of 130 km/h, maximum acceleration of  $3.0 \text{ m/s}^2$  and a duration of 11 minutes driving time. However, not every experimental test had that high maximum vehicle speed due to the limitation of the real-world traffic conditions. Figure 4-3 shows one typical experimental test conducted on the designed route. It is notable to detect that about 70% of the driving time was spent on the accelerations and decelerations.

**Table 4-3** Definitions of The Four Modal Analysis Variables

	Modal Name	Definition
1	Idle	$V \leq 3 \text{ km/h}$ and $ a  \leq 0.1 \text{ m/s}^2$
2	Acceleration	$a > 0.1 \text{ m/s}^2$
3	Deceleration	$a < -0.1 \text{ m/s}^2$
4	Cruise	$V > 3 \text{ km/h}$ and $ a  \leq 0.1 \text{ m/s}^2$

Two routes were chosen along the Highway 2 between Edmonton city and Leduc city to simulate the Highway Fuel Economy test cycle. The driving distance is about 20 km with an average vehicle speed of 80 km/h, maximum speed of 100 km/h and a duration of 13 minutes. The vehicle speed trace and the driving modals distribution of an experimental test are shown in Figure 4-4. In contrast to the urban route tests and the high-acceleration, high-speed aggressive driving tests, the vehicle spent more than 50% of the total time on cruise.

## 4.4 RESULTS AND DISCUSSIONS

The basic direct measurement test results consist of time traces of exhaust concentration ( $\text{NO}_x$ ,  $\text{CO}$ ,  $\text{CO}_2$ ,  $\text{HC}$ ,  $\text{O}_2$ ), vehicle speed, intake mass air flow rate, air fuel ratio and ambient temperature. The basic calculated test results include the time traces of vehicle acceleration, tractive power calculated using a vehicle dynamic model, <sup>[8]</sup> mass flow rates for tailpipe emissions, and fuel consumption rate calculated by MAF and AFR (APPENDIX B).

### 4.4.1 FUEL EFFICIENCY ANALYSIS

The vehicle fuel efficiency is measured as vehicle tractive work divided by fuel energy consumed (LHV basis) expressed by Equation 1. The lower heating value of Iso-Octane ( $\text{C}_8\text{H}_{18}$ ) obtained from reference <sup>[9]</sup> is used for the efficiency calculation.

$$\begin{aligned}
 \text{Efficiency} &= \frac{\text{Vehicle Work (kJ)}}{\text{Energy Released From Fuel Consumed (kJ)}} \times 100\% \\
 &= \frac{\text{Vehicle Power (kW)}}{\text{Fuel Consumption Rate (g/s)} \times \text{LHV (kJ/g)}} \times 100\% \quad [1]
 \end{aligned}$$

Figure 4-5 shows the relationship between vehicle fuel efficiency and tractive power. Fuel efficiency is inherently zero at idle but increases rapidly to reach a plateau value when tractive power is above 20-30% of the rated vehicle peak power. The plateau efficiency value varied: about 33% for the Chevrolet Silverado and the newest automatic transmission car, 32% for the AWD manual transmission car, 30% for the oldest FWD car and only 25% for the very high mileage GMC Savana van. Considering ideal Otto cycle efficiency and the fact that these are post-drivetrain efficiency values, the in-use efficiency values are quite impressive. However, as also shown in Figure 4-5, it was notable that, for typical driving conditions as represented by these tests, the vehicles spent 60% of their time at less than 10% of rated power and 82% at less than 20% of rated power. Hence, average in-use fuel efficiency was typically much lower than the maximum plateau values.

By further examining the vehicle fuel efficiency data, it can be found that the fuel efficiency starts dropping slightly when the vehicle power is over 50% of the rated power. Normally, the higher vehicle tractive power is associated with higher engine speed. Theoretically, the rich mixture combustion increases the specific fuel consumption and decreases the fuel efficiency. Since there is a limitation of the real-world driving conditions, the further fuel efficiency trend cannot be interpreted clearly only using the present experimental data.

Another way of looking at vehicle fuel consumption is to consider the relationship between tractive energy demand, fuel consumption and average vehicle speed as shown for these test vehicles in Figures 4-6 to 4-10. The graphs show that the average vehicle energy demand is typically high (due to accelerations) at low road speed and rises again (due to aerodynamic drag) at high test road speed. The minimum energy demand is

generally in the 60 to 80 km/hr average speed range. Reflecting the energy demand, vehicles moving at low road speed typically have high fuel consumption because they are using high power to accelerate and /or they are running at low power and low efficiency. Vehicles moving at very high speed have high fuel consumption due to higher aerodynamic drag. The optimum speed for low fuel consumption generally falls in the 60 to 100 km/h vehicle average speed range. This presents an interesting challenge for traffic management since it is difficult to maintain such high average speeds without using massive traffic infrastructure (freeways). However, vehicle fuel consumption is typically about three times higher when average vehicle speed is reduced to typical traffic speeds on the order of 20 km/h show in Figure 4-6 to 4-10.

#### 4.4.2 FUEL ECONOMY COMPARISON AMONG THE DIFFERENT TESTING PATTERNS

A significant share of customers will take the vehicle fuel economy (L/100km or MPG) into account for their next automobile purchase. With the increasing competition in the automotive industry, the fuel economy is becoming one of the most important sale points for the vehicle manufacturers. However, the rated fuel economy by the manufacturer is developed from the dynamometer test through the designed driving cycles (Urban Cycle & Highway Cycle) under the standard conditions (such as 20°C). Fuel economy will change with the different ambient temperature, air humidity, traffic conditions and the different driving behaviors. Figure 4-11 shows the in-use tested fuel economies of all vehicles driving at three different patterns. Vehicles driving on the highway have good fuel economy, because the vehicle average speed is between 80 km/h and 100 km/h which is located in the low fuel consumption range indicated in Figure 4-6 to 4-10, and there is no idle time during the trip. The vehicles have worse fuel economy while driving on the US06 simulation routes with over 120 km/h maximum speed and more than 2.5 m/s<sup>2</sup> acceleration described in Figure 4-3. However, the fuel economy is still better than the urban tests fuel economy due to high average vehicle speed and the quite small fraction of the idle time (less than 5%). With about one quarter of the total driving time at idle and the low average speed, the vehicles have the worst fuel

economy while driving on the urban routes. The value of the fuel economy is proportional to the vehicle engine displacement shown in Figure 4-11, and the reason could be that the vehicle with bigger engine size usually has the higher weight and higher rated power, which tends to be compensated by consuming more fuel.

#### 4.4.3 RELATIONSHIP BETWEEN CO<sub>2</sub> EMISSION AND FUEL CONSUMPTION

Carbon dioxide (CO<sub>2</sub>) and water vapor are the major products of hydrocarbon combustion. These two gases are normal atmospheric constituents and are considered non-toxic, but CO<sub>2</sub> is one of the basic greenhouse gases which have significant influence upon warming the earth climate. In addition to the criteria emissions (CO, HC, NO<sub>x</sub>), the significant contribution of CO<sub>2</sub> from the internal combustion engine is drawing great attention all over the world. Because CO<sub>2</sub> cannot be reduced by an exhaust after-treatment system, reduction of fuel consumption from cars is an effective method for CO<sub>2</sub> emission abatement. <sup>[10]</sup> This section focuses on analyzing the relationship between CO<sub>2</sub> emission rate and the fuel consumption rate and creating a general relationship function for all light duty gasoline vehicles.

Based on the experimental test results, it is not hard to find that the CO<sub>2</sub> emission and fuel consumption are strongly correlated in different driving patterns which indicates that there is a great potential to calculate the CO<sub>2</sub> emission from the fuel consumption value. Figure 4-12 illustrates three typical tests of Urban, Highway and US06 simulation cycle respectively. Three linear fit lines almost overlap together, but there is a slight difference. From the different slopes of the straight lines, it can be stated that the vehicle produces the CO<sub>2</sub> emission at most from the Highway tests and at least from the US06 tests when the vehicle has the same fuel consumption rate. While driving on the highway, the vehicle's ECM tends to let the engine run at a slightly fuel lean mixture (the AFR is larger than the Stoichiometric AFR) to increase the fuel efficiency due to less acceleration and deceleration period. The extra air helps the engine to produce more final combustion products (CO<sub>2</sub> & H<sub>2</sub>O) and less intermediate products (HC, CO). In contrast, the vehicle engine runs at a fuel rich mixture (the AFR

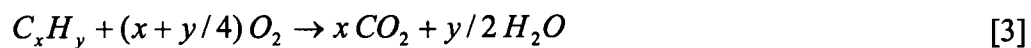
is less than the Stoichiometric AFR) at a great large fraction of time during the aggressive driving tests. Therefore, the vehicle produces less CO<sub>2</sub> and more HC/CO as expected. When operating on the urban routes, the engine runs at fuel rich, stoichiometric, fuel lean mixtures alternatively, so the CO<sub>2</sub> emission from the urban routes test is between those of the Highway test and the US06 test.

It is more realistic that the vehicle is driven under the mixed driving patterns during a longer period time, not only driven on the highway or on the urban roads. Therefore, it is necessary to average all driving patterns' data and produce one function for the vehicle to get the relationship between the CO<sub>2</sub> emission rate and fuel consumption rate shown in Figure 4-12. Using the same method, the other four vehicles are examined and similar CO<sub>2</sub> emission rate functions are developed as illustrated in Figure 4-13. With further averaging, these five functions are then summarized into one general CO<sub>2</sub> emission function for the whole light duty gasoline vehicles. Because the CO<sub>2</sub> emission and the fuel consumption are measured or calculated at the same time trace, the general function in Figure 4-13 can be integrated to produce the cumulative CO<sub>2</sub> emission function expressed by the following equation:

$$CCO_2 = 3.07 CFC \quad [2]$$

*CCO<sub>2</sub>* : Cumulative CO<sub>2</sub> Emission [g]

*CFC* : Cumulative Fuel Consumption [g]



Theoretically, the full combustion process can be expressed as Equation 3 if all carbon of gasoline is assumed to transfer into CO<sub>2</sub>. Therefore, the ratio of CO<sub>2</sub> emission against fuel consumption can be calculated as follow:

$$\frac{CO_2 (mass)}{C_xH_y (mass)} = \frac{44x}{12x + y} = \frac{44}{12 + y/x}$$

From the experimental results analysis, the average hydrogen-to-carbon ratio ( $y/x$ ) of fuel consumed by the vehicles is 1.96, which can be determined by balancing the typical gasoline combustion equation illustrated in Appendix B. The mass emission of  $\text{CO}_2$  is then 3.15 times of fuel consumed under the theoretical assumption. However, the real experimental result of 3.07 is 2.5% less than the ideal value. This may be caused by the small fraction of CO and HC in any tailpipe exhaust emissions. Hence, Equation 2 is reasonably accurate to link the greenhouse gas  $\text{CO}_2$  with fuel consumption for the light duty gasoline vehicles.

#### 4.4.4 FUEL CONSUMPTION FUNCTION DEVELOPMENT

Having analyzed the influences on the fuel efficiency and the fuel economy from the vehicle speeds and the driving patterns, it only supplies the general knowledge of lowering the fuel consumption strategies, but does not provide enough information about how to link the instantaneous fuel consumption rate with the vehicle performance (such as vehicle power) at the same time. This section explores a method to calculate and predict the fuel consumption as well as mass emission of  $\text{CO}_2$  from the other known or estimated parameters instead of using MAF and AFR.

The top graph in Figure 4-14 shows the instantaneous fuel consumption rate (g/s) and vehicle speed time traces. When the vehicle speed increases from zero to 50 km/h (point A) rapidly, the fuel flow rate increases from 0.5 g/s to 3.8 g/s in the same time interval. However, when the vehicle speed increases from 17 km/h to 75 km/h (point B), the fuel flow rate only increases from 0.6 g/s to 2 g/s because the slope of the speed time trace of this section is noticeably lower than that of the previous acceleration section. Another typical acceleration section in the same truncated test plot shows that the fuel flow rate only increases 0.5 g/s when the vehicle is slowly accelerated from 45 km/h to 65 km/h (point C). After calculating the acceleration and the vehicle power, the bottom graph in the same figure can be developed, which clearly indicates that fuel flow rate is proportional to the acceleration and the vehicle power rather than the vehicle speed.

The fuel consumption and tractive power traces can be integrated to give cumulative fuel consumption and cumulative vehicle work. The vehicle power-based fuel consumption factor (g/kW.h) is then the slope of a plot of fuel consumption against vehicle tractive work as shown in Figure 4-15. The intercept value between the solid line and the Y-axis can be determined by the initial idle fuel consumption rate (g/s) multiplied by initial idle time (s). All five vehicles' idle fuel flow rates (both cold-start and warmed-up) were measured and the average values were calculated. Figure 4-16 shows that the idle fuel flow rates in both cases could be correlated well with engine displacement. The cold-start idle fuel flow rates of the vehicle with 5.4 L engine displacement are three times higher than that of the vehicle with 1.8 L engine displacement. However, the difference of the idle fuel flow rates between these two cases is much lower after the engine warmed-up.

The vehicle power-based fuel consumption factor (g/kW.h) of each vehicle could also be compared with vehicle positive tractive power as shown in Figure 4-17. All vehicles shared a similar trend of specific fuel consumption falling from an infinite level for zero tractive power towards a realistic value (around 400 g/kW.h) at some low tractive power level. The high-mileage GMC Savana clearly stood out as having higher relative fuel consumption than the rest of the vehicles which clustered reasonably close together. This confirmed that some feature of the van, (probably the transmission) was significantly hurting its tractive efficiency. This GMC Savana van does not represent the other vehicles in the same class, but does exist in the real world. For the other four vehicles, the fuel consumption trend curved over towards a stable, lower value once tractive power exceeded approximately 20 kW. In this presentation, it is clear the AWD car (Audi Quattro) had a slightly higher fuel consumption function than the average while the newest FWD car (Pontiac Vibe) had the lowest specific fuel consumption function. The best values of measured fuel consumption factors approached 200 g/kW.h which is an impressive level for spark ignition engines considering that this is an at-the-wheel value.

Further attempts need to be made to combine the fuel consumption results for the four light duty spark ignition vehicles since the high-mileage GMC Savana should not contribute much on the average specific fuel consumption. Twenty-five evenly spaced points between 0 and 50 kW vehicle power were taken from the power fits shown in Figure 4-17 for Audi Quattro, Pontiac Vibe, Chevrolet Cavalier and Chevrolet Silverado respectively. An unbiased average trend function can be developed by power fitting the total one hundred sampled points for all four vehicles illustrated in Figure 4-18. The difference between the vehicle original fuel consumption factor value and the average trend value is shown in Figure 4-19. Just for the comparison purpose, the high-mileage GMC Savana fuel consumption rates are also summarized, and the real value is 67% higher than the average value with a highest Standard Deviation of 16%. However, the real fuel consumption factor for Chevrolet Cavalier and Chevrolet Silverado is very close to the average trend with no more than 3% of the difference. Operating the fuel rich mixture condition at most of time, Audi Quattro produces higher vehicle power based specific fuel consumption rates than the average values after the vehicle power is over 10 kW. The average difference between the real values of Audi Quattro and the average values is +11%. On the other hand, the newest Pontiac Vibe produces lower specific fuel consumption rates than the average trend after the vehicle power is over 5 kW, and the average difference is about -10%. By considering the complex traffic conditions and the weather conditions in the real world, the Equation 4 is fairly accurate to represent the four tested vehicles as well as a significant fraction of the on road fleet.

$$FCF = 150 + \exp(-0.857 \ln(P) + 7.356) \quad [4]$$

*FCF* : Fuel Consumption Factor [g/kW.h]  
*P* : Vehicle Power [kW]

From the idle fuel flow functions, the general fuel consumption factor against vehicle power function (Equation 4) and CO<sub>2</sub> emission function (Equation 2), a basic model can be established for these four vehicles by supplying or estimating a few vehicle operation parameters, such as the driving time, vehicle speed trace, etc. The major

benefit for this basic model is to make it possible to predict the cumulative fuel consumption (g) and the greenhouse gas CO<sub>2</sub> emission (g) for the vehicles similar to those tested without using the complicated fuel consumption and tailpipe emission measurement system.

#### 4.5 MODELING RESULTS VALIDATION

For comparative purposes, Table 4-4 lists the experimental results and modeling results of four cases for three light duty passenger cars and one light duty gasoline pickup truck. It clearly indicates that the modeling fuel consumption and CO<sub>2</sub> emission are lower than those of the experimental results for Audi Quattro and Chevrolet Silverado. In contrast, for the Pontiac Vibe, the modeling values of the fuel consumption and CO<sub>2</sub> emission are over predicted comparing with the experimental results. With less mile age (22,700 km), newer transmission/transaxle system and newer TPS, EGR, IMP sensors, it is reasonable for the Pontiac Vibe to produce less CO<sub>2</sub> emission than the smoothed out modeling results. The modeling fuel consumption value for Chevrolet Cavalier is impressively accurate comparing with the experimental data with only 1.4% error. Every modeling value listed in Table 4-4 is fully compliant with the way to develop the general fuel consumption function demonstrated previously.

**Table 4-4** Comparison Between the Experiment Results and Modeling Results

Vehicle Type	Sample Case	Driving Distance	Experimental Fuel Consumption	Modeling Fuel Consumption	Fuel Consumption Error	Experimental CO <sub>2</sub>	Modeling CO <sub>2</sub>	CO <sub>2</sub> Error
LDGVA	Case 1	12.75 km	999 g	902 g	-9.7%	3024 g	2769 g	-8.4%
LDGVV	Case 2	13.24 km	880 g	931 g	5.8%	2760 g	2858 g	3.6%
LDGVC	Case 3	11.89 km	811 g	823 g	1.4%	2383 g	2527 g	6.0%
LDGTSP	Case 4	20.84 km	2005 g	1881 g	-6.2%	6066 g	5775 g	-4.8%

The average errors between the modeling results and the experimental values for the four typical vehicles are less than 10%, which indicates the established fuel consumption and CO<sub>2</sub> emission model has sufficient accuracy to examine the tested

vehicles' fuel consumption and CO<sub>2</sub> emission. There is also a great potential to evaluate the cumulative fuel consumption and CO<sub>2</sub> emission for other vehicles within the same classes using this basic model.

## 4.6 CONCLUSION

This chapter has examined the capability of an on-board & in-use measurement system to measure the fuel consumption and CO<sub>2</sub> emission for five vehicles while in real service. The test results show that the vehicles have high fuel efficiency when operating in the 60 km/h to 100 km/h average speed range or when the vehicle tractive power is over 30% of rated peak power. The distance-based fuel consumption (in g/km) increases most significantly when operating at an average vehicle speed below 40 km/h because of increased idling and acceleration-related fuel consumption. Vehicles generally have low vehicle energy demand and low fuel consumption rate when operating around 80 km/h average speed. Those experimental results emphasize the potential for fuel savings and the green house gas emission reductions through improvements of road structure and traffic control to reduce congestion.

A basic cumulative fuel consumption and greenhouse gas CO<sub>2</sub> mass emission prediction model was established by developing a general vehicle power-based fuel consumption function, two idle fuel flow rate functions and one CO<sub>2</sub> emission function from seventy repeated experimental tests using five typical vehicles conducted under three different driving patterns. Comparison with the experimental data shows that the model is sufficiently accurate for examining real-world fuel consumption of vehicles similar to those tested and for use as a reference for general behavior of light duty gasoline vehicles.

## **4.7 FUTURE WORK**

Beyond fuel consumption, this portable in-use measurement system is capable of quantifying tailpipe criteria pollutant emissions (HC, CO and NO<sub>x</sub>) in real service. Development of comprehensive real-world toxic emission factors and modeling analysis is an on-going and future task.

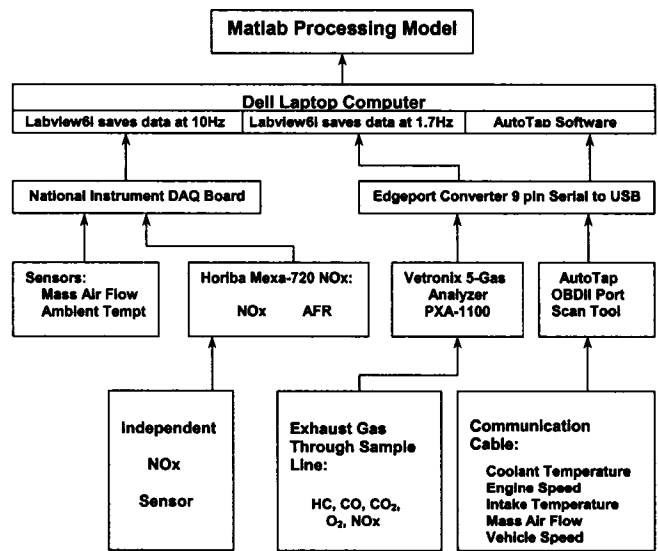


**Figure 4-1** Schematic of Test Instruments and Calculations

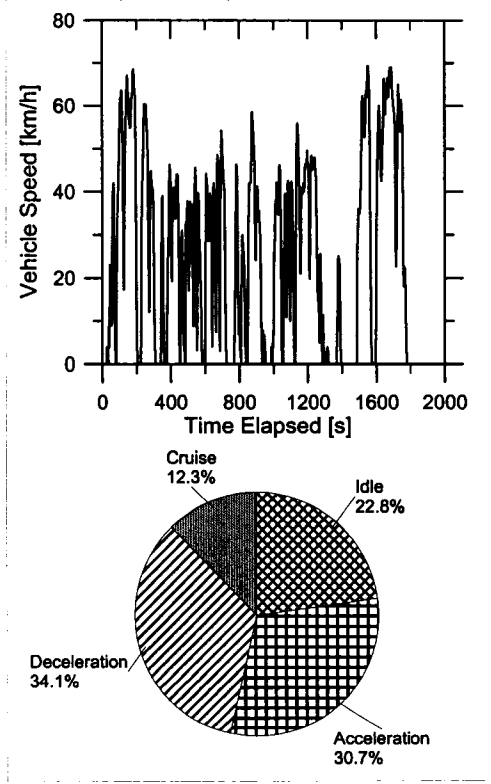


**Figure 4-2** Urban Test Route Speed Trace and Modal Fraction (Using 2004 Pontiac Vibe)

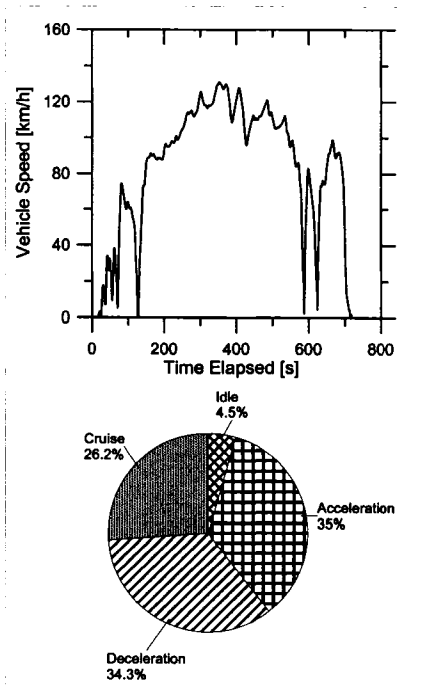


**Figure 4-3** US06 Test Route Speed Trace and Modal Fraction  
(Using 2001 GMC Savana)

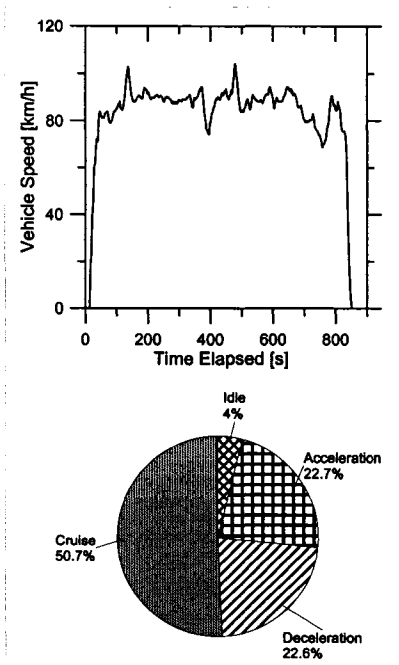


**Figure 4-4** Highway Test Route Speed Trace and Modal Fraction  
(Using 1999 Audi Quattro)

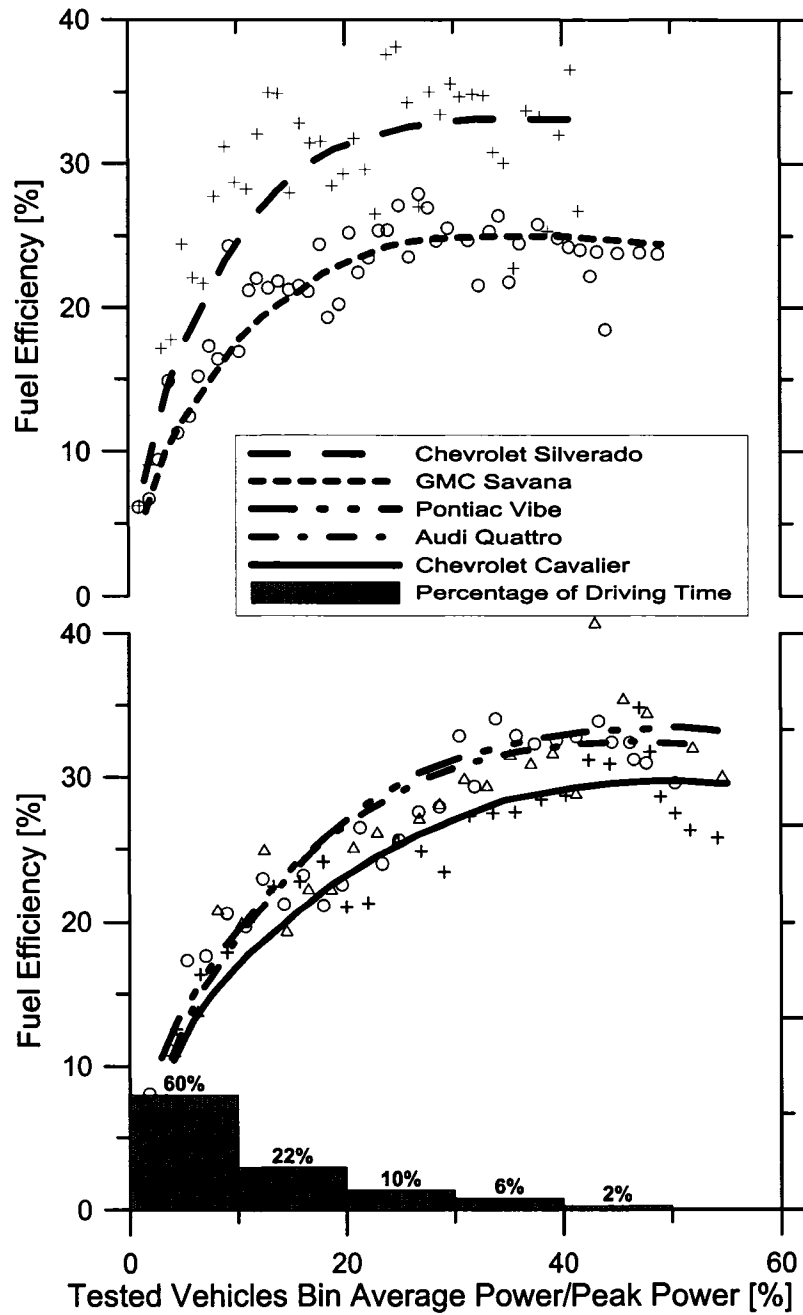
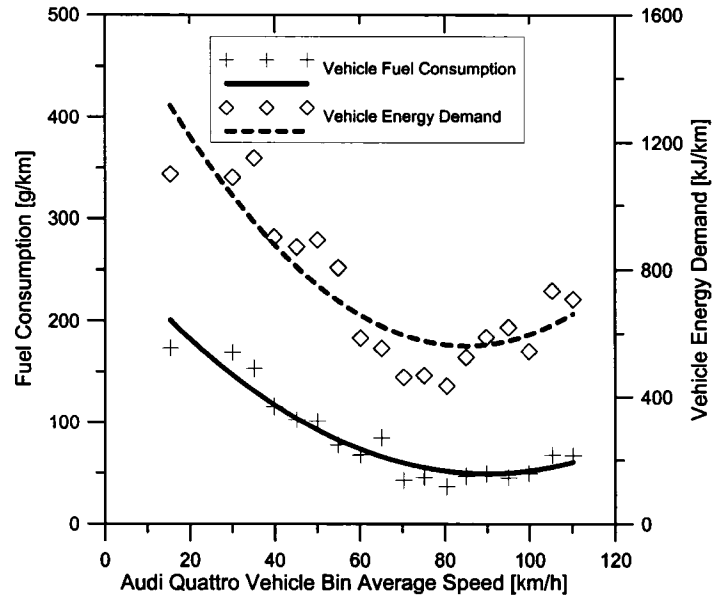
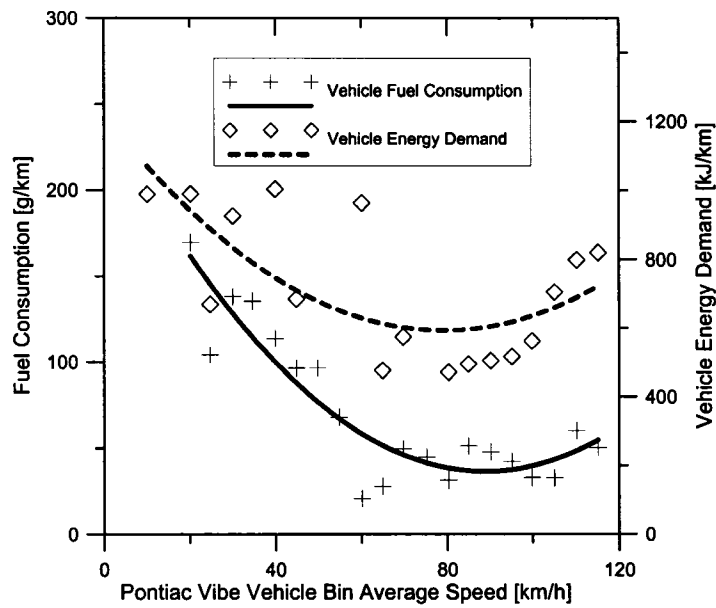


Figure 4-5 Vehicle Fuel Efficiency and Tractive Power



**Figure 4-6** Fuel Consumption and Tractive Energy: Audi Quattro



**Figure 4-7** Fuel Consumption and Tractive Energy: Pontiac Vibe

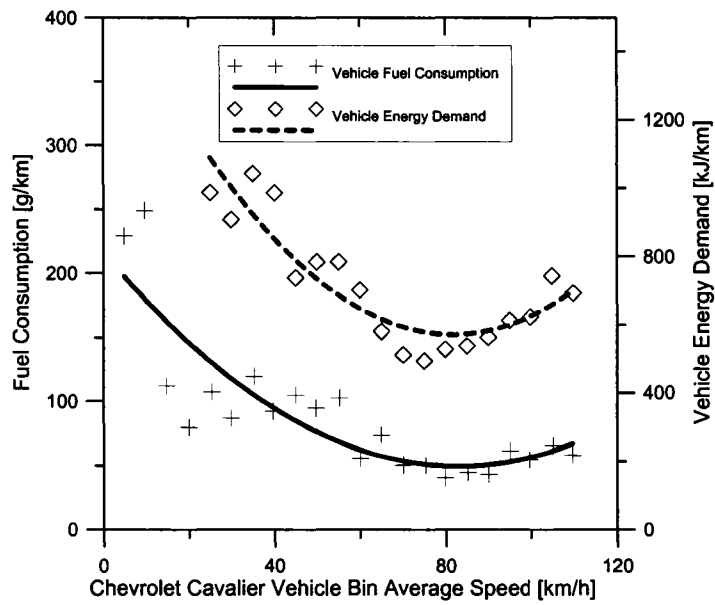


**Figure 4-8** Fuel Consumption and Tractive Energy: Chevrolet Cavalier

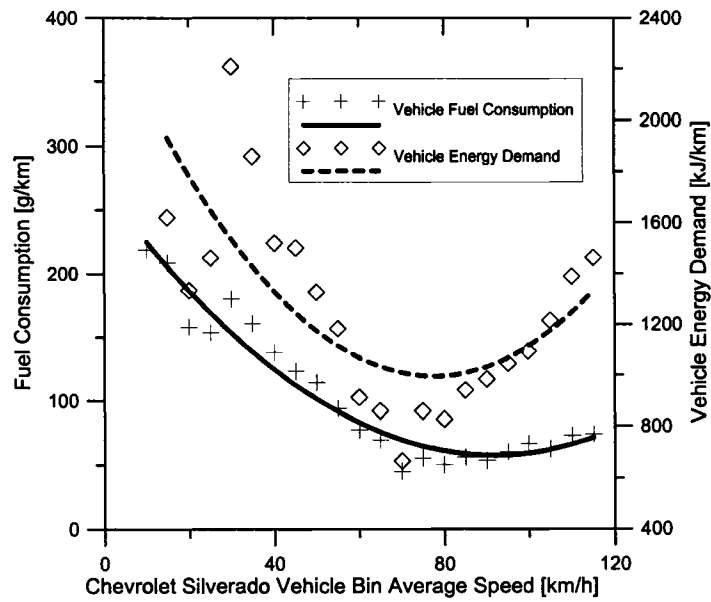


**Figure 4-9** Fuel Consumption and Tractive Energy: Chevrolet Silverado

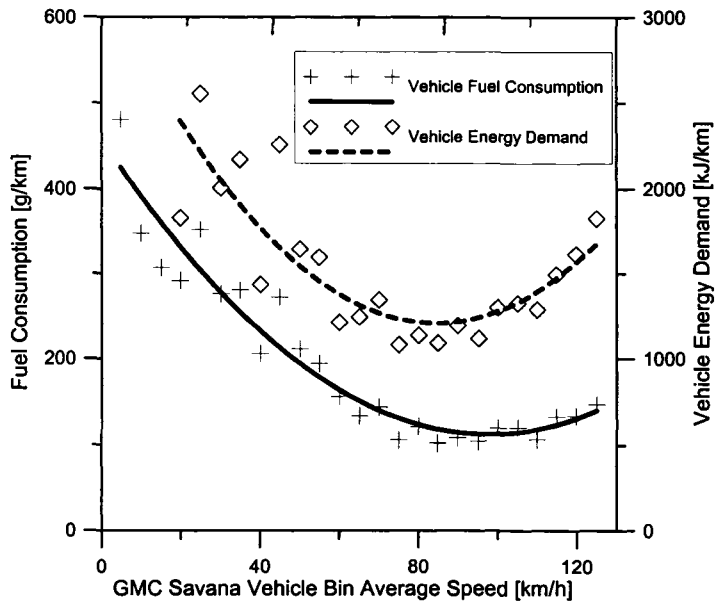


**Figure 4-10** Fuel Consumption and Tractive Energy: GMC Savana

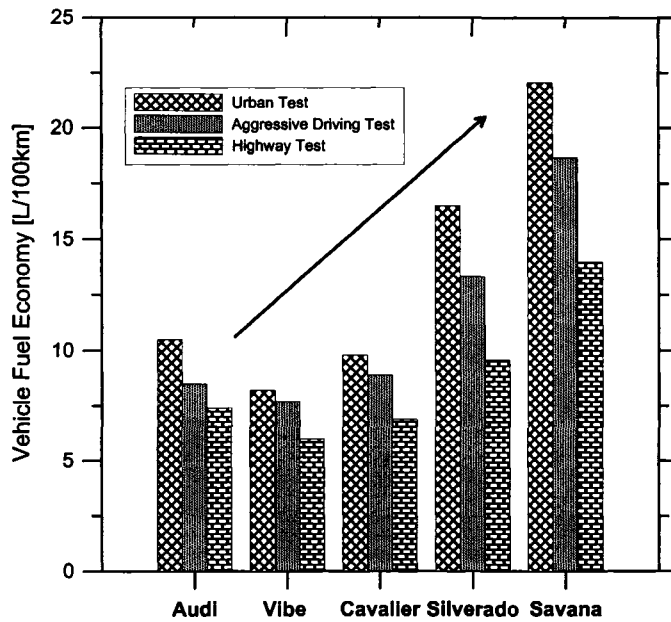


**Figure 4-11** Vehicle Fuel Economies Comparison to Three Driving Patterns

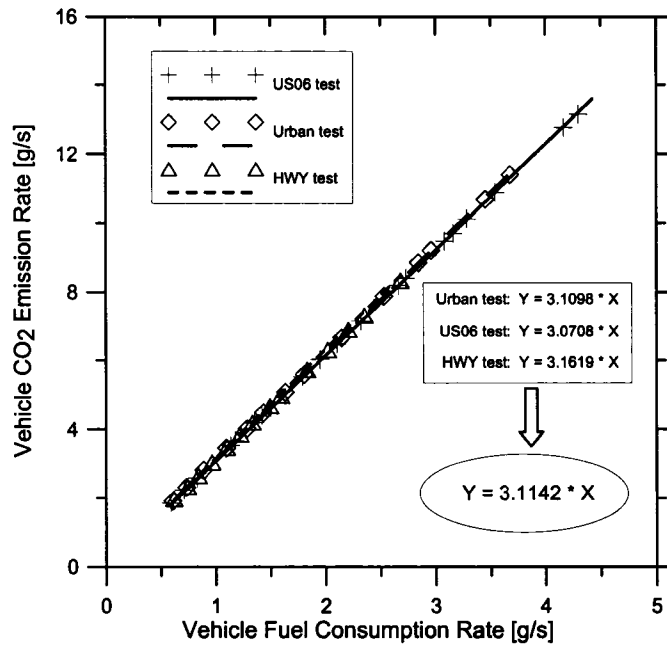


**Figure 4-12** Relationship Between Instantaneous CO<sub>2</sub> and Fuel Consumption of Chevrolet Silverado

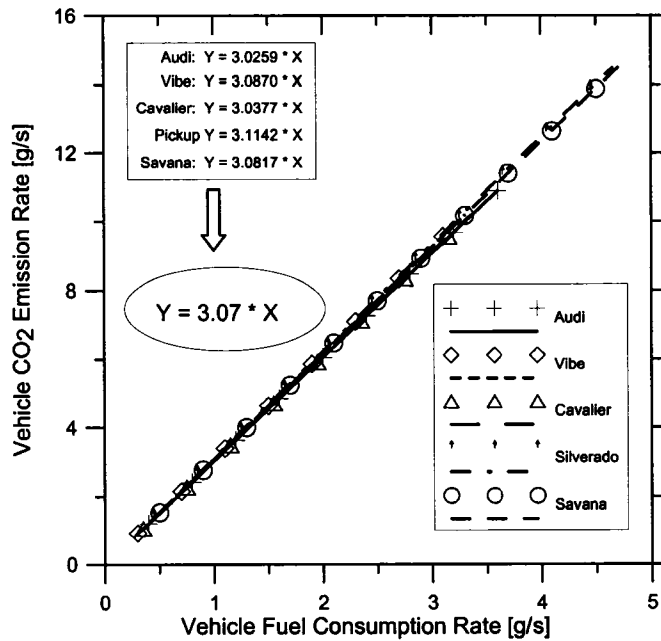


**Figure 4-13** General Relationship Function Between CO<sub>2</sub> and Fuel Consumption

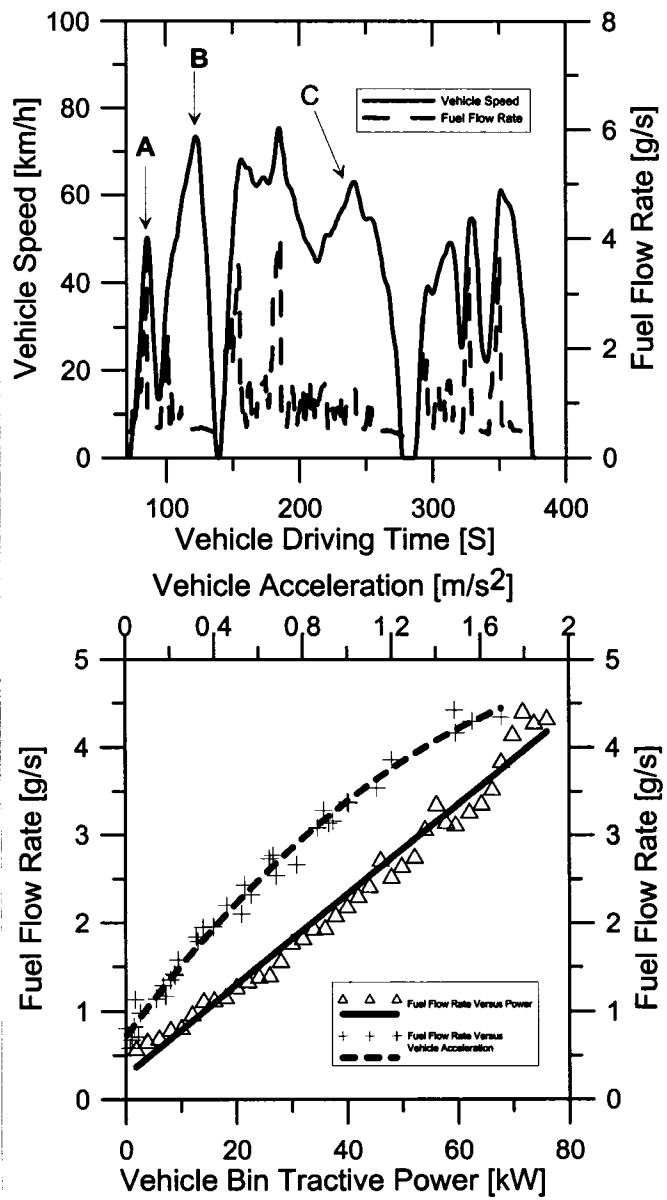
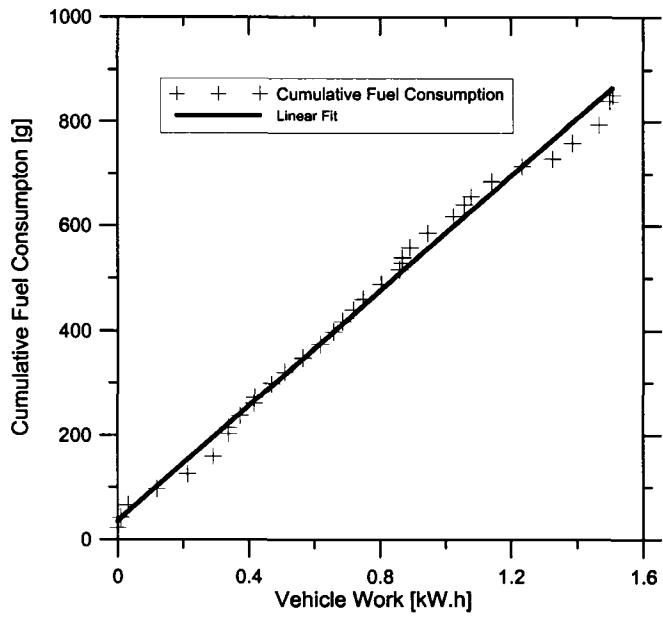
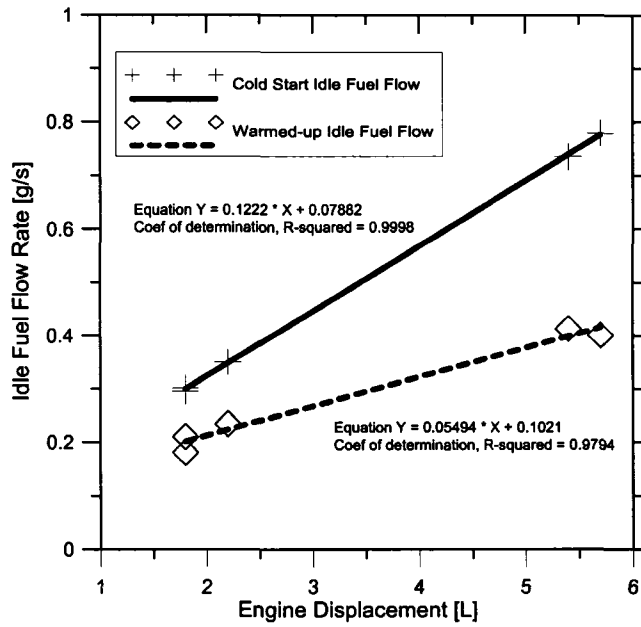


Figure 4-14 Vehicle Speed and Fuel Flow Rate Time Trace



**Figure 4-15** Cumulative Fuel Consumption Trend Against Vehicle Work  
(Using Pontiac Vibe)



**Figure 4-16** Vehicle Idle Fuel Flow Rate

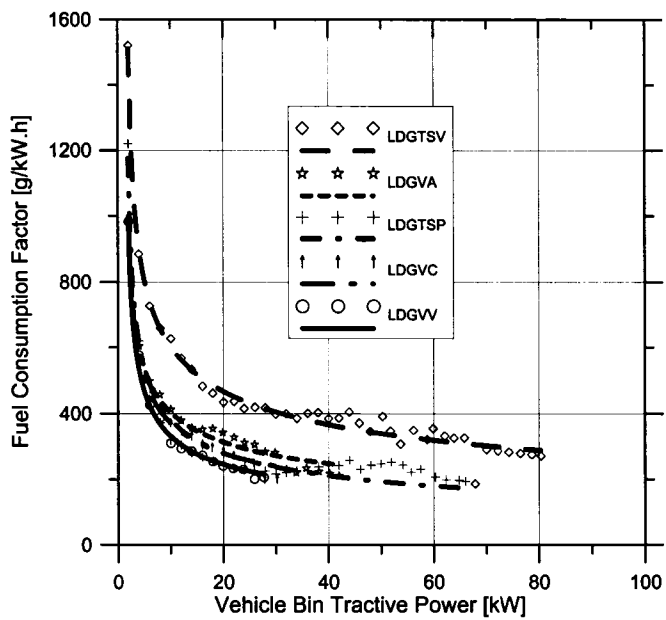


**Figure 4-17** Relationships Between Vehicle Fuel Consumption Factor and Power  
(Refer Table 4-2 for vehicle symbol)

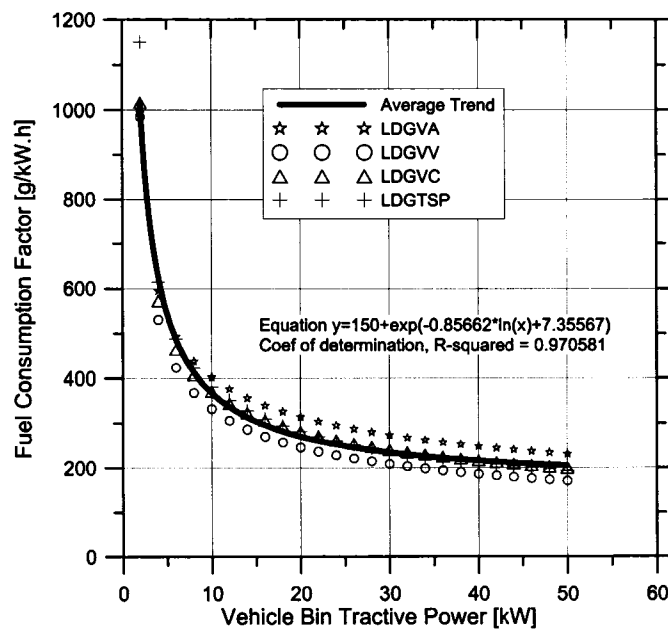


**Figure 4-18** General Fuel Consumption Function  
(Refer Table 4-2 for vehicle symbol)

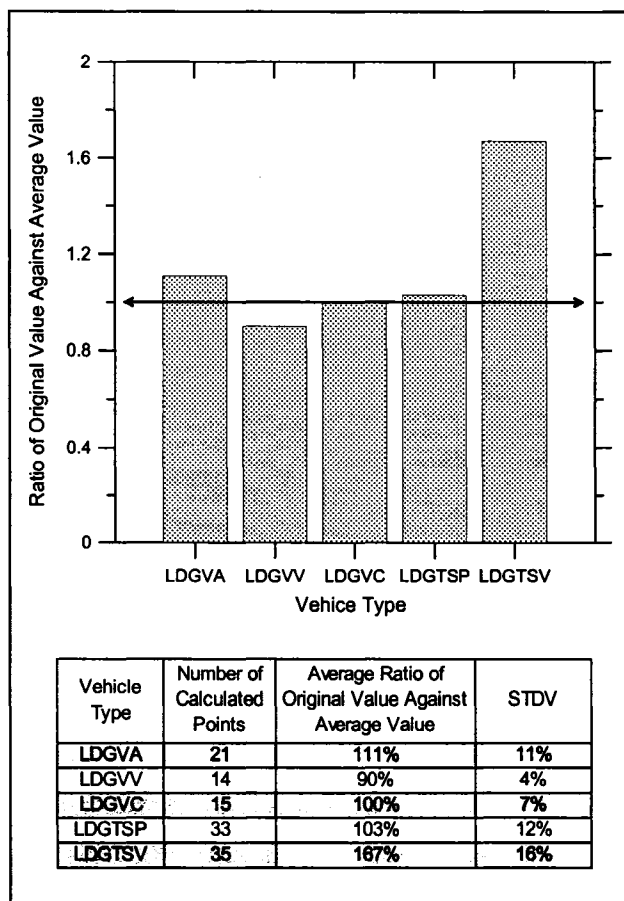


**Figure 4-19** Average Ratio of Vehicle Original Value against Average Trend Value

## REFERENCES

1. Jason D. Hawirko; M.David Checkel. "Quantifying Vehicle Emission Factors for Various Ambient Conditions using an On-Road, Real-Time Emissions System", SAE Paper 2003-01-0301, Society of Automotive Engineers, 2003.
2. Kurt Engeljehringer. "Trends of Future Emission Legislation and its Measurement Requirements", SAE Paper 2004-01-3291, Society of Automotive Engineers, 2004.
3. Fuel Consumption Test Notes #15 – FVMS2000, Integrated Measurement & Control. <http://www.imc-berlin.de>
4. H. Christopher Frey, Nagui M. Roupail, A. Unal, and James D. Colyar. "Measurement of On-Road Tailpipe CO, NO, and Hydrocarbon Emissions Using a Portable Instrument", In proceedings, Annual Meeting of the Air & Waste Management Association, June 24-28, 2001, held in Orlando, Florida, and published by A & WMA, Pittsburgh, PA.
5. Jason D. Hawirko; M. David Checkel. "Real-Time, On-Road Measurement of Driving Behavior, Engine Parameters and Exhaust Emissions", SAE Paper 2002-01-1714, Society of Automotive Engineers, 2002.
6. PXA-1100 Gas Analyzer Operator's Manual, Vetronix Corporation. Printed in USA, July 1996.
7. Michal Vojtisek-Lom, Joseph E. Allsop. "Development Of Heavy-Duty Diesel Portable, On-Board Mass Exhaust Emissions Monitoring System With NO<sub>x</sub>, CO<sub>2</sub> And Qualitative PM Capabilities", SAE Paper 2001-01-3641, Society of Automotive Engineers, 2001.
8. Andy D. B. Yates and Samson Mkwanzazi. "Methodology for Determining Octane Response at Different Altitudes for Vehicles Equipped with Knock Sensors", SAE Paper 2002-01-1663, Society of Automotive Engineers, 2002.
9. Stephen R. Turns. "An Introduction to Combustion", Second Edition.
10. Wojciech Gis and Piotr Bielaczyc. "Emission of CO<sub>2</sub> and Fuel Consumption for Automotive Vehicles", SAE Paper 1999-01-1074, Society of Automotive Engineers, 1999.

## CHAPTER 5

### **Emission Factors Analysis For Multiple Vehicles Using an On-Board And In-Use Emissions Measurement System**

*Despite more stringent emission regulations implemented in recent years, vehicle tailpipe emissions are still the major source of air pollution problems in most urban areas. To control and reduce the toxic emissions (HC, CO and NO<sub>x</sub>), it is critical to understand in-use emissions as well as to implement further emission standards. At present, the emission factors are mainly studied and determined by traditional chassis dynamometer methods. However concerns have been raised about the extent to which emissions produced by on-road vehicles can be predicted using emission factors developed from the standard test procedures.*

*This Chapter demonstrates the use of an on-board, in-use vehicle emissions measurement system capable of measuring tailpipe emission rates while the vehicle is in real service experiencing complex traffic conditions, driver behavior and weather conditions. The instantaneous mass flow rate (g/s) of fuel and five typical emission gases (NO<sub>x</sub>, HC, CO, CO<sub>2</sub>, O<sub>2</sub>) in addition to vehicle operation parameters (mass air flow rate, vehicle speed, engine speed, ambient temperature, coolant temperature, etc) are measured using an ECM OBD-II scanner, a Mass Air Flow meter and two emissions analyzers. All measurements are coordinated and recorded using a laptop computer. At only 38 lbs in weight, the measurement system is adapted for easy transition from vehicle to vehicle while providing minimal impact on vehicle operation.*

*Chapter 5 presents an analysis of vehicle emission factors based on multiple on-road tests with five typical mid-life vehicles in urban, highway and aggressive driving situations. Emission factors for HC, CO and NO<sub>x</sub> developed from sixty repeated tests are expressed in terms of g/kW.h, g/km and g/kgFuel. The tailpipe emission factors expressed as g/kW.h and g/km are strongly correlated with vehicle tractive power and vehicle speed respectively. However, emission factors expressed in terms of g/kgFuel are relatively independent of vehicle power and speed. Based on these emission functions and the vehicle idle emission rate measurements, an in-use emission model can be established for use in estimating tailpipe cumulative emissions for vehicles experiencing real-world driving conditions with significant differences from the standard test sequences.*

*This chapter is based on a technical paper submitted for publication to SAE World Congress & Exhibition 2007.*

## 5.0 INTRODUCTION

Carbon monoxide, hydrocarbons and oxides of nitrogen are common toxic gases released from most on-road vehicles, and vehicles are known to be the major source of urban air pollution, contributing significantly to urban environmental and public health problems. <sup>[1][2][3]</sup> To understand and control the air pollution problems, accurate emission measurement should be developed and accurate emission inventories are needed. <sup>[4][5]</sup>

Currently, vehicle emission factors are mainly determined from traditional chassis dynamometer tests carried out in the lab under strictly controlled, repeatable conditions, complying with the legislated driving cycles. <sup>[6]</sup> The standard driving cycles such as EPA FTP75, EPA HWFET, European NEDC cycle and Japanese 10-15 cycle were designed and utilized to simulate the stop-start urban driving conditions and sustained vehicle speed highway driving conditions. <sup>[7][8]</sup> MOBILE6, a popular emission inventory prediction program developed by U.S. EPA, estimates emissions of hydrocarbons, carbon monoxide, and oxides of nitrogen for cities or regions using a travel-based emission factor expressing emissions in grams per kilometer (g/km). With emission factors developed for 28 different vehicle classes, the total emission inventory is calculated as the number of cars of different classes multiplied by the appropriate vehicle driving distances. <sup>[5][9]</sup> However, concerns have been raised about whether emission factors developed from the standard test procedures truly represent emissions associated with real-world driving. <sup>[10]</sup>

Since 1990, high-quality portable vehicle emission measurement equipment have become available which significantly contributes to development of in-use vehicle emission measurement systems capable of measuring the mass emissions from the on-road vehicles experiencing various weather conditions, wide range of vehicle power demands and complex traffic influences. <sup>[3-6][10-22]</sup> This chapter introduces an on-board emission measurement system that can be easily and quickly installed on multiple light

duty gasoline vehicles while in the regular everyday duty, and illustrates a comprehensive analysis for three in-use emission factors expressed in term of g/kW.h, g/km and g/kgFuel for HC, CO and NOx developed from sixty repeated tests using five typical mid-life vehicles in urban, highway and aggressive driving situations. The goal is not only to demonstrate the capability of this on-board & in-use emissions measurement system to measure the real time instantaneous emissions, but also introduce the method to build a basic in-use emissions estimation model using the vehicle power based emission functions which can be referenced to examine further more vehicles.

**Table 5-1 Instrument Specification**

Value	Range	Resolution	Sensitivity	Accuracy (Rated)
5 Gas HC	0-20,000 ppm	1 ppm	N/A	5% of reading
5 Gas CO	0-10%	0.01%	N/A	5% of reading
5 Gas CO <sub>2</sub>	0-20%	0.10%	N/A	5% of reading
5 Gas O <sub>2</sub>	0-25%	0.01%	N/A	5% of reading
5 Gas NOx	0-4000 ppm	1 ppm	N/A	32 ppm at 0-1000 ppm 60 ppm at 1001-2000 ppm 120 ppm at 2001-4000 ppm
Horiba NOx	0-3000 ppm	1 ppm	N/A	30 ppm at 0-1000 ppm 3% at 1001-2000 ppm 5% at 2001-3000 ppm
Horiba A/F	3.99-500	0.01 A/F	N/A	0.35 A/F at 9.5-Stoich 0.15 A/F at Stoich 0.40 A/F at Stoich-20.00 A/F 0.90 A/F at 20.01-30.00 A/F 1.70 A/F at 30.01-40.00 A/F 2.60 A/F at 40.01-50.00 A/F 3.70 A/F at 50.01-60.00 A/F 0.5 vol% O <sub>2</sub> at >=60.01 A/F
Siemens HFM 62B	2-153 g/s	27.72 mg/s	22.72 (g/s) / V	1.0 g/s
AD 590	-55 - 150 °C	0.12 °C	1000 °C / V	0.5 °C

## 5.1 EXPERIMENTAL CONFIGURATION

Figure 5-1 provides a schematic of the emission analyzers, sensors and data acquisition system used as an on-board & in-use measurement system. Vehicle speed, operating

parameters and mass flow rate (g/s) of fuel and exhaust emissions (NO<sub>x</sub>, CO, CO<sub>2</sub>, HC, O<sub>2</sub>) were all measured using an ECM OBD-II scanner (Autotap), a Mass Air Flow sensor (Siemens), and two emissions analyzers (Horiba and Vetronix) with the rated resolution and accuracy values shown in Table 5-1. All measurements were coordinated and recorded using a Dell laptop computer. The raw experimental data files were processed by a dedicated MATLAB program to calculate the vehicle power, mass emission rate, fuel consumption rate and other parameters of interest, as illustrated in more detail by Appendix A and Appendix B. Hereinafter, the equipment details will be expounded.

VETRONIX FIVE-GAS ANALYZER: The PXA-1100, a self-contained device which operates from vehicle electrical power (12v), is a portable, light weight (13 lbs) diagnostic exhaust gas analyzer. It is equipped with quick connect hoses, which include one sampling line, two exhaust lines and one drainage line with a check valve. A flexible probe assembly at the end of the sampling hose is designed to insert into the vehicle tailpipe and secured by a chain during road tests. The emission samples are pumped into the Five-Gas Analyzer by a built-in vacuum pump. The mole fraction of Hydrocarbon (as hexane, HC), Carbon Monoxide (CO), Carbon Dioxide (CO<sub>2</sub>), Oxygen (O<sub>2</sub>) and Oxides of Nitrogen (NO<sub>x</sub>) are measured and displayed on screen as well as being transmitted to the computer via a RS-232 serial link. These emission gases are analyzed by two different methods: non-dispersive infrared (NDIR) for HC, CO and CO<sub>2</sub> composition and two electro-chemical detectors for O<sub>2</sub> and NO<sub>x</sub> detection. The gas analyzer takes approximately 15 minutes from the time it is powered up for the internal, infrared gas detectors and sample chamber to complete the warm-up cycle. One of the start-up steps is a 'Zero Gas Data' step where the gas analyzer adjusts its readings to zero using a sample of ambient air. Therefore, it is critical to locate the analyzer in a place with a supply of ventilated fresh air. To ensure measurement accuracy, the PXA-1100 was calibrated every two weeks using a premixed blend. <sup>[4][23]</sup>

HORIBA MEXA-720 NO<sub>x</sub> ANALYZER: The Mexa-720 NO<sub>x</sub> analyzer is a light weight (1 kg), compact (130×75×200 mm), multi-function portable Oxides of Nitrogen (NO<sub>x</sub>) emissions analyzer with zirconia-ceramic sensor. The single unit provides fast-response measurements of both Oxides of Nitrogen (NO<sub>x</sub>) and Oxygen (O<sub>2</sub>) as well as giving Air/Fuel Ratio (AFR) and Excess Air Ratio ( $\lambda$ ). The sensor was directly inserted into the vehicle exhaust flow using an exhaust gas oxygen sensor fitting added downstream of the catalytic converter. This location minimizes measurement time delays due to dead-volume sampling. The Mexa-720 NO<sub>x</sub> analyzer operated on vehicle electrical power (12v) and needed approximately three minutes warm-up time. The NO<sub>x</sub> concentration and AFR were read and recorded directly by the data acquisition system. A monthly four-point calibration, (Zero, Middle, Span, High NO<sub>x</sub>) was conducted.

ECM OBD-II PORT SCANNER: An Auto Tap OBD-II Diagnostic Scanner was used to read the ECM sensor data, (which is available in real-time from all 1996 and later vehicles complying with OBD-II requirements). Operating parameters such as vehicle speed, engine speed, coolant temperature, intake air temperature, etc could be displayed in table, graph, meter or gauge visual displays as well as being transmitted via USB connection to the Dell laptop computer for recording.

MASS AIR FLOW METER: Vehicle intake air consumption was measured by a Siemens HFM 62B MAF meter manually mounted in the vehicle air system of each vehicle. This MAF meter is a compact, light weight (160g) device operating on the vehicle electrical power (12v). The MAF was allowed to warm up for 15 minutes prior to road testing and covered a 2 g/s to 153 g/s range with an analog voltage output. To ensure accuracy and stability, the MAF was calibrated every three months. The calibration was accomplished by measuring the flow drawn through an ASME standard nozzle as described in SAE standard J244.

TEMPERATURE SENSOR: Ambient temperature was measured with an AD590 integrated-circuit temperature transducer fastened to the vehicle radio antenna. The AD590 was powered by the vehicle electrical power (12v) and produces a linear current output ( $1 \mu A / K$ ) over the range  $-55^{\circ}C$  to  $150^{\circ}C$ . The calibration curve was developed with a three-point calibration conducted every three months. The voltage-to- $^{\circ}C$  calculation was achieved by the data acquisition program.

DATA ACQUISITION SYSTEM: The data acquisition system included a Dell Inspiron-1100 laptop computer, a National Instruments AL-16E-4 PCMCIA data acquisition card and two Labview 6i programs. The DAQ Card is capable of monitoring eight differential channels of analog input with twelve bit resolution and selectable gains of 1, 2, 5, 10, 20, 50 and 100. The data acquisition card collected data from HFM 62B MAF meter, AD590 ambient temperature sensor and Horiba Mexa-720 NOx. Labview 6i program codes are written to process the analog inputs from the data acquisition card as well as to communicate with PXA-1100 gas analyzer via RS-232 interface cable. The data acquisition system is able to read and record all instantaneous data from the measurement equipment into the Dell laptop computer [5]. All experimental data are recorded after the user manually composes the recorded files names for each program and triggers the record buttons. After conducting the experiments, the user needs to record the weather conditions, test routes number and start time as references for the later research analysis.

The whole system weighing 17 kg (38 lbs) is installed in a designed steel case to be quite convenient for the operator to carry from vehicle to vehicle. This on-board & in-use emission measurement system is capable of being installed easily on a wide variety of vehicles, being used during the regular everyday duty of the vehicle. Since the light weight system can be belted on the passenger seat and the emission sampling hose is secured along the vehicle body, the measurement system does not pose a real or perceived danger to the vehicle drivers, passengers or the general public. [22]

## 5.2 TEST VEHICLES

Five typical mid-life vehicles of model year 1997 to 2004 were used for these tests. As listed in Table 5-2, these vehicles included three passenger cars, one light duty pickup truck and one cargo van. Engine displacement varied from 1.8 L to 5.7 L with four automatic transmissions and one manual transmission. Vehicle odometer reading varied from 22,000 to 442,000 km. All vehicles were in “normal” operating conditions with no diagnostic trouble codes or obvious faults. The vehicle classes represented by these vehicles represent a significant fraction of the on-road fleet.

In order to minimize the extra engine load from the accessories, the radio/CD player and air conditioner were turned off, but the ventilation fan was set at the lowest level during experimental tests on every vehicle.

**Table 5-2 Vehicle Features**

Vehicle Type	LDGV	LDGV	LDGV	LDGT2	LDGT3
Vehicle Model	Audi Quattro	Pontiac Vibe	Chevrolet Cavalier	Chevrolet Silverado	GMC Savana
Vehicle Symbol	LDGVA	LDGVV	LDGVC	LDGTSP	LDGTSV
Model Year	1999	2004	1997	1999	2001
Odometer Reading	101,000 km	22,700 km	129,600 km	122,000 km	442,300 km
Engine & ECM Maker	Audi, Germany	Toyota, Japan	Chevrolet, USA	Chevrolet, USA	GMC, USA
Engine Type / Size	1.8 L L4 AWD	1.8 L L4 FWD	2.2 L L4 FWD	5.4 L V8 4WD	5.7 L V8 RWD
Supply OBDII Port Data	Yes	Yes	Yes	Yes	Yes
Real Weight During Test	1557 kg	1407 kg	1357 kg	2360 kg	2690 kg

## 5.3 DRIVING ROUTES

Six urban routes were selected in Edmonton city, each of which is similar to FTP 75 urban driving cycle consisting of one fraction of the congested stop-start urban roads including one way, one lane each way, two lanes each way, and two fractions of relatively high-speed suburban roads. Those routes have an average distance of 16 km with an average vehicle speed of 30 km/h, maximum vehicle speed of around 80 km/h and a duration of 27 minutes. An example of vehicle speed trace and the four driving

modals distribution of experimental test is shown in Figure 5-2. The graph shows that there are 23 stops and frequent accelerations. 65% of the driving time is used on acceleration and deceleration, and idle time occupies almost one quarter of the total driving time. The definitions of idle, acceleration, deceleration and cruise modals are listed in Table 5-3.

**Table 5-3** Definitions of The Four Modal Analysis Variables

	Modal Name	Definition
1	Idle	$V \leq 3 \text{ km/h}$ and $ a  \leq 0.1 \text{ m/s}^2$
2	Acceleration	$a > 0.1 \text{ m/s}^2$
3	Deceleration	$a < -0.1 \text{ m/s}^2$
4	Cruise	$V > 3 \text{ km/h}$ and $ a  \leq 0.1 \text{ m/s}^2$

Two routes were chosen along the Whitemud Freeway at the south of Edmonton city to simulate the aggressive driving behaviors represented by the EPA US06 driving cycle. The driving distance was about 10 km with an average vehicle speed of 80 km/h, designed maximum vehicle speed of 130 km/h, maximum acceleration of  $3.0 \text{ m/s}^2$  and a duration of 11 minutes driving time. However, not every experimental test had that high maximum vehicle speed due to the limitation of the real-world traffic conditions. Figure 5-3 shows one typical experimental test conducted on the designed route. It is quite easy to detect that about 70% of the driving time was spent on the accelerations and decelerations.

Two routes were chosen along the Highway 2 between Edmonton city and Leduc city to simulate the Highway Fuel Economy test cycle. The driving distance is about 20 km with an average vehicle speed of 80 km/h, maximum speed of 100 km/h and a duration of 13 minutes. The vehicle speed trace and the driving modals distribution of an experimental test are shown in Figure 5-4. In contrast to the urban route tests and the high-acceleration, high-speed aggressive driving tests, the vehicle spent more than 50% of the total time on cruise.

## 5.4 RESULTS AND ANALYSIS

The basic direct measurement test results consist of time traces of exhaust molar concentration (NO<sub>x</sub>, CO, CO<sub>2</sub>, HC, O<sub>2</sub>), vehicle speed, intake mass air flow rate, air fuel ratio and ambient temperature. The basic calculated test results include the time traces of vehicle acceleration, tractive power calculated using a vehicle dynamic model (Appendix A), mass flow rates for tailpipe emissions (Appendix B), and fuel consumption rate calculated by MAF and AFR.

### 5.4.1 INSTANTANEOUS EMISSION TRACES

One typical experimental test is chosen to demonstrate the instantaneous mass emission rates of HC, CO, CO<sub>2</sub>, O<sub>2</sub> and NO<sub>x</sub> shown in Figure 5-5. The test lasted about 30 minutes with a cold start and the driving distance was 22 km. The emission trace shows a significant rise in CO emission rate between 0s and 200s which indicates the loss of emission control before the catalyst light-off. Over this period, the average CO mass emission rate is 0.153 g/s and the peak value is 1.6 g/s. From 200s to the end of the test, the CO emission rate drops sharply and stabilizes at quite low value with 0.00906 g/s average rate. The CO average emission rate of the pre-catalyst light-off is seventeen times higher than that of the post-catalyst light-off. The same scenario can be found in HC and NO<sub>x</sub> mass emission rate traces. HC emission rate averages 0.0041 g/s and reaches 0.012 g/s peak value at the pre-catalyst light-off region and averages 0.00023 g/s at post-catalyst light-off region. It is surprising to detect that the HC emission rate is near zero at most time after 700s drive which indicates the catalyst is very efficient to reduce the HC emission. On the other hand, the vehicle runs at the lean mixture after the engine totally warmed-up because relatively higher O<sub>2</sub> emission from the tailpipe can be observed in Figure 5-5. NO<sub>x</sub> emission rate averages 0.0049 g/s and reaches 0.040 g/s at the pre-catalyst light-off region and averages 0.00092 g/s at post-catalyst light-off region. By further study the NO<sub>x</sub> emission at post-catalyst light-off region, it is easy to tell that the NO<sub>x</sub> emission is not stable and there are still a lot of peak values of 0.020 g/s. As mentioned previously, the vehicle runs at the lean mixture condition

and tends to produce more NO<sub>x</sub>, another reason probably is that the catalyst is less efficient to minimize the NO<sub>x</sub> emission. In contrast to the distinctive emission rates of HC, CO, NO<sub>x</sub> at two situations, closer examination of O<sub>2</sub> and CO<sub>2</sub> mass emission rate traces shows that there is no obvious difference between the pre-catalyst light-off and the post-catalyst light-off regions. From this case, it should be stated that this on-board & in-use emission measurement system has ability to capture the vehicle emissions on a second by second basis.

#### 5.4.2 CUMULATIVE EMISSIONS

Basically, the toxic emissions from the vehicle tailpipe drawing the most air pollution concerns in the urban city are CO, HC and NO<sub>x</sub> varying a lot with different vehicle power demand or the efficiency of exhaust after treatment system. This chapter will focus on the comprehensive CO, HC and NO<sub>x</sub> emission factors development.

The instantaneous emissions of HC, CO and NO<sub>x</sub> can be integrated to give the cumulate emissions. Figure 5-6 shows the cumulative emissions of HC, CO and NO<sub>x</sub> against the total driving distance respectively. All of the curves show a similar pattern where cold starts have a higher slope during the engine open loop operation followed by a short transition period. The curves then stabilize at a lower slope after full catalyst light-off. The slope of these three cumulative mass emission curves represent the emission factors in unit of g/km. The intercept values on each curve measure the mass of pollutant emitted from the tailpipe during the cold start and the initial idle period. The initial value of HC, CO and NO<sub>x</sub> are 0.33 g, 14.6 g and 0.041 g respectively. To clarify the pre-catalyst light-off region and the post-catalyst light-off region, an example of HC emission trend is highlighted in the bottom graph of the Figure 5-6. The steep initial slope of the cold start occurred before 0.7 km driving distance and the fairly flat stabilized slope was achieved after 2.5 km. A transition region with a progressively decreasing slope is visible between 0.7 km and 2.5 km and the change over point can be determined within this region.

The similar emission pattern can be demonstrated by plotting the cumulative emissions against vehicle work or cumulative fuel consumption shown in Figure 5-7. The vehicle work and the cumulative fuel consumption can be achieved by integrating the instantaneous vehicle tractive power and mass fuel flow rate. The slopes of the cumulative emission trend curves in term of  $g/kW.h$ ,  $g/km$ ,  $g/kgFuel$  called emission factors in this chapter can link the cumulative emissions with the vehicle work, driving distance and cumulative fuel consumed. In order to predict the total emissions of one trip from the estimated vehicle work, driving distance and total fuel consumption, it is critical to determine the value of the emission factors if they are constant or to develop the emission functions if the emission factors vary with other driving parameters.

Figure 5-8 and 5-9 illustrate two examples of driving patterns which are truncated from the same experimental test data file. As displayed in the congested segment of the test (the bottom graph in Figure 5-8), an average vehicle speed of 26 km/h was obtained whereas the average vehicle tractive power was 4 kW. In contrast, the free-flow profile displayed by the bottom graph in Figure 5-9 had an average vehicle speed of 48 km/h and an average vehicle tractive power of 6 kW. In order to illustrate the general influence from the different driving patterns, the test vehicle's engine had reached the operating temperature before the start of the congested segment and the free-flow segment. In addition, since these two segments were part of single experimental test, the influences from ambient temperature and pressure are neglected. The cumulative emission profiles (as functions of vehicle work, fuel consumption and distance traveled) are demonstrated for the congested driving pattern in the Figure 5-8. Each of three kinds of emission factors ( $g/kW.h$ ,  $g/kgFuel$ ,  $g/km$ ) based on the slope of the cumulative emission profiles are developed for the HC, CO and NO<sub>x</sub> emissions respectively. A similar diagram, with respect to the free-flow traffic scenario, is shown in Figure 5-9. By comparing with the emission factors from the previous traffic congested driving pattern, it has shown a significant decrease in emission factor (especially for  $g/kW.h$  and  $g/km$ ) with a 50% increase in average vehicle tractive power or 85% increase in average vehicle speed.

The above emission factors analysis of the typical stop-start and free-flow driving patterns has found:

1. The same real-world experiment includes the different driving profiles.
2. The different emission factors are found for different driving profiles.
3. All emission factors with the unit of g/kW.h, g/kgFuel and g/km vary with the vehicle tractive power and vehicle speed to some extent.

#### 5.4.3 INFLUENCES FROM THREE TYPICAL DRIVING PATTERNS ON EMISSION FACTORS

To further clarify the influence on the emission factors (g/kW.h, g/km and g/kgFuel) from different driving patterns, the average values of those factors were calculated from the typical urban tests, highway tests and aggressive driving tests for each vehicle illustrated in Figures 5-10 to 5-12. For the reasonable comparison with the highway and aggressive driving tests, the warmed-up start urban tests were chosen to eliminate the cold start influence on the emissions. It clearly indicates from the graphs that HC, CO and NO<sub>x</sub> average emission factors of urban tests have the highest values and those of highway tests have the lowest values for Audi Quattro, Pontiac Vibe and Chevrolet Silverado. HC emission factors for Chevrolet Cavalier and GMC Savana also have the similar trend as the other vehicles, but the CO and NO<sub>x</sub> average emission factors of the aggressive driving tests for Cavalier and Savana have the highest values instead of those from the urban tests. As a general rule proved by the above results, a vehicle produces the most emissions in terms of the same vehicle work, driving distance and fuel consumption while driving on the stop-start traffic conditions because there are more idle time, lower vehicle speed/vehicle power, and more frequent acceleration and deceleration. In contrast, a vehicle produces the least pollutants while driving on the highway since there are negligible idle time, higher vehicle speed, less acceleration and medium vehicle power and load. However, some vehicles such as Chevrolet Cavalier and GMC Savana are quite sensitive to acceleration since they produce the most CO and NO<sub>x</sub> through the fast acceleration and higher vehicle load.

By comparing the emissions factors among those five vehicles, 2004 Pontiac Vibe produced the least emissions in all category, which is not surprise that the very low emission rate vehicle can be achieved after so many years with more stringent emission regulations compliment. Audi Quattro stands out from the peers by producing the highest HC and CO in all driving patterns with about six times higher than the Chevrolet Silverado which is not common for 1.8 L engine displacement vehicle, but emits reasonably lower NO<sub>x</sub> than the Chevrolet Silverado or GMC Savana. These experimental data indicates that the air/fuel ratio experienced a rich excursion for Audi Quattro under all driving patterns. This is a special case which does not represent the other on-road fleet in the same class, but does exist in the real world. The emission trends from these three driving situations indicate increasing emission factors of NO<sub>x</sub> pollutant from the other four tested vehicles with engine displacement increasing from 1.8 L to 5.7 L. However, the HC and CO emission factors have no any clear trends among the same four vehicles.

#### 5.4.4 COMPREHENSIVE EMISSIONS FUNCTIONS DEVELOPMENT

In order to determine the correlation between the vehicle emission factors and the vehicle power/average speed, sixty experimental tests using five typical vehicles were conducted. Since the dedicated Matlab program is capable of calculating the instantaneous mass emission rates, vehicle power and fuel consumption rate based on the same time trace of the vehicle speed, the emission factors of g/kW.h, g/km and g/kgFuel are easily derived from the above parameters and saved into the same data file. To avoid the occasional uncertainty influences during the experiments, the average value of emission factors are calculated and used for the following analysis.

##### 5.4.4.1 Post-Catalyst-Light-Off Emission Factors Analysis

Since the catalyst pre-light off stage only occupies a small fraction of the whole driving distance, it is necessary to start analyzing the emission factors from the warmed-up

stable emission experiments which more represent the real driving profiles. Figures 5-13 to 5-15 illustrate NO<sub>x</sub>, CO and HC emission factors of Chevrolet Cavalier as functions of vehicle power and average vehicle speed. The emission factors are determined by examining the experimental tests with a fully operating catalyst and a stabilized engine temperature.

The top graph of Figure 5-13 shows a power correlation for the NO<sub>x</sub> emission factor (g/kW.h) with the vehicle tractive power. As presented in the figure, the specific NO<sub>x</sub> emission has the maximum value of about 1.7 g/kW.h when vehicle power is less than 5 kW. A logical result of decreasing of NO<sub>x</sub> emission factor is found with increasing average vehicle power, and the relatively stable and low values are achieved after the vehicle power is over 20 kW. A four times difference can be notified for the NO<sub>x</sub> emission factor over the average power range of 5 to 35 kW. With low average vehicle power, the vehicle is usually driven with a lower average velocity experiencing frequent accelerations and decelerations expressed by the congested traffic driving pattern in Figure 5-8. The higher NO<sub>x</sub> emission can be achieved from the faster acceleration and thus higher emission factor. The correlations between the other two NO<sub>x</sub> emission factors (g/kgFuel, g/km) and vehicle power are shown in the middle and bottom graphs of Figure 5-13. In contrast to factor g/kW.h, the HC emission factors of g/kgFuel and g/km have no clear correlations with the vehicle power because of the widely scattered data set along the whole range of the vehicle tractive power.

Besides the vehicle tractive power, vehicle speed is another important vehicle performance parameter. The relationship between three NO<sub>x</sub> emission factors (g/kW.h, g/kgFuel, g/km) and average vehicle speed shown in the same figure. The factor g/km is strongly correlated with vehicle speed similar to the relationship between g/kW.h and vehicle power as analyzed above. The emission factor has the higher value of more than 0.45 g/km when the average vehicle speed is less than 5 km/h. The value of the emission factor decreases rapidly when the vehicle speed increases from 5 km/h to 35 km/h, and reaches the lowest specific NO<sub>x</sub> emission with the wide vehicle speed range of 35 km/h to 85 km/h. In term of the overall test, the NO<sub>x</sub> emission value is reduced

surprisingly 10 times when the vehicle speed is raised from 5 km/h to 85 km/h. NO<sub>x</sub> emission factors of g/kW.h and g/kgFuel shows a different scenario that it is hard to find the reasonable trends with the whole vehicle speed range.

Three CO emission factors against vehicle tractive power and average speed are presented in Figure 5-14. Similar to the NO<sub>x</sub> emission factor, a power fit describes the CO emission factor g/kW.h over the average vehicle power range. The specific CO emission can be as high as 9 g/kW.h when the vehicle power is less 5 kW with frequent acceleration and low vehicle speed. The fuel enrichment strategies accepted in the acceleration modal result in higher instantaneous CO emission rates and thus higher emission factors. The specific CO emission decreases and stabilizes at 3 g/kW.h value with increasing the vehicle power. A three times difference is found for the CO emission factors over an average power range of 5 to 35 kW. Similarly, the other two CO emission factors (g/kgFuel, g/km) have no clear correlation with the average vehicle power. For the CO emission factors with respect to vehicle speed, it is quite easy to find the correlation function in spite of the more scattered data set than that of NO<sub>x</sub> emission. Again, there is no clear correlation between CO emission factors of g/kW.h or g/kgFuel and the vehicle speed.

Figure 5-15 illustrates the HC emission factors as functions of average vehicle tractive power and average speed. In the data set of g/kW.h with respect to vehicle power shown in the top graph of the figure, the specific HC emission value decreases with increasing the vehicle power for the same reasons as presented above. Overall, a five times emission difference is found over 5 to 35 kW average vehicle power range. By comparing with HC and CO emission factor, NO<sub>x</sub> data set with the unit of g/kW.h has weak relationship with vehicle tractive power. However, the factor of g/km is strongly correlated with the vehicle speed decreasing 20 times over 5 km/h to 85 km/h speed range. No any obvious trend between the factor of g/kgFuel with the vehicle tractive power or average speed can be found from Cavalier experimental results.

The above analysis of Cavalier emission factors of g/kW.h, g/kgFuel and g/km with respect to vehicle tractive power and average vehicle speed has shown:

1. The emission factors of HC, CO and NO<sub>x</sub> are affected by the vehicle driving performances mainly represented by vehicle tractive power and average speed.
2. The emission factor of g/kW.h is correlated with the average vehicle power for HC, CO and NO<sub>x</sub> sharing the similar trend of the specific emission falling from an infinite level for zero tractive power towards a realistic value at some low tractive power level, then stabilizes at a low value with further vehicle power increasing. The associated emission factor functions can be easily derived from the power fit curves.
3. The emission factor of g/km is strongly correlated with the average vehicle speed (km/h) for HC, CO and NO<sub>x</sub>, but there is no obvious correlation with vehicle tractive power. Similar to trend of the emission factor g/kW.h with respect to vehicle power, the value of g/km is found to decrease with increases of the average vehicle speed.
4. The emission factor of g/kgFuel is relatively independent of vehicle power and speed.

The emission factors of other vehicles were also examined by the same methodology considering one driver was used as well as the same test routes. For simplicity, the correlations of the emission factors of g/kW.h and g/km with the vehicle tractive power and average speed respectively will be presented in the chapter because the similar conclusion can be drawn that the factor of g/kgFuel for HC, CO and NO<sub>x</sub> is less dependent on either vehicle power or vehicle speed.

Figures 5-16 to 5-19 show the experimentally determined emission factors of HC, CO and NO<sub>x</sub> with the unit of g/kW.h against vehicle tractive power for Audi Quattro, Pontiac Vibe, Chevrolet Silverado and GMC Savana respectively. Each figure presents measured data points and fitted curves for the tested vehicle specific emissions of HC, CO and NO<sub>x</sub>. Similar to Chevrolet Cavalier emission factors, the value of HC and CO emission factors for the other four vehicles decrease dramatically when the vehicle tractive power increases from 2 to 15 kW, and reach the lower stabilized emission rate after the vehicle power is over 15 kW. By studying the graphs of HC and CO emission

factor closely, it is not a surprise to find that Pontiac Vibe produces the lowest HC and CO emission rate due to its lowest mileages and newest catalyst converter. However, Audi Quattro produces the most HC and CO emission rate among the five tested vehicles. From the experimental data set of Audi Quattro shown in Figure 5-16, the specific HC emission values vary from 0.5 to 3 g/kW.h, and the specific CO emission values vary from 15 to 80 g/kW.h with the different vehicle tractive power. On the other hand, the Pontiac Vibe produces 0.008 to 0.06 g/kW.h HC and 3 to 10 g/kW.h CO, the Chevrolet Cavalier produces 0.011 to 0.04 g/kW.h HC and 4 to 10 g/kW.h CO, the Chevrolet Silverado produces 0.02 to 0.25 g/kW.h HC and 4 to 25 g/kW.h CO, the GMC Savana produces 0.035 to 0.14 g/kW.h HC and 4 to 18 g/kW.h CO respectively. Those listed data verify the conclusion summarized above that the specific emissions increase with the increasing engine displacement, but there is some exemptions existing in the real-world fleet.

For NO<sub>x</sub> emission factor, Audi Quattro, Pontiac Vibe, Chevrolet Cavalier and Chevrolet Silverado share the similar emission trend with the higher emission rate at the lower vehicle power and lower stabilized emission rate at the higher vehicle power. However, GMC Savana's NO<sub>x</sub> emission factor of g/kW.h produces a different scenario shown in Figure 5-19. The relatively high NO<sub>x</sub> emission values are found when the vehicle power is either less than 15 kW or over 45 kW, and the lowest NO<sub>x</sub> emission value of about 0.5 g/kW.h is located somewhere in the middle segment of the vehicle power. The possible reason could be that the 2001 Cargo Van has high mile age of 442,000 km and NO<sub>x</sub> emission reduction ability of the catalyst was limited after 5 years intensive operation time.

Figures 5-20 to 5-23 show the experimentally determined emission factors of HC, CO and NO<sub>x</sub> with the unit of g/km against vehicle average speed for Audi Quattro, Pontiac Vibe, Chevrolet Silverado and GMC Savana respectively. All vehicles share the similar emission trend for HC, CO and NO<sub>x</sub> that the emission factor of g/km decreases with the increase of the vehicle speed. Especially, it is worth to mention is that the NO<sub>x</sub> emission factor of g/km for GMC Savana has a reasonable correlation with the vehicle

average speed although the correlation of its factor of g/kW.h with the vehicle power was taken as a special case as illustrated above. Comparing with other vehicles, the Pontiac Vibe again produces the least specific emission rates of HC, CO and NO<sub>x</sub>, the Audi Quattro produces the most HC and CO emission rates.

#### 5.4.4.2 Pre-Catalyst-Light-Off Emission Factors Analysis

The pre-catalyst light-off emission factors are determined from examining emissions data of the first small region of driving distance. The data from the experimental tests show that the catalytic converter starts to oxidize HC, CO and reduces NO<sub>x</sub> at the specific point and the emissions rates are stabilized at the lower values from the much higher untreated emissions values. The change-over points of HC, CO and NO<sub>x</sub> are identical for Audi Quattro, Pontiac Vibe or GMC Savana, but the NO<sub>x</sub> change-over points are slightly different from those of HC and CO for Chevrolet Cavalier and Silverado as shown in Table 5-4. All emissions change-over points are not more than 1.2 km, but vary a lot with different vehicle type. Pontiac Vibe has the fastest reaction time because of its lower mile age; On the other hand, the GMC Savana has the longest pre-light-off distance probably due to the worse catalyst conditions after quite long driving distances in the past. It is worth to indicate that those catalyst light-off change-over points are determined based on about 60 seconds initial idle. In addition, there are no heavy traffic congestions within the pre-light-off region and there are no aggressive driving behaviors (i.e. the vehicle speed is less than 80 km/h and the acceleration is less than 1.5 m/s<sup>2</sup>).

**Table 5-4** Vehicle Catalyst Light-Off Change-Over Point

Vehicle	Audi Quattro	Pontiac Vibe	Chevrolet Cavalier	Chevrolet Silverado	GMC Savana
HC	1.1 km	0.5 km	1.0 km	0.6 km	1.2 km
CO	1.1 km	0.5 km	1.0 km	0.6 km	1.2 km
NO <sub>x</sub>	1.1 km	0.5 km	0.9 km	0.7 km	1.2 km

Figures 5-24 to 5-28 illustrate the HC, CO and NO<sub>x</sub> emission factors with the unit of g/kW.h as functions of each vehicle average tractive power for the pre-light-off region. Figures 5-29 to 5-33 show those emission factors with the unit of g/km as functions of each vehicle average speed for the pre-light-off region. The correlations of the emissions factors for HC, CO and NO<sub>x</sub> with the vehicle power or average speed have the similar trends as those of the post-light-off region analyzed above. However the differing scales in each figure range from high scales for the pre-light-off period to lower scales for the post-light-off period. The difference in scale shows the importance of the cold-start, pre-light-off emission rates relative to stabilized, post-light-off emission rates.

#### 5.4.5 DESCRIPTION OF THE EMISSION MODEL ESTABLISHMENT

The emission profiles of the tested vehicle for cold and warmed-up start application can be described by the emission model based on the above emission functions. Figure 5-34 shows the vehicle emission calculations in two different cases, one for cold start (at least 10 hours soak period before start) and one for warmed-up start applications (coolant temperature is over 80° C). The vehicle cumulative emissions of one cold-start trip can be achieved by calculating the mass emissions from cold start initial idle period, pre-catalyst light-off region and post-catalyst light-off region. The initial cold start emission rates and warmed-up start emission rates are summarized in Table 5-5 and the emissions during the whole initial idle period can be easily calculated by multiplying the initial idle emission rates (g/s) with the last time (s). The pre-light-off region emissions and post-light-off region emissions can be calculated by the emission factor either in term of g/kW.h or g/km developed previously. Similarly, but there are less steps for the emission calculation of the warmed-up start trips. The cumulative emissions can be achieved by calculating the mass emissions from warmed-up start initial idle period and the post-catalyst light-off region. The intermediate warmed-up start vehicle emissions inventory (i.e. the coolant temperature is between the ambient temperature and 80° C) cannot be predicted by the model shown in Figure 5-34 due to

lack of the intermediate warmed-up start idle mass emission rates and the vehicle catalyst light-off change over point.

Instantaneous Emission factor of g/km is calculated from the instantaneous mass emission rate (g/s) divided by vehicle speed (km/h) which is less dependent on the vehicle acceleration and power demand. Therefore, the emission factor of g/km faces the major shortcoming that it only represents the overall emissions profiles, but hard to represent the details of high power demand and fast acceleration at low speed situations during the trip. In contrast, the power-based emission factor of g/kW.h is calculated from the instantaneous mass emission rate (g/s) divided by vehicle tractive power (kW) which is dependent on the vehicle speed, acceleration, vehicle mass illustrated in Appendix A. Having priority over g/km, emission factor of g/kW.h with ability to link the emissions with the whole on-road driving profiles will be utilized in the in-use emission model calculations.

**Table 5-5 Idle Emission Rates For Five Vehicles**

Vehicle Type		Audi Quattro	Pontiac Vibe	Chevrolet Cavalier	Chevrolet Silverado	GMC Savana
HC at idle [g/s]	Cold Start	0.006313	0.001633	0.003618	0.023340	0.012091
	Warmed-up	0.000270	0.000003	0.000038	0.000263	0.000146
CO at idle [g/s]	Cold Start	0.171440	0.089438	0.161829	0.370955	0.221206
	Warmed-up	0.007004	0.002019	0.000876	0.002735	0.002958
NOx at idle [g/s]	Cold Start	0.000385	0.000165	0.000452	0.000493	0.000648
	Warmed-up	0.000158	0.000065	0.000087	0.000286	0.000077

#### 5.4.6 COMPARISON WITH AVAILABLE MODEL

MOBILE6 developed by U.S. EPA is a standard vehicle emission inventory prediction model consisting of a running emission (slope in g/km or g/mile) and a start emission (intercept in grams).<sup>[9]</sup> It can evaluate the vehicle HC, CO and NOx emissions under the urban driving cycle with 60 seconds cold start initial idle time. MOBILE6 is capable of estimating emission factors for any calendar year between 1952 and 2050 for 28 individual vehicle types, however those emission factors were developed by the

traditional chassis dynamometer method in the lab which draws a lot of concerns of reflecting the real-world driving profiles. According to MOBILE6 vehicle classifications, the Pontiac Vibe and Chevrolet Cavalier belong to LDGV (Light-Duty Gasoline Vehicle/Passenger Cars), the Chevrolet Silverado belongs to LDGT1 (Light-Duty Gasoline Trucks 1) and the GMC Savana belongs to LDGT2 (Light-Duty Gasoline Trucks 2).

For the comparison purpose, typical cold-start urban tests using four vehicles were carried out. The emissions output from the basic in-use model described above in this chapter, the emissions from the direct experimental measurement, and the emissions of the same class of vehicle predicted by MOBILE6 model are summarized in Figure 5-35. The bar chart can show that the power-based in-use model and MOBILE6 model approaches are able to produce estimates of on-road emissions inventories though the results from both models have disagreement with the experimental data somewhat. However, a closer study of the data listed in the table in the same figure can find out the calculation results from in-use model have good compliance with the experimental data with 11% average absolute error for HC, CO, NO<sub>x</sub> cumulative emissions from four tested vehicles. Although higher error can be observed in some case occasionally, it is not a surprise considering the fact that emission functions are derived from the average data summarized from several similar tests for each vehicle. On the other hand, there is less agreement between the results from MOBILE6 model and the experimental data with 70% average absolute error. Especially for the very low emission vehicle Pontiac Vibe, the HC emission is overestimated by 209%. The in-use model results are much closer to the experimental data than those from MOBILE6 model for the random selected cold-start urban tests using four tested vehicles. The reason could be that the emission factors MOBILE6 model is using were developed from the standard test procedures raising concerns about the representative of emissions produced by specific on-road vehicle.

In contrast to travel or power-based emission factors, the fuel-based emission factor has less dependence on the vehicle power and average speed as illustrated previously.

Hence the regional fuel-based emission inventory estimation can be achieved by multiplying the weighted vehicle fuel-based emission factors with the total fuel consumption obtained from sales tax data at the state level. However, this methodology also faces the great challenges that uncertainty in the fuel-based inventory results from uncertainty in the emission factors measured for each vehicle model year and from the weighting factors used to combine the emission factor data. <sup>[1]</sup> The trip cumulative emissions from Pontiac Vibe, Chevrolet Cavalier, Chevrolet Silverado and GMC Savana are also shown in Figure 5-35 calculated from the average fuel-based emission factors summarized in Table 5-6. With 37% average absolute error for HC, CO and NOx from all tested vehicles, the fuel-based emission calculation is less accurate than the results from vehicle in-use power/work-based model because the smoothed out non-constant fuel-based emission factor raises some uncertainty to what extent emission rates increase with the fuel flow rate and how well the driving modes from which emission factors were measured represent the specific tests under study.

**Table 5-6** Vehicle Fuel-Based Emission Factor From Urban Tests

Emission Factor	Audi Quattro	Pontiac Vibe	Chevrolet Cavalier	Chevrolet Silverado	GMC Savana
HC g/kgFuel	6.58	0.15	0.20	1.50	0.87
CO g/kgFuel	98.44	11.88	12.24	27.71	12.37
NOx g/kgFuel	2.43	0.52	1.40	4.08	3.55

## 5.5 CONCLUSION

A portable on-board, in-use emission measurement system has been used to measure emissions from five typical vehicles operating on repeated tests covering a range from urban to highway to aggressive driving behavior. The results have been analyzed to develop mass emission functions and factors in terms of g/kW.h, g/km and g/kgFuel.

The specific energy-based emission factors for HC, CO and NOx, (ie. factors in terms of g/kW.h), rise rapidly to peak values determined by idle emission rates when vehicle tractive power is less than 5 kW. Similarly, the distance-based emission factors, (in

terms of g/km), rise rapidly for low average vehicle speeds. A logical result of decreasing of the emission factors is found with increasing vehicle power and average speed. These features emphasize the importance of vehicle idle and low-speed operation in determining overall emission levels. However, the specific fuel consumption-based emission factors, (in terms of g/kgFuel) are relatively independent on both vehicle power and speed, since the fuel consumption rate and emission rate both vary with vehicle power and average speed.

The influences of driving pattern on emissions were analyzed by comparing the vehicle emissions from the three typical driving patterns, (urban, highway and aggressive). Generally speaking, the specific emission rates from the urban tests were the highest for all three criteria pollutants (HC, CO and NO<sub>x</sub>), and the specific emission rates from the highway tests were the lowest. However, there were exceptions depending on the state of the vehicle and its control system calibration. This raises a significant challenge for any emission inventory prediction model since real urban emissions depend on the behavior of millions of vehicles accounting for thousands of model / age combinations.

Based on the emission functions developed in this chapter, a basic in-use model has been established to calculate the cumulative HC, CO and NO<sub>x</sub> mass emissions for vehicles similar to those tested. The calculations from in-use model have been compared with the experimental values by using the same speed trace as well as the results from MOBILE6. Though the results from the different approaches are not in perfect agreement, they show that the model based on in-use data is able to produce emissions inventories that are more sensitive to actual real-world driving conditions than a MOBILE6 estimate. The simplest emission estimate based on fuel consumption (g/kgFuel) is less accurate than the more complex, power-based model but still provides a reasonable method of estimating emissions where fuel consumption is measured.

## **5.6 FUTURE WORK**

The basic in-use model can examine the on-road emission inventories for a few vehicle types, which is not sufficient to confidently estimate regional on-road emission inventories. Future work should extend this basic model by testing more light-duty vehicle types using the same methodology illustrated in this chapter.

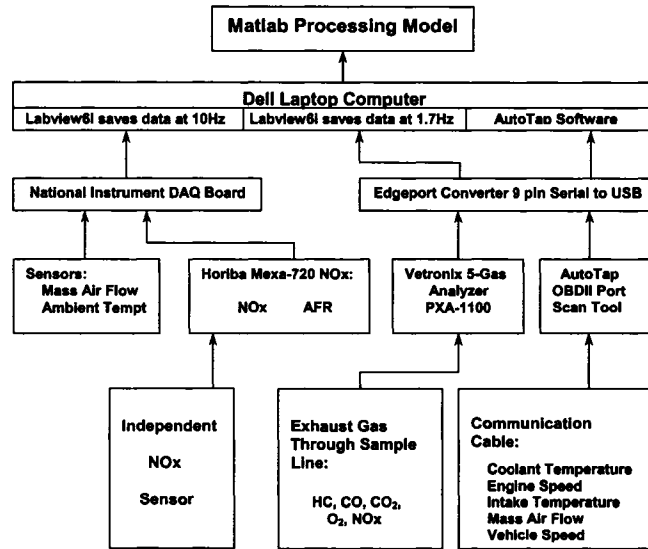


**Figure 5-1** Schematic of Test Instruments and Calculations

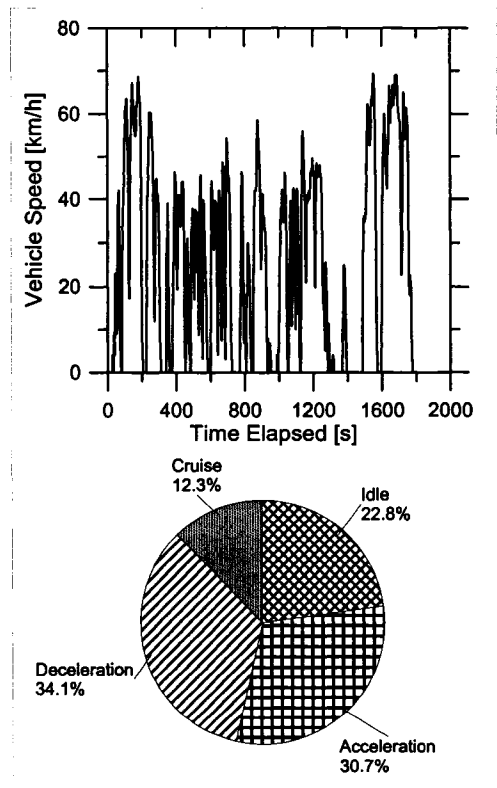


**Figure 5-2** Urban Test Route Speed Trace and Modal Fraction (Using 2004 Pontiac Vibe)

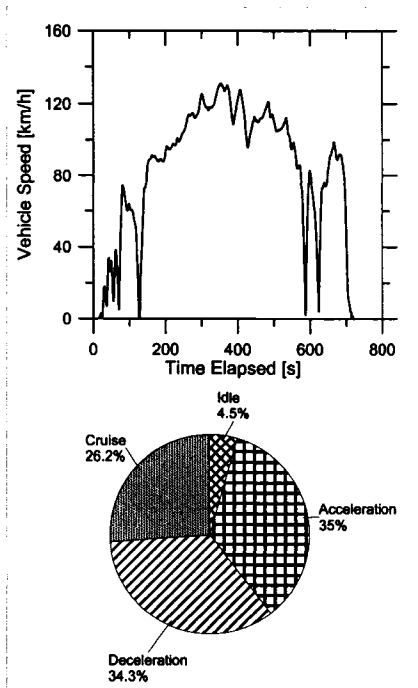


**Figure 5-3** US06 Test Route Speed Trace and Modal Fraction  
(Using 2001 GMC Savana)

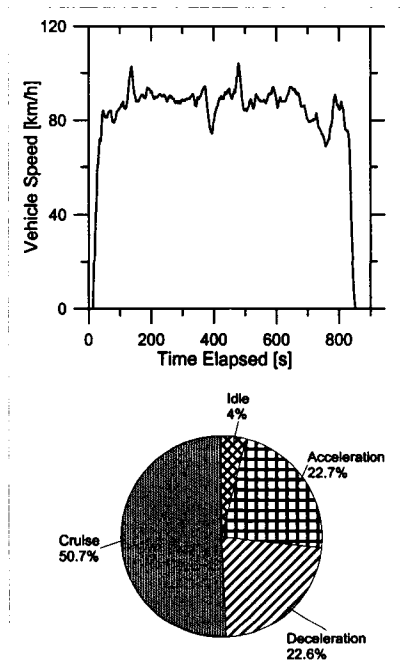


**Figure 5-4** Highway Test Route Speed Trace and Modal Fraction  
(Using 1999 Audi Quattro)

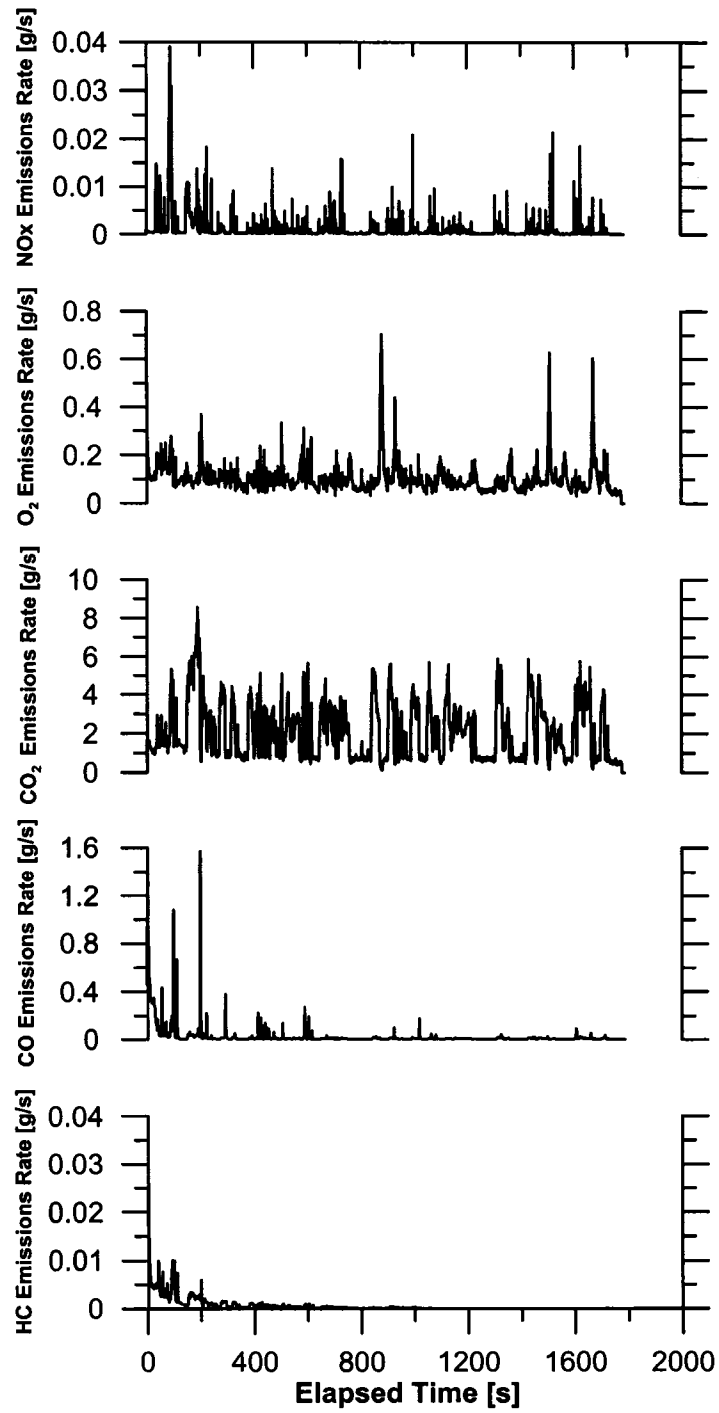


**Figure 5-5** Instantaneous Emission Traces Obtained From Chevrolet Cavalier

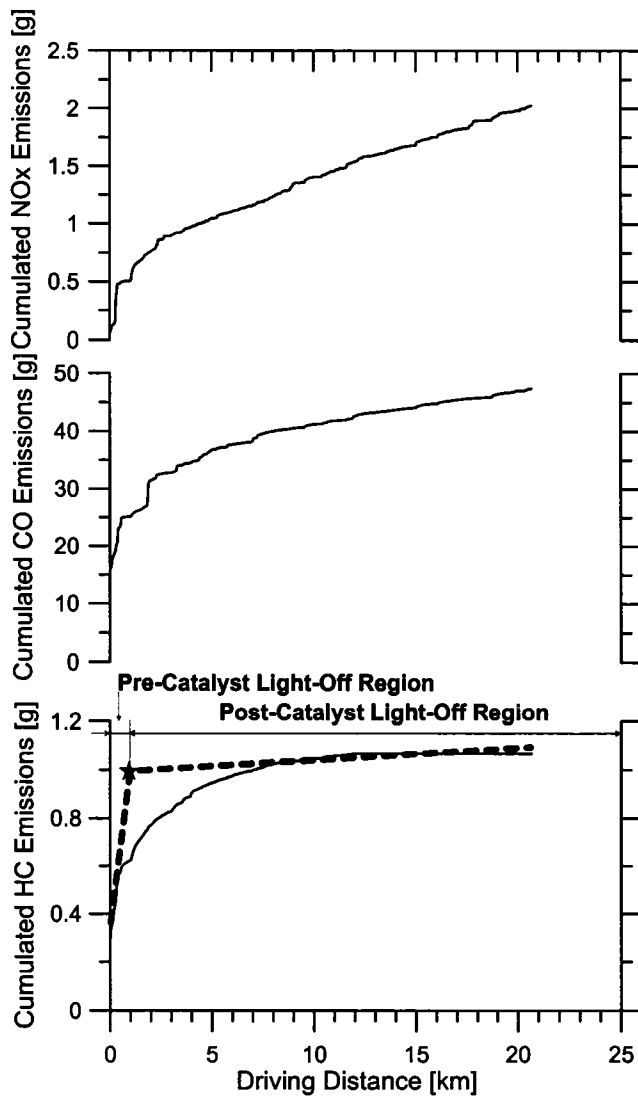


**Figure 5-6** Trends Of Cumulative Emissions With Driving Distance  
(Using Chevrolet Cavalier)

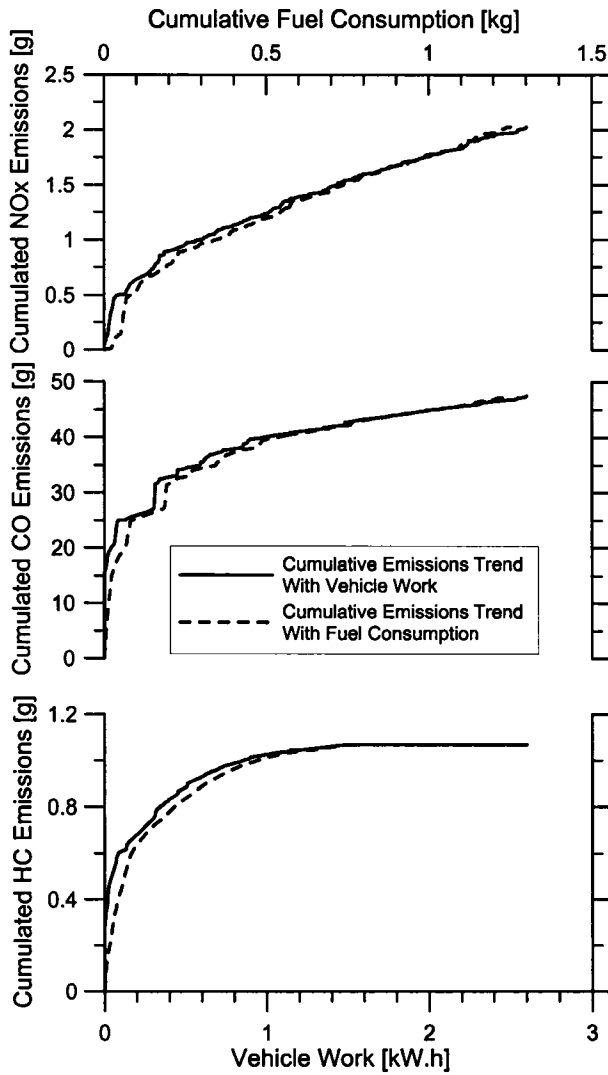


**Figure 5-7** Trends Of Cumulative Emissions With Work/Fuel Consumption  
(Using Chevrolet Cavalier)

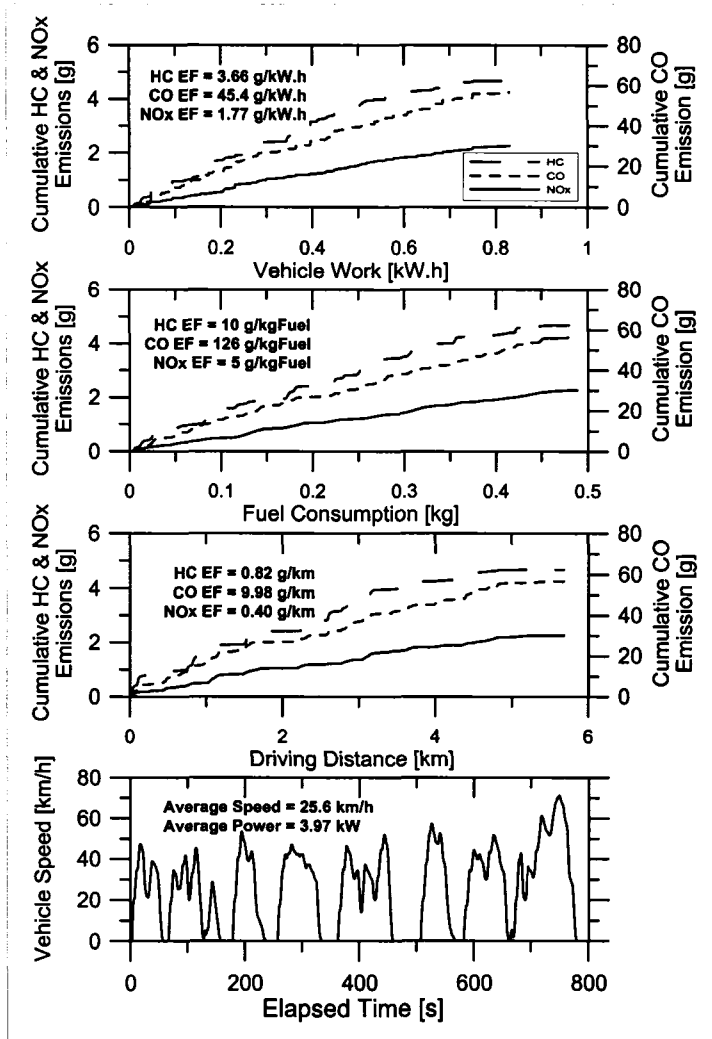


**Figure 5-8** Emission Factors of Congested Driving Pattern From Truncated Data (Using Chevrolet Cavalier)

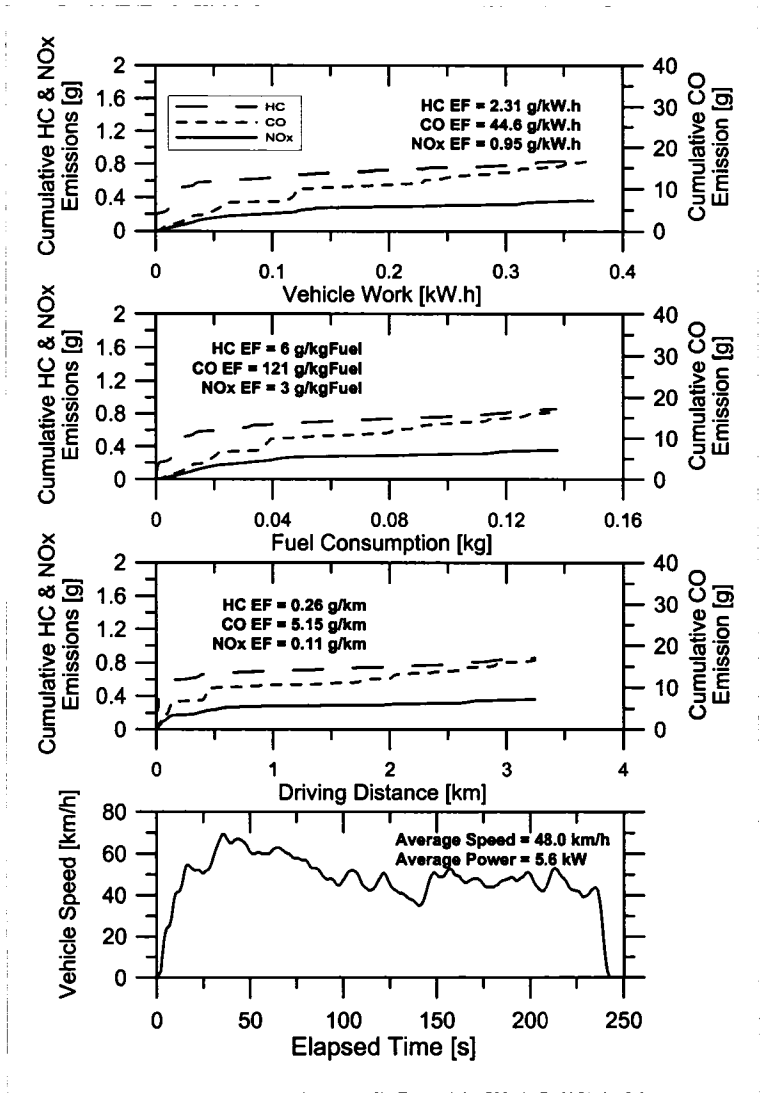


**Figure 5-9** Emission Factors of Free Flow Driving Pattern From Truncated Data (Using Chevrolet Cavalier)

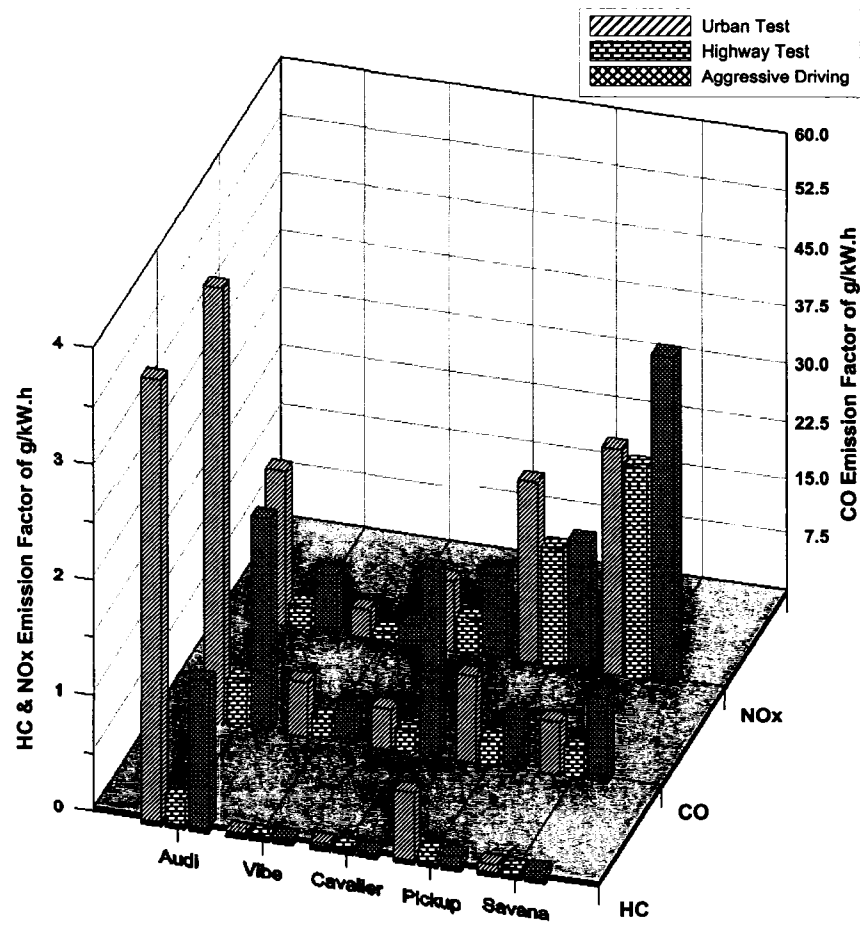


**Figure 5-10** The Comparison of g/kW.h Among Different Driving Patterns

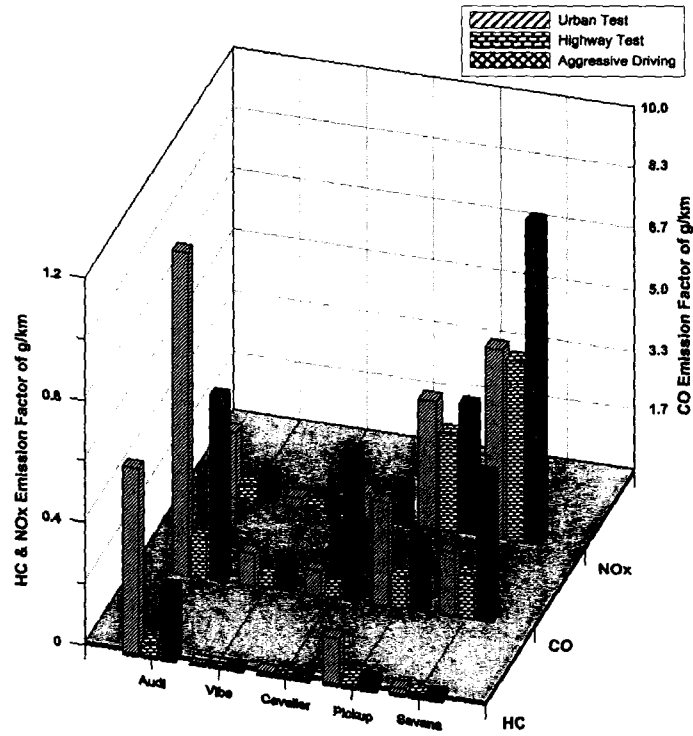


Figure 5-11 The Comparison of g/km Among Different Driving Patterns

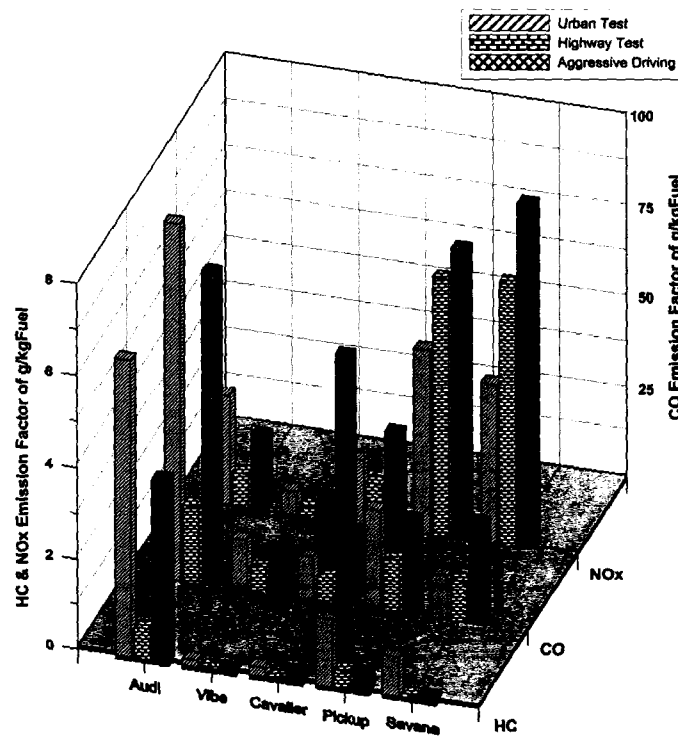
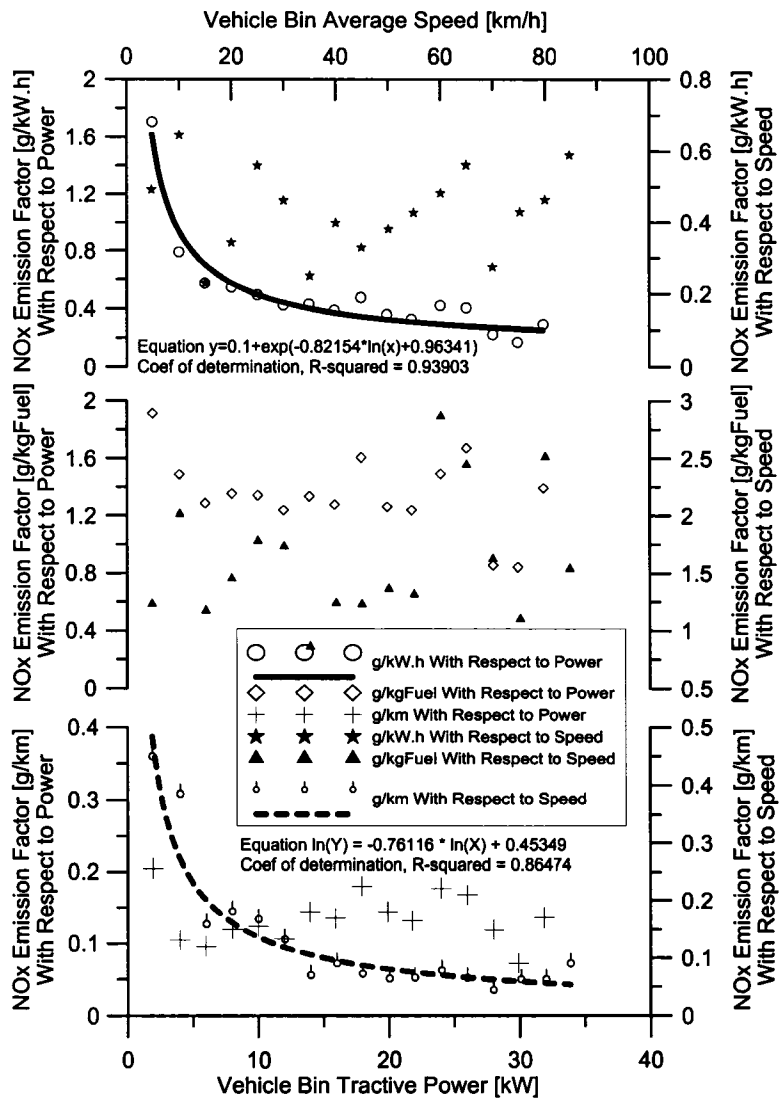
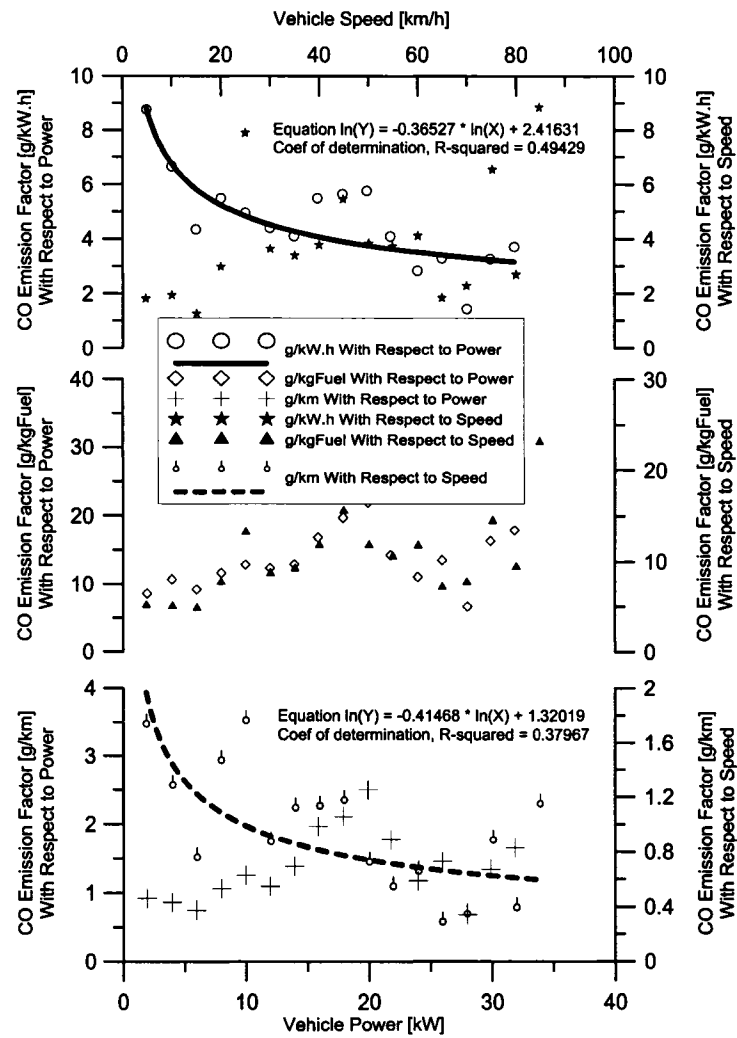


Figure 5-12 The Comparison of g/kgFuel Among Different Driving Patterns



**Figure 5-13** Correlation Of Chevrolet Cavalier Post-Catalyst Light-Off NOx Emission Factors With Bin Vehicle Power and Bin Average Speed



**Figure 5-14** Correlation Of Chevrolet Cavalier Post-Catalyst Light-Off CO Emission Factors With Bin Vehicle Power and Bin Average Speed

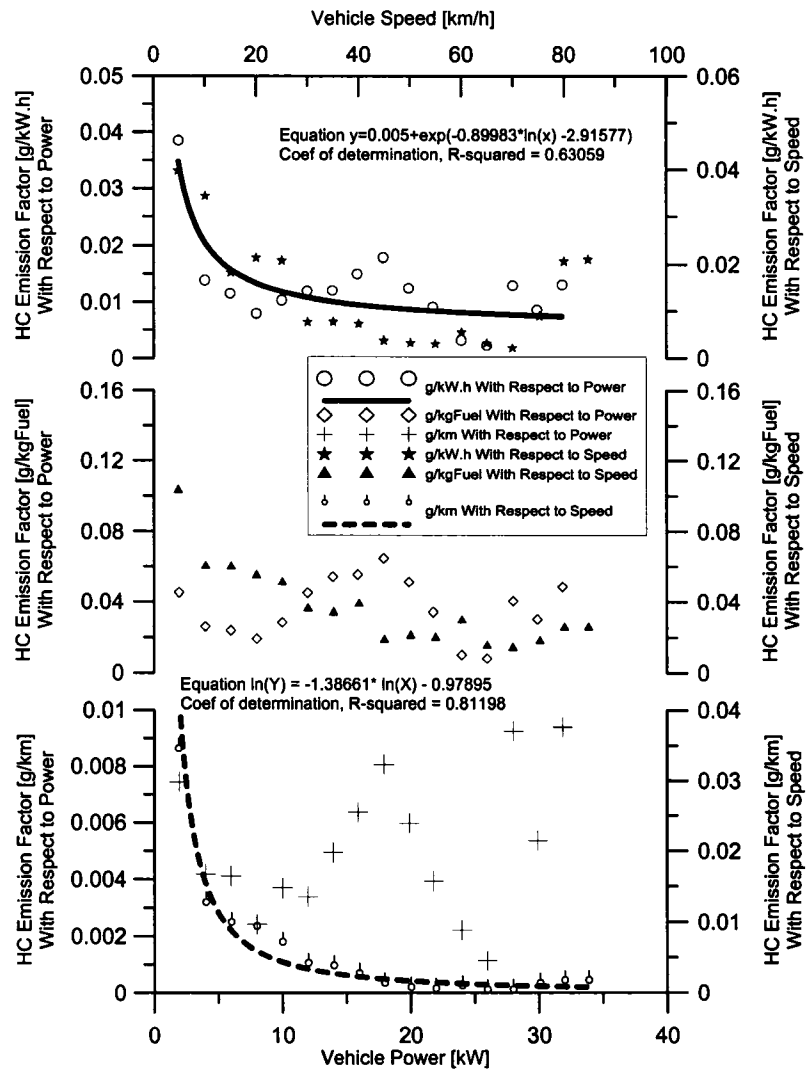


**Figure 5-15** Correlation Of Chevrolet Cavalier Post-Catalyst Light-Off HC Emission Factors With Bin Vehicle Power and Bin Average Speed

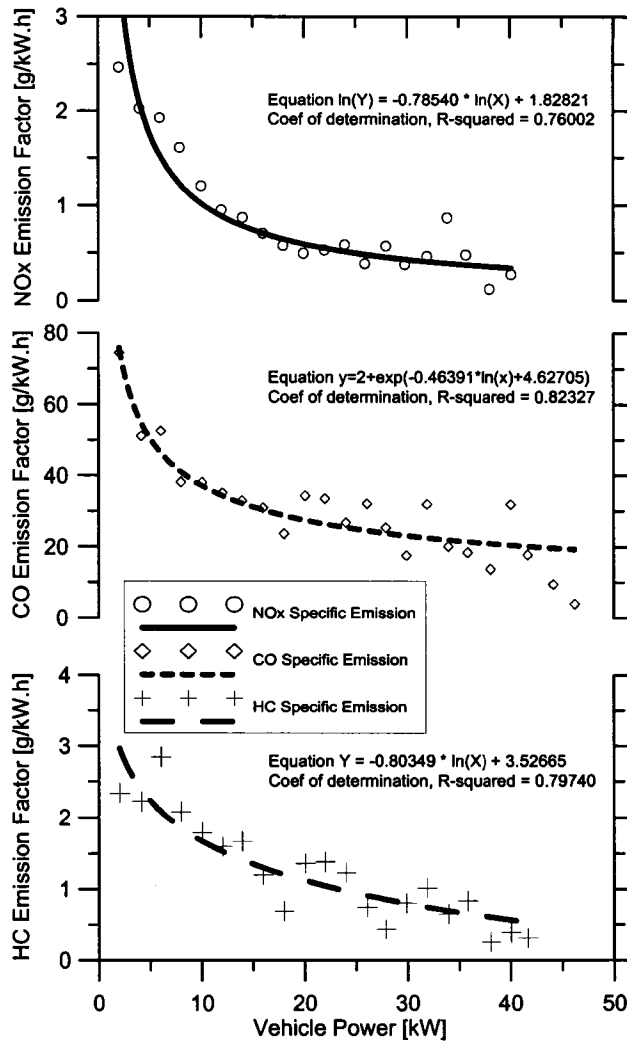


**Figure 5-16** Correlation Of Audi Quattro Post-Catalyst Light-Off Emission Factors With Bin Vehicle Power

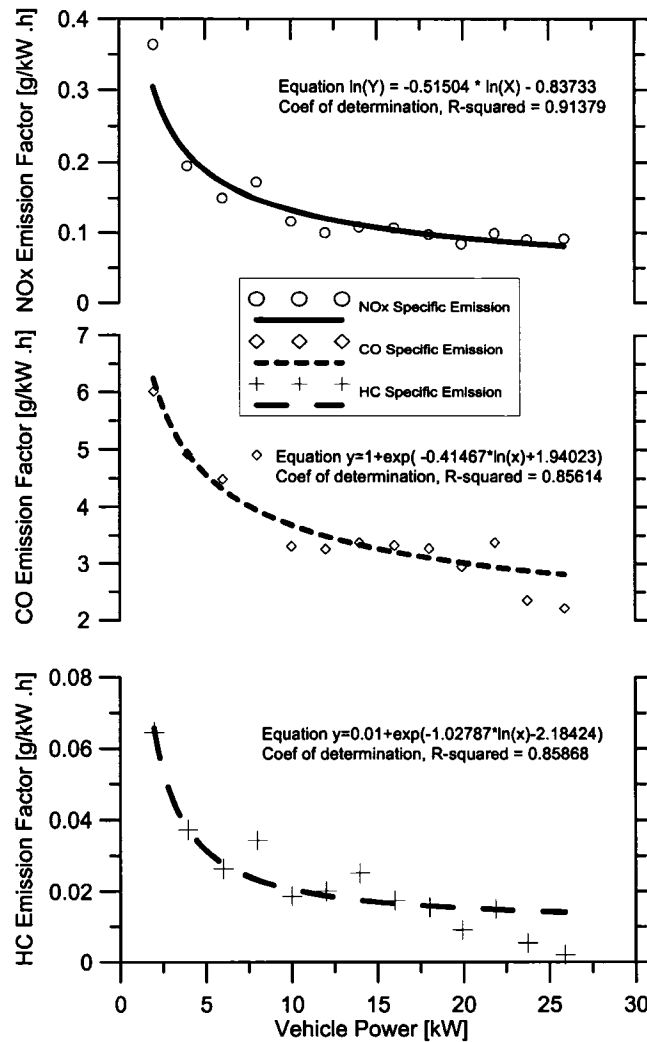


**Figure 5-17** Correlation Of Pontiac Vibe Post-Catalyst Light-Off Emission Factors With Bin Vehicle Power

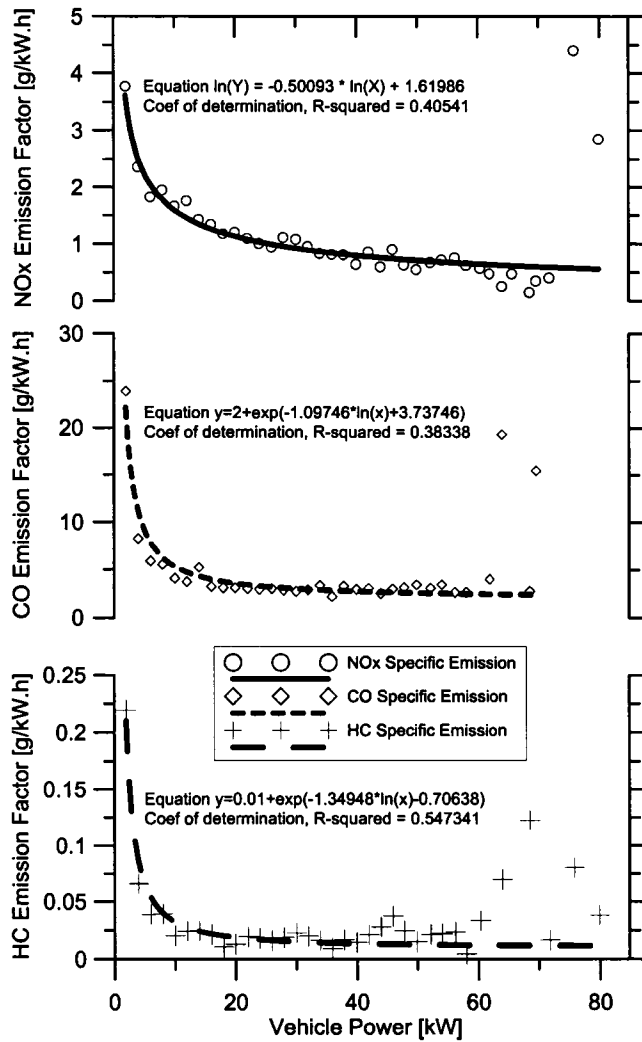


**Figure 5-18** Correlation Of Chevrolet Silverado Post-Catalyst Light-Off Emission Factors With Bin Vehicle Power

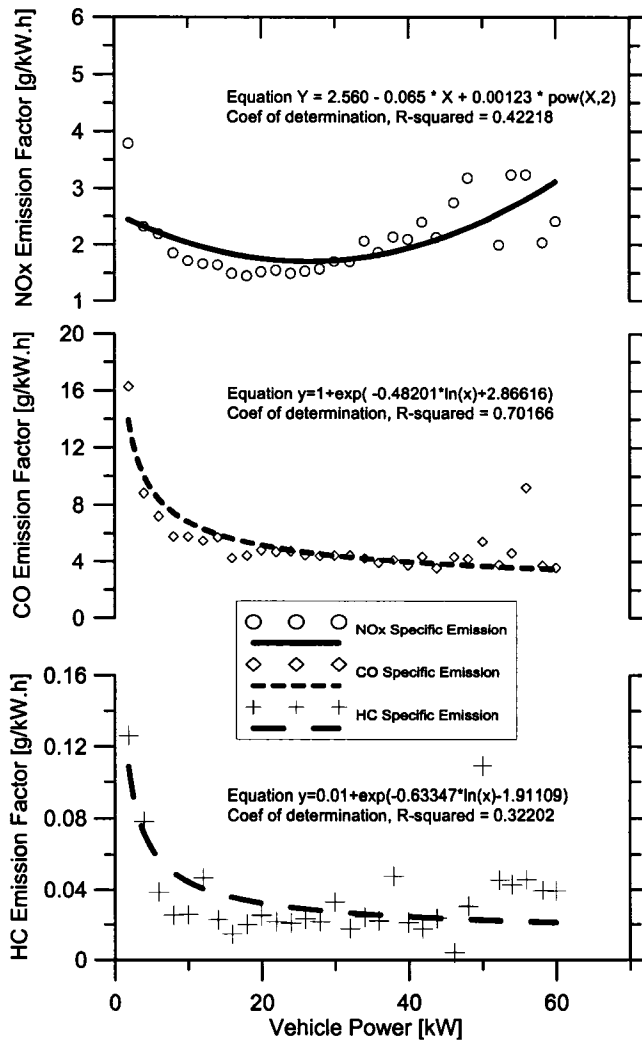


**Figure 5-19** Correlation Of GMC Savana Post-Catalyst Light-Off Emission Factors With Bin Vehicle Power

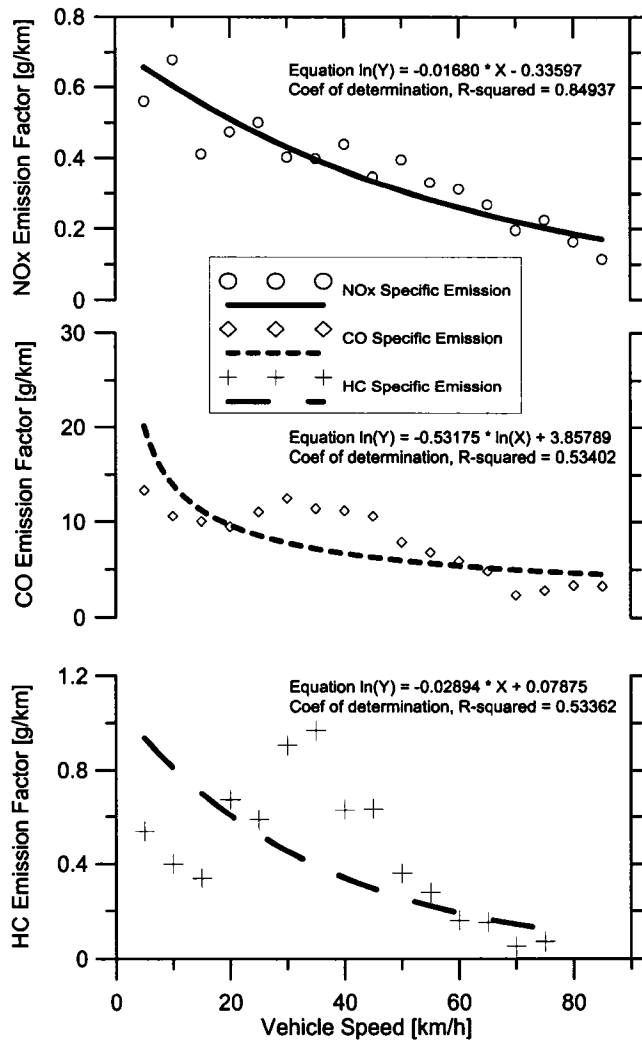


**Figure 5-20** Correlation Of Audi Quattro Post-Catalyst Light-Off Emission Factors With Bin Average Vehicle Speed

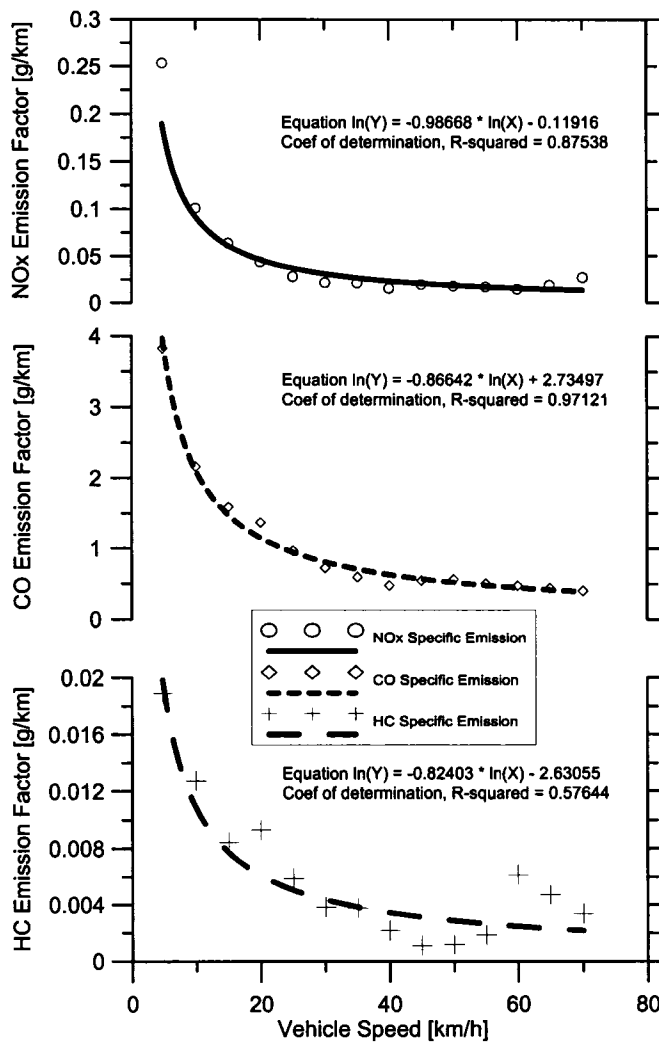


**Figure 5-21** Correlation Of Pontiac Vibe Post-Catalyst Light-Off Emission Factors With Bin Average Vehicle Speed

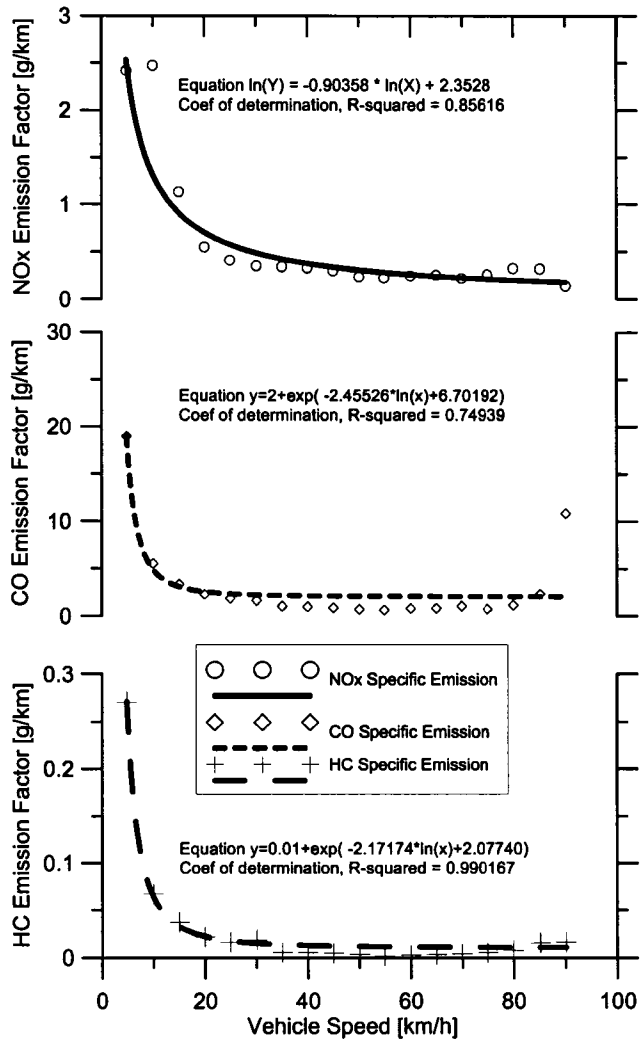


**Figure 5-22** Correlation Of Chevrolet Silverado Post-Catalyst Light-Off Emission Factors With Bin Average Vehicle Speed

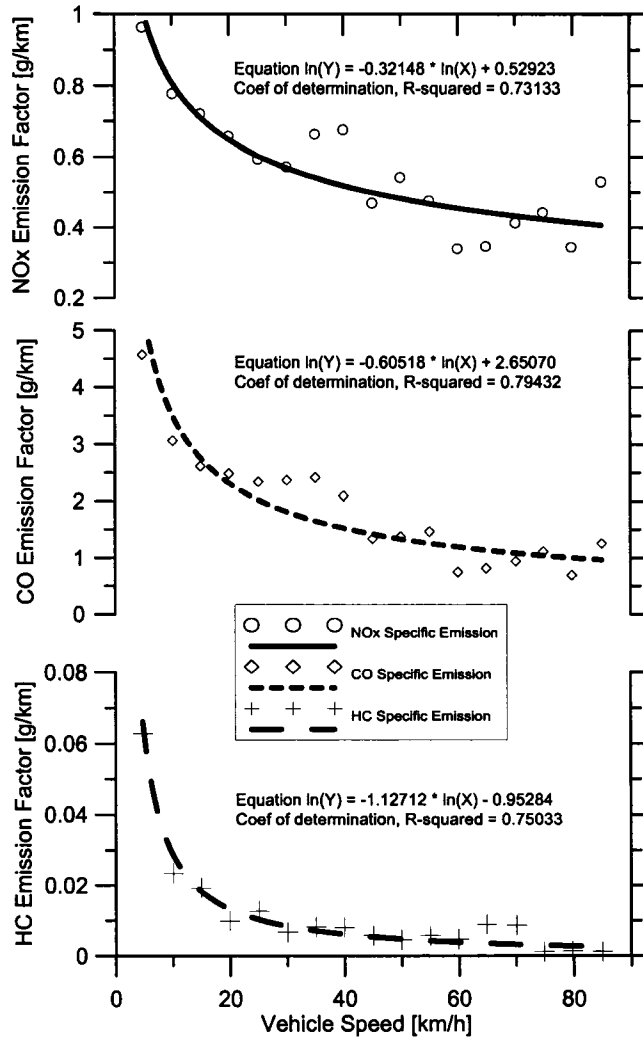


**Figure 5-23** Correlation Of GMC Savana Post-Catalyst Light-Off Emission Factors With Bin Average Vehicle Speed

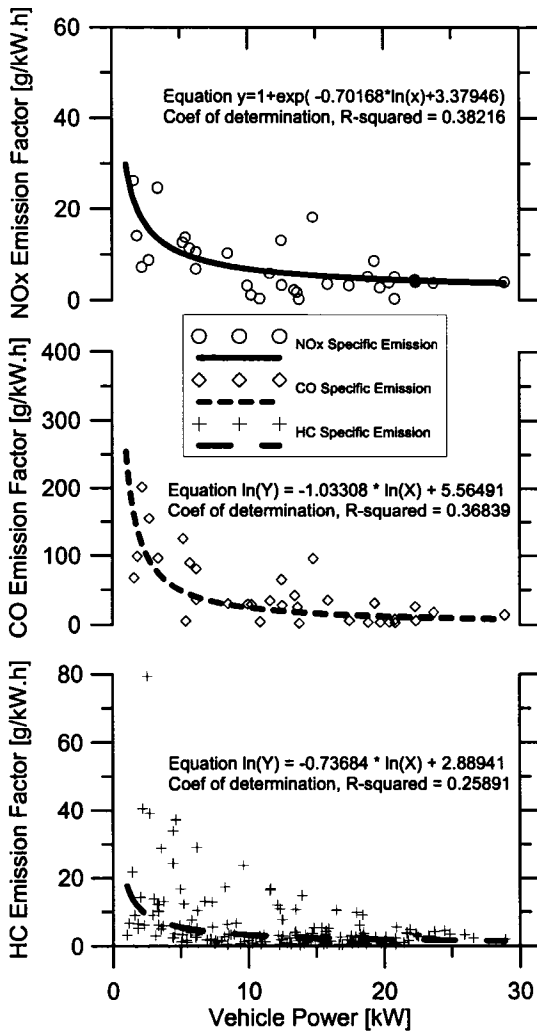


**Figure 5-24** Correlation Of Audi Quattro Pre-Catalyst Light-Off Emission Factors With Bin Vehicle Power

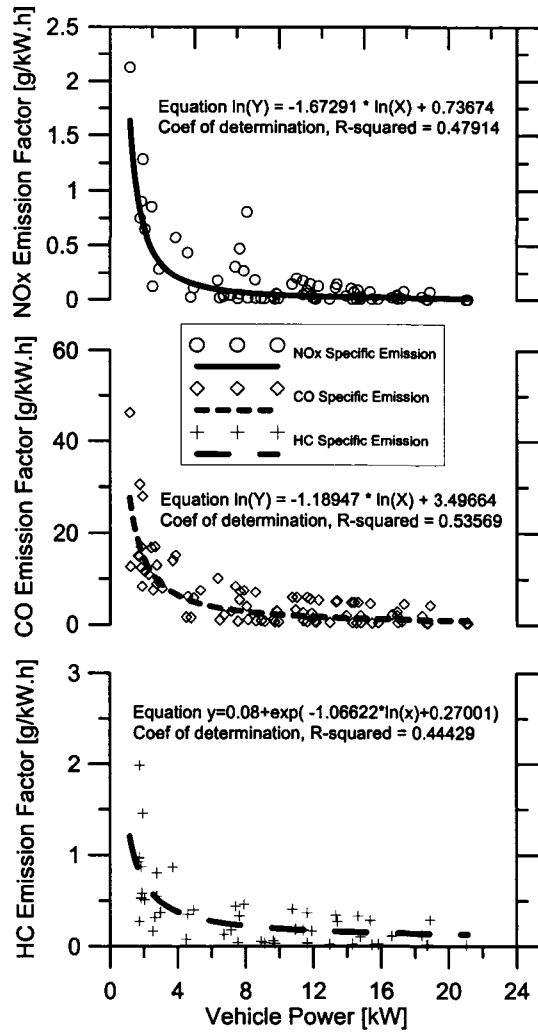


**Figure 5-25** Correlation Of Pontiac Vibe Pre-Catalyst Light-Off Emission Factors With Bin Vehicle Power

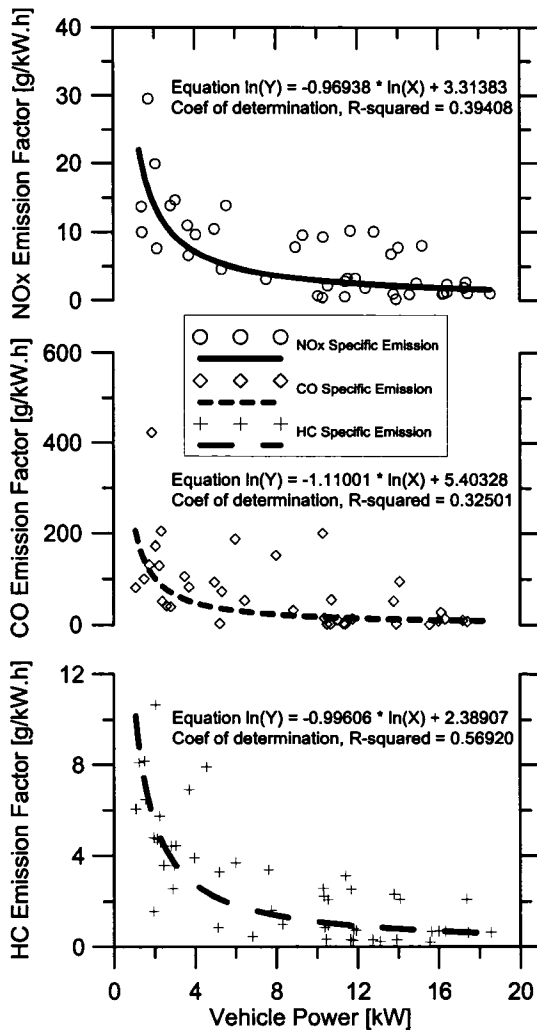


**Figure 5-26** Correlation Of Chevrolet Cavalier Pre-Catalyst Light-Off Emission Factors With Bin Vehicle Power

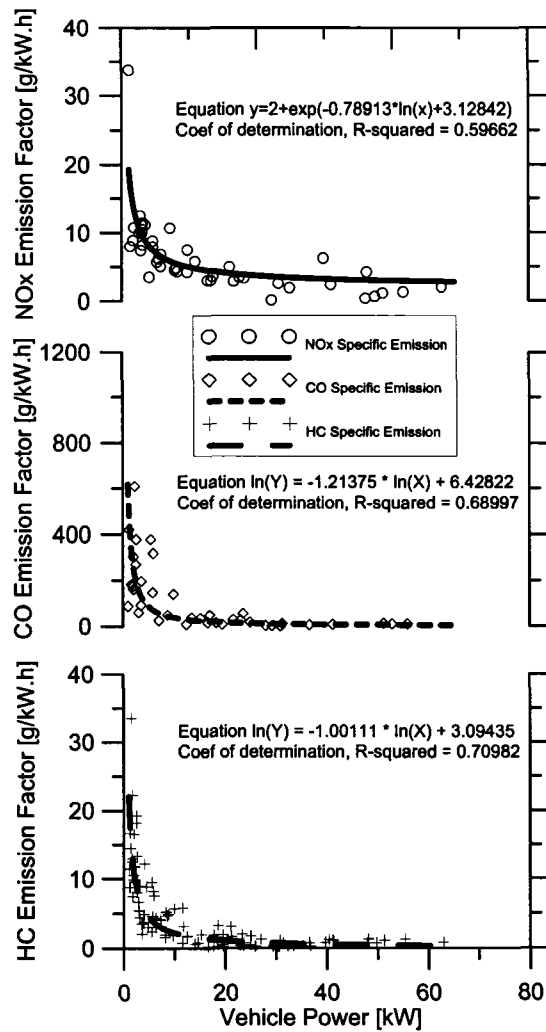


**Figure 5-27** Correlation Of Chevrolet Silverado Pre-Catalyst Light-Off Emission Factors With Bin Vehicle Power

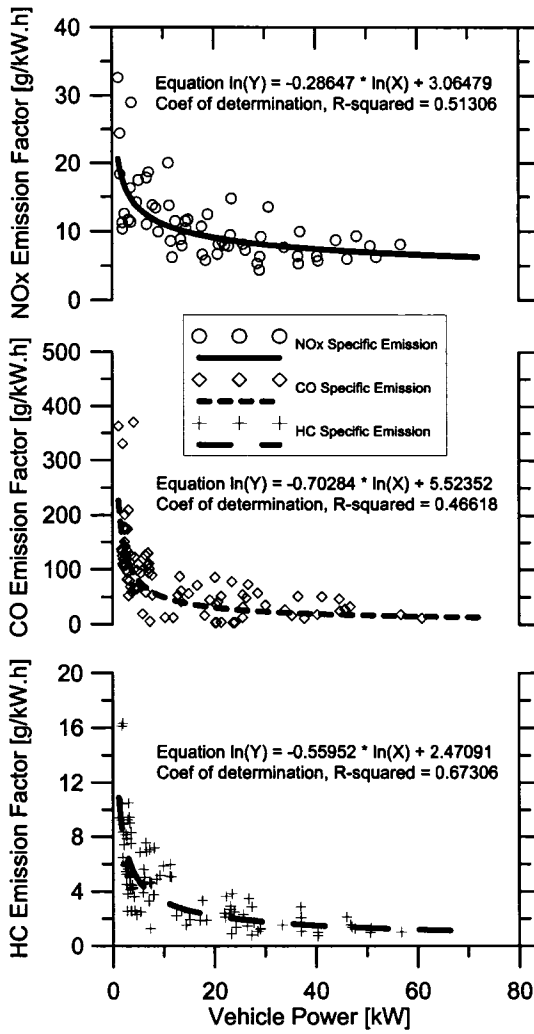


**Figure 5-28** Correlation Of GMC Savana Pre-Catalyst Light-Off Emission Factors With Bin Vehicle Power

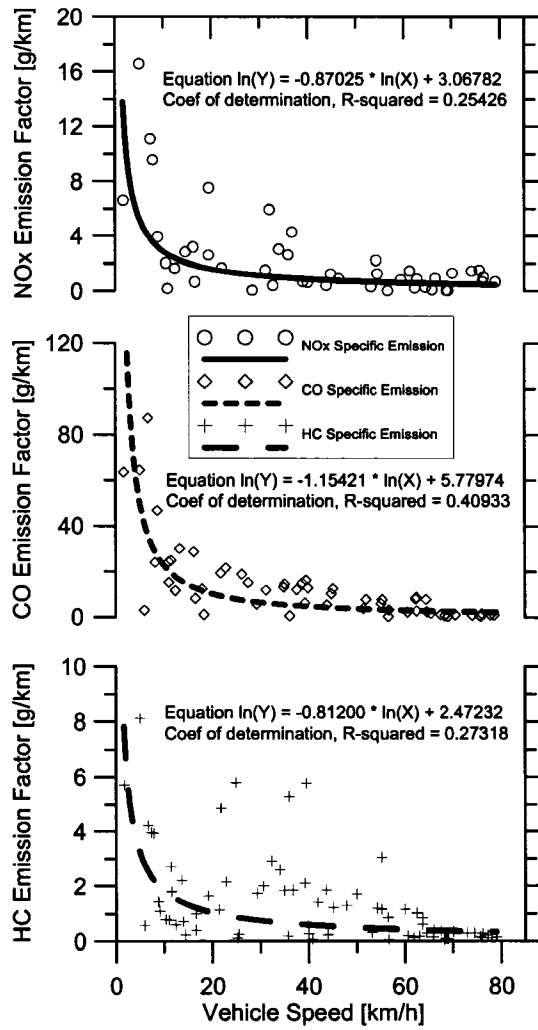


**Figure 5-29** Correlation Of Audi Quattro Pre-Catalyst Light-Off Emission Factors With Bin Average Vehicle Speed

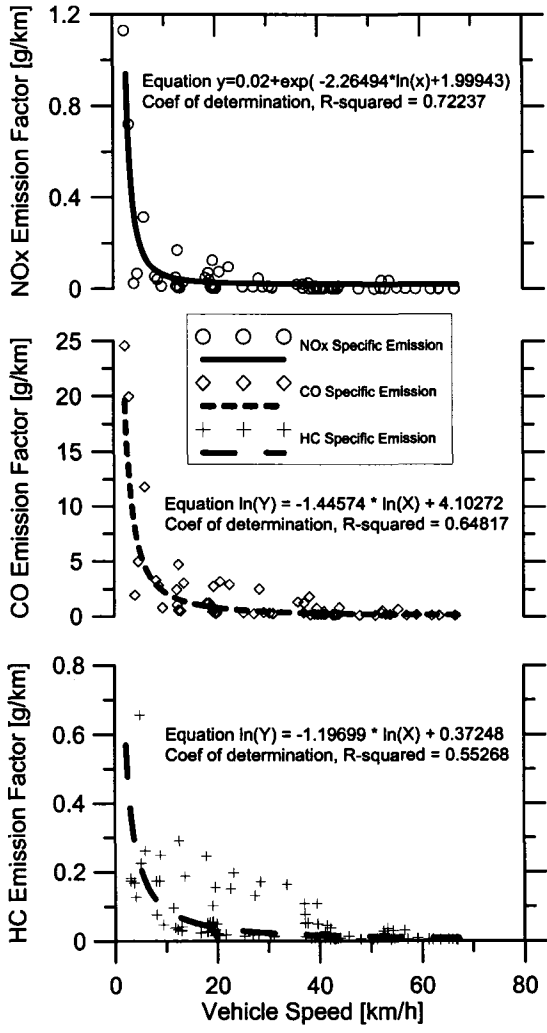


**Figure 5-30** Correlation Of Pontiac Vibe Pre-Catalyst Light-Off Emission Factors With Bin Average Vehicle Speed

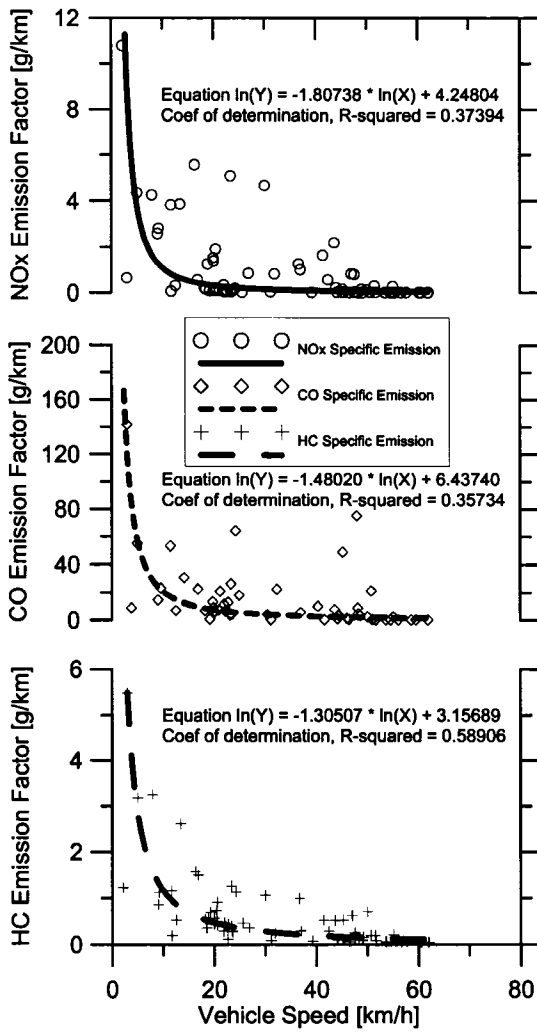


**Figure 5-31** Correlation Of Chevrolet Cavalier Pre-Catalyst Light-Off Emission Factors With Bin Average Vehicle Speed

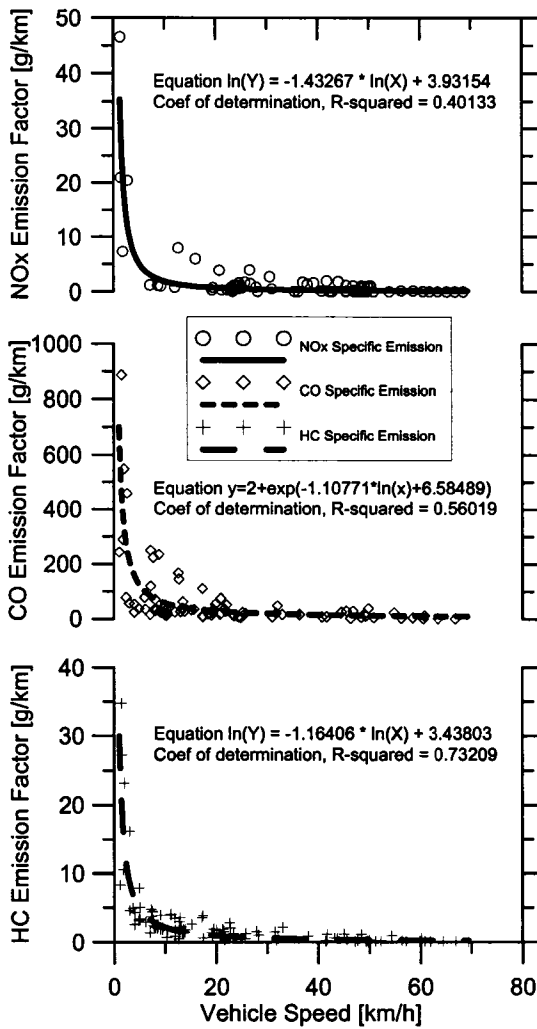


**Figure 5-32** Correlation Of Chevrolet Silverado Pre-Catalyst Light-Off Emission Factors With Bin Average Vehicle Speed

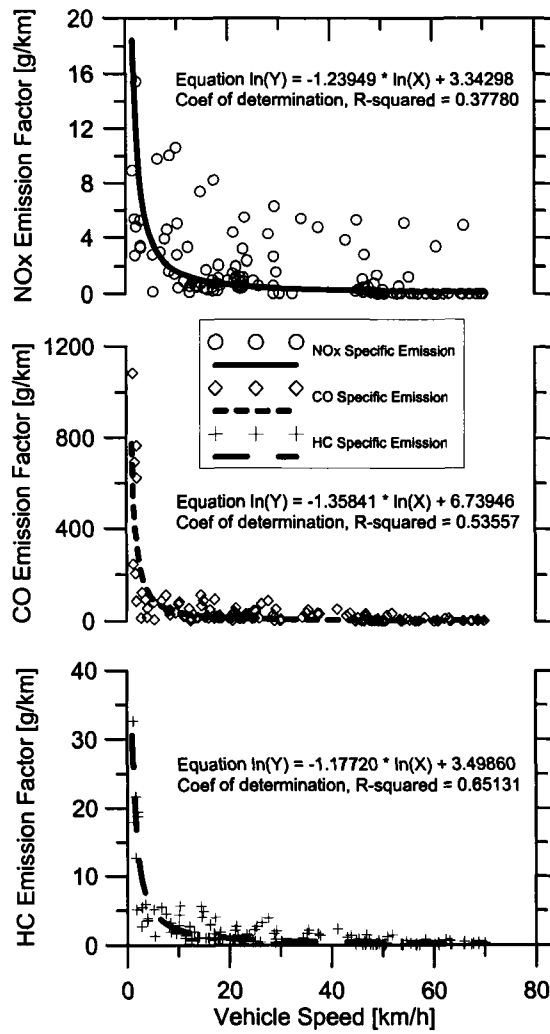


**Figure 5-33** Correlation Of GMC Savana Pre-Catalyst Light-Off Emission Factors With Bin Average Vehicle Speed

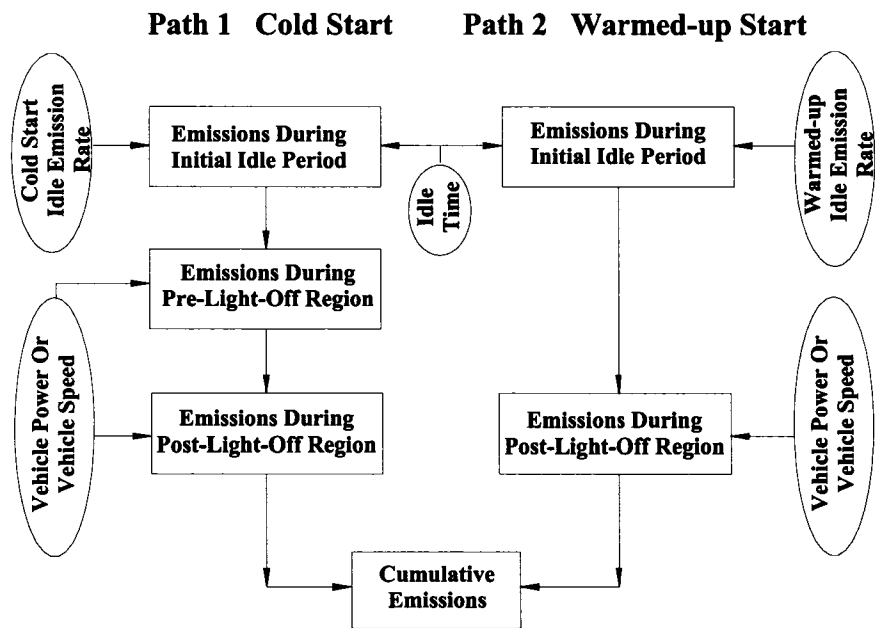


**Figure 5-34** Basic Power-Based In-Use Emissions Prediction Model

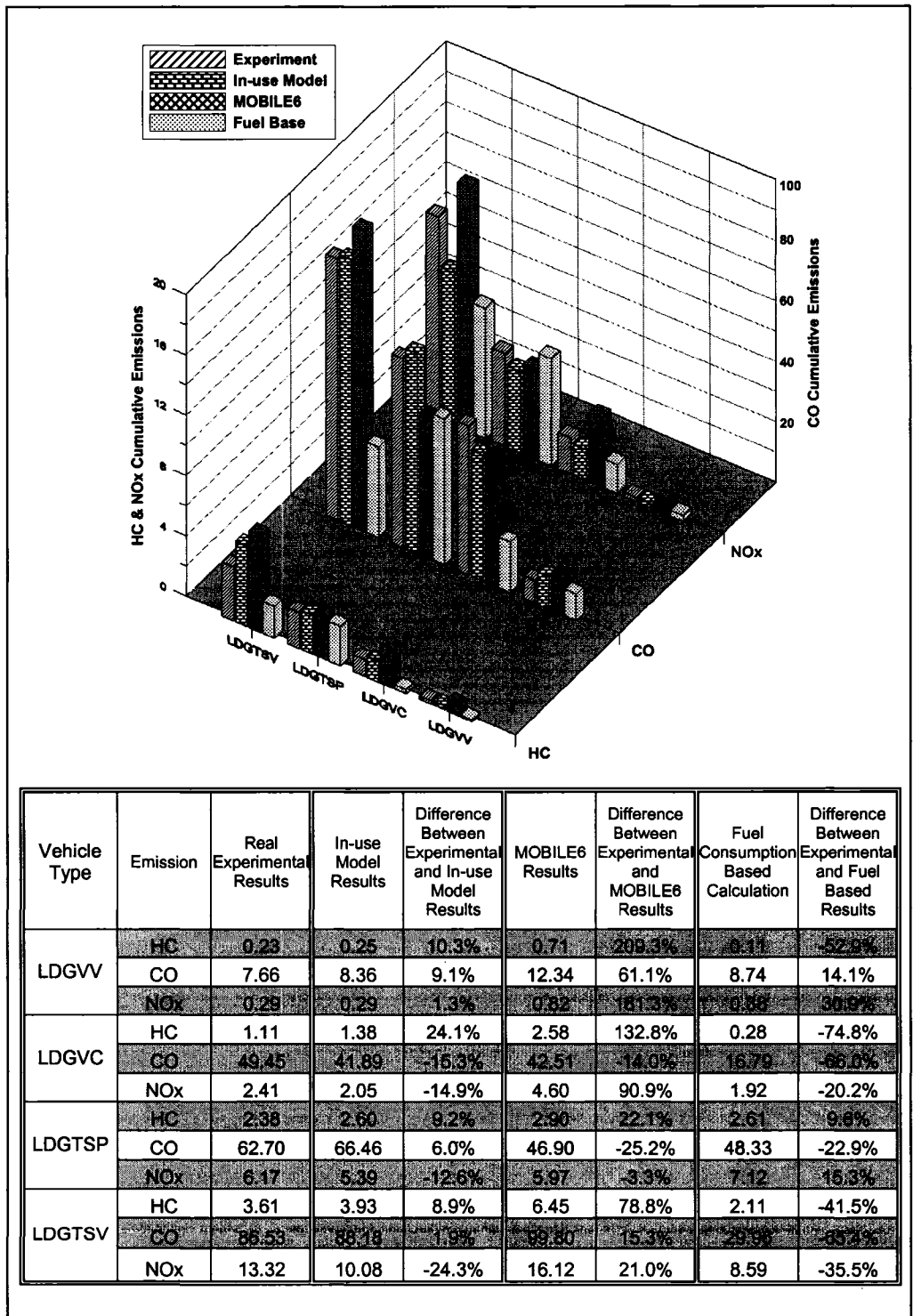


**Figure 5-35 Emissions Values Comparison Among the Experiment, In-use Model, Fuel Based Calculation and MOBILE6**

## REFERENCES

1. Brett C. Singer and Robert A. Harley. "A Fuel-Based Motor Vehicle Emission Inventory", Journal of the Air & Waste Management Association, Volume 46, PP. 581-593, 1996.
2. M. D. Checkel. "Mec E 541 Combustion Engines Lecture Notes", September 2004.
3. Travis B. Manchur, M. David Checkel. "Time Resolution Effects on Accuracy of Real-Time NOx Emissions Measurements", SAE Paper 2005-01-0674, Society of Automotive Engineers, 2005.
4. Jason D. Hawirko; M. David Checkel. "Real-Time, On-Road Measurement of Driving Behavior, Engine Parameters and Exhaust Emissions", SAE Paper 2002-01-1714, Society of Automotive Engineers, 2002.
5. Jason D. Hawirko; M. David Checkel. "Quantifying Vehicle Emission Factors for Various Ambient Conditions using an On-Road, Real-Time Emissions System", SAE Paper 2003-01-0301, Society of Automotive Engineers, 2003.
6. Jeff Jetter; Shinji Maeshiro; Seiji Hatcho; Robert Klebba. "Development of an On-Board Analyzer for Use on Advanced Low Emission Vehicles", SAE Paper 2000-01-1140, Society of Automotive Engineers, 2000.
7. Website: <http://www.epa.gov/otaq/sftp.htm#cycles>.
8. S Samuel, L Austin, D Morrey. "Automotive Test Drive Cycles for Emission Measurement and Real-World Emission Levels-A Review", ISSN: 0954-4070, Proc Instn Mech Engrs Vol 216, PP. 555-564, Part D: J Automobile Engineering, 2002.
9. Website: <http://www.epa.gov/OMSWWW/m6.htm#m60>.
10. H. Christopher Frey, Nagui M. Roupail, A. Unal, and James D. Colyar. "Measurement of On-Road Tailpipe CO, NO, and Hydrocarbon Emissions Using a Portable Instrument", In proceedings, Annual Meeting of the Air & Waste Management Association, held in Orlando, Florida, and published by A & WMA, Pittsburgh, PA, June 24-28, 2001
11. H. Christopher Frey, Nagui Roupail, Alper Unal, and James Colyar. "Emissions And Traffic Control: An Empirical Approach", Proceedings, CRC On-Road Vehicle Emissions Workshop, held in San Diego, CA, March 2000.

12. Michal Vojtisek-Lom; James T. Cobb, Jr. "Vehicle Mass Emissions Measurements Using a Portable 5-gas Exhaust Analyzer and Engine Computer Data", In proceedings- Emissions Inventory, Planning for the Future, Air & Waste Management Association; Pittsburgh, PA, 1997.
13. Christine A. Gierczak, Gerald Jesion, John W. Piatak, J.W. Butler; Ford Research Laboratory; Ford Motor Company. "On-Board Vehicle Emissions Measurement Program", Final Report, CRC Report No, VE-11-1, April 1994.
14. Timothy J. Truex ; John F. Collins; Jeff J. Jetter; Benjamin Knight; Tadayoshi Hayashi; Noriyuki Kishi and Norio Suzuki. "Measurement of Ambient Roadway and Vehicle Exhaust Emissions-An Assessment of Instrument Capability and Initial On-Road Test Results with an Advanced Low Emission Vehicle", SAE Paper 2000-01-1142, Society of Automotive Engineers, 2000.
15. Christopher S. Weaver and Marco V. Balam-Almanza. "Development of the 'RAVEM' Ride-Along Vehicle Emission Measurement System for Gaseous and Particulate Emissions", SAE Paper 2001-01-3644, Society of Automotive Engineers, 2001.
16. Christopher S. Weaver and Lawrence E. Petty. "Reproducibility and Accuracy of On-Board Emission Measurements Using the RAVEM™ System", SAE Paper 2004-01-0965, Society of Automotive Engineers, 2004.
17. Mark Dearth, James Butler, Alex Colvin. "SemtechD: The Chassis Roll Evaluation of a Commercial Portable Emission Measurement System (PEMS)", SAE Paper 2005-01-0673, Society of Automotive Engineers, 2005.
18. Basil Daham, Gordon Andrews, Hu Li. "Application of a Portable FTIR for Measuring On-road Emissions", SAE Paper 2005-01-0676, Society of Automotive Engineers, 2005.
19. Gordon Andrews, Hu Li, J.A. Wylie, Grant Zhu. "Influence of Ambient Temperature on Cold-start Emissions for a Euro 1 SI Car Using In-vehicle Emissions Measurement in an Urban Traffic Jam Test Cycle", SAE Paper 2005-01-1617, Society of Automotive Engineers, 2005.
20. Yutaka Takada, Norifumi Takada, Norimasa Lida. "Transient NOx Characteristics of Freight Vehicles with EGR System in Real Traffic Conditions", SAE Paper 2005-01-1619, Society of Automotive Engineers, 2005.
21. Michal Vojtisek-Lom, Joseph E. Allsop. "Development Of Heavy-Duty Diesel Portable, On-Board Mass Exhaust Emissions Monitoring System With NOx,

CO<sub>2</sub> And Qualitative PM Capabilities”, SAE Paper 2001-01-3641, Society of Automotive Engineers, 2001.

22. Mridul Gautam, Gregory Thompson, Daniel Carder. “Measurement of In-Use, On-Board Emissions from Heavy-Duty Diesel Vehicles: Mobile Emissions Measurement System”, SAE Paper 2001-01-3643, Society of Automotive Engineers, 2001.

23. PXA-1100 Gas Analyzer Operator’s Manual, Vetronix Corporation, Printed in USA, July 1996.

24. Stephen R. Turns. “An Introduction to Combustion”, Second Edition.

## **CHAPTER 6**

### **Conclusions**

*Chapter 6 states the general conclusions summarized from the research, and reiterates the work achievements.*

This M.Sc. thesis is a study on quantifying a portable on-board & in-use emissions and fuel consumption measurement system adapted to multiple vehicles and examining the fuel consumption factors and emissions factors from series of repeated experimental tests using five typical mid-life vehicles with engine displacement varying from 1.8 L to 5.7 L representing a significant fraction of the on-road fleet.

The first achievement of the research was to rebuild a portable on-board & in-use measurement system adapted to multiple vehicles, which would allow real-time vehicle tailpipe instantaneous mass emissions and fuel consumption measurement to be made. The whole system was put into a steel box and could be belted onto the passenger seat while testing on the roads. The system weighs 17 kg (38 lb) and is quite easy to transport from vehicle to vehicle. Chapter 3 illustrates the ability of the system to accurately capture and record the vehicle emissions and fuel consumption as well as vehicle performance traces.

The second achievement of the research was to develop a general correlation function relating the fuel consumption factor ( $\text{g/kW.h}$ ) with the vehicle tractive power ( $\text{kW}$ ). A fuel consumption model for the light duty gasoline vehicles was established to be able to predict the fuel consumptions by any given vehicle speed trace and the initial vehicle idle time. From the fuel efficiency analysis of Chapter 4, it is not hard to find the trend that vehicles have low energy demand (in  $\text{kJ/km}$ ) and low distance-based fuel consumption (in  $\text{g/km}$ ) at 60 km/h to 100 km/h average vehicle speed range, and the values of  $\text{g/km}$  increase sharply when the average vehicle speed is lower than 40 km/h. The fuel efficiency can reach the maximum value (about 30%) when the small passenger vehicle produces 30% of its peak power and the light duty truck produces 25% of its peak power respectively.

The third achievement of the research was to finish an analysis of vehicle emission factors based on multiple on-road tests in urban, highway and aggressive driving situations. The tailpipe emission factors expressed as  $\text{g/kW.h}$  and  $\text{g/km}$  are strongly correlated with vehicle tractive power and average vehicle speed respectively. The

results analysis proved that these emission factors decreased rapidly from the infinite level for zero tractive power and vehicle speed and stabilized at a low value with increasing vehicle power and average speed respectively. Therefore, the associated correlation functions relating these emission factors to either vehicle power or average speed can be developed in both pre-catalyst light-off region and post-catalyst light-off region for five test vehicles. However, emission factor expressed in terms of  $\text{g/kgFuel}$  are relatively less dependent of travel based parameters such as vehicle power and average speed. Hence the practical fuel-based emission inventories prediction can be achieved simply by multiplying the average emission factor ( $\text{g/kgFuel}$ ) with the total vehicle fuel consumption although there are some uncertainty to what extent emission rates increase with the fuel flow rate and how well the driving modes from which emission factors were measured represent the specific tests under study. Based on the measurement of idle mass emission rates both at cold-start and warmed-up start situations as well as the emission functions developed in Chapter 5, a basic in-use work /travel-based model can be established not only to estimate the cumulative mass emissions of HC, CO and NO<sub>x</sub> from vehicles similar to those tested with reasonable accuracy, but also provide valuable references for the general behavior and the emissions inventory estimation for the other light-duty gasoline vehicles.

Based on knowledge of the present on-board & in-use measurement system and the dedicated experimental results analysis, future work could be recommended as follows:

1. More research is required to test a wide range of vehicles using the same on-board & in-use measurement system to develop in-use general emission functions weighted by the vehicle type and vehicle age factors helping to increase the capability of estimating the mass emissions from the wide variety of the on-road light duty gasoline vehicles by the emission inventories prediction model.
2. One of the advantages of the diesel engine is to produce less HC, CO and CO<sub>2</sub>, however it usually emits more NO<sub>x</sub> and PM. With the population of diesel

vehicle increasing on the road, it is necessary to modify the present on-board & in-use measurement system by adding equipment capable of measuring PM. Hence, the important pollutants from both the on-road gasoline fueled vehicles and diesel fueled vehicles can be examined by this new generation of real-time measurement system.

## APPENDIX A

### Vehicle Dynamic Model And Uncertainty Analysis

*Tractive power demand is one of the most important parameters while the vehicle is in real service experiencing the wide range of road speed, acceleration and road conditions. By building the relationship function among the forces and the resistances experienced by any on-road vehicle, the vehicle dynamic model allows the vehicle power,  $C_d$  (Coefficient of drag),  $C_r$  (Coefficient of Rolling) to be calculated, which is the fundamental concept and tool to determine the fuel consumption factor and emission factor in term of g/kW.h. This appendix describes the equations and the methodology to determine the  $C_d$  and  $C_r$  for any given vehicle. Root Sum Square error formula is used for overall instrument accuracy calculations through combining component errors.*

Coast down testing is typically used to determine a vehicle's drag coefficient and rolling coefficient. The usual procedure of coast down testing involves finding a flat and level road of about 2 km length on which to conduct the tests. In the Edmonton area, coast down testing is easily conducted because the Highway 2 allows sufficient space and time to complete the tests. The detailed experimental method is that a vehicle is accelerated up to a speed of 110 km/h, then the transmission is shifted to neutral and the vehicle is allowed to coast along the road to end up a stop. During the experiment, the vehicle speed vs. time and ambient temperature and pressure are recorded.

The simplified vehicle dynamic model is illustrated in Figure A-0. There are four forces exerting on the vehicle, which are Aerodynamic Resistance ( $F_{aero}$ ), Vehicle Rolling Resistance ( $F_{rolling}$ ), Inertial Resistance ( $F_{inertial}$ ), Vehicle Climbing Force ( $F_{climb}$ ).<sup>[1][2][3][4]</sup> Usually,  $F_{inertial}$  is positive at acceleration and negative at deceleration,  $F_{aero}$  and  $F_{rolling}$  are negative, and  $F_{climb}$  is negative when the vehicle climbs, positive when the vehicle declines.

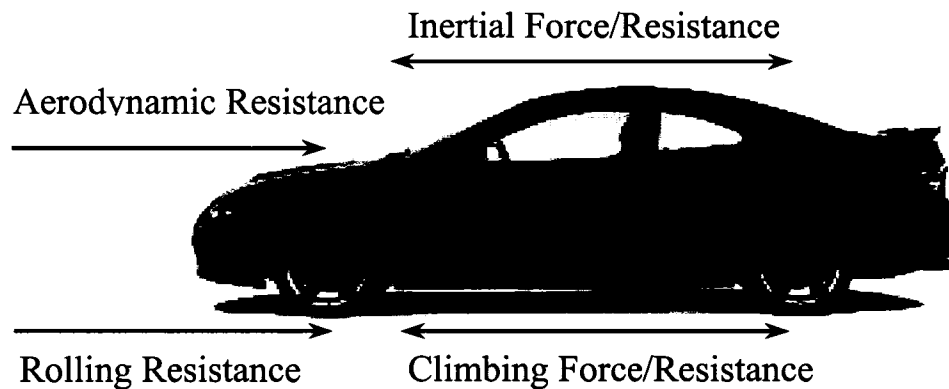


**Figure A-0** Schematic Of Dynamic Vehicle Resistances

The Vehicle Tractive Force:

$$F_{tractive} = F_{inertial} + F_{aero} + F_{rolling} + F_{climb} \quad A1$$

From Newton's 2<sup>nd</sup> law,  $\sum F = ma$ , the Vehicle Inertial Resistance is:

$$F_{inertial}(t) = m \times a(i) \quad \text{A2}$$

$$a(i) : \text{Vehicle Acceleration} \quad [\text{m/s}^2]$$

The error of inertial force is:

$$\varepsilon_{F_{inertial}} = F_{inertial} \times \left[ \left( \frac{\varepsilon_m}{m} \right)^2 + \left( \frac{\varepsilon_a}{a} \right)^2 \right]^{1/2}$$

After getting the data file of vehicle speed vs. time, the vehicle acceleration or deceleration can be calculated by the following equation:

$$a(i) = \frac{V_{i+1} - V_{i-1}}{T_{i+1} - T_{i-1}} \quad \text{A3}$$

$$\begin{aligned} V & : \text{Vehicle Velocity} & [\text{m/s}] \\ T & : \text{Time} & [\text{s}] \end{aligned}$$

Assuming there is no error in the time stamp value and the error in  $V_{i+1}$  is the same as  $V_{i-1}$ , the error of acceleration is:

$$\varepsilon_a = \frac{\sqrt{2} \times a_i \times \varepsilon_v}{V_{i+1} - V_{i-1}}$$

The Aerodynamic Resistance is defined as Equation A4:

$$F_{aero}(t) = \frac{1}{2} \rho_{air} \times C_d \times A \times (V(t) + V_{wind}(t))^2 \quad \text{A4}$$

$$\begin{aligned} \rho_{air} & : \text{Air Density} & [\text{kg/m}^3] \\ C_d & : \text{Coefficient of Drag} \\ A & : \text{Front Area of The Vehicle} & [\text{m}^2] \\ V(t) & : \text{Vehicle Velocity} & [\text{m/s}] \\ V_{wind}(t) & : \text{Wind Velocity} & [\text{m/s}] \end{aligned}$$

Yates and Mkwanzazi <sup>[1]</sup> illustrate that wind velocity plays a factor in the aerodynamic drag on the vehicle. But instantaneous wind speeds were not considered in these calculations. Therefore the error of vehicle aerodynamic resistance is

$$\varepsilon_{Faero} = F_{aero} \times \left[ \left( \frac{\varepsilon_{\rho_{air}}}{\rho_{air}} \right)^2 + \left( \frac{\varepsilon_{Cd}}{C_d} \right)^2 + \left( \frac{\varepsilon_A}{A} \right)^2 + \left( 2 \times \frac{\varepsilon_V}{V} \right)^2 \right]^{1/2}$$

Frontal area of the vehicle can be approximately determined from the published overall width and overall height data for the vehicle. The height of the vehicle is based on the vehicle's maximum road height and the width is the distance from mirror to mirror. Therefore the actual frontal area is smaller than the multiplication between the vehicle height and width. The current accepted method in determining the frontal area is to take 80% of the road height and width product as the following equation:

$$A = 0.8 \times W \times H \quad \text{A5}$$

$W$  : The Width of Vehicle [m]  
 $H$  : The Height of Vehicle [m]

The error of vehicle frontal area is

$$\varepsilon_A = A \times \left[ \left( \frac{\varepsilon_W}{W} \right)^2 + \left( \frac{\varepsilon_H}{H} \right)^2 \right]^{1/2}$$

The Air Density can be calculated by the recorded ambient temperature and ambient pressure:

$$PV = mRT = m \times \frac{R_u}{MW_{air}} \times T$$

Rearrange above equation, we can get the Air Density:

$$\rho_{air} = \frac{P \times MW_{air}}{R_u \times T} \quad \text{A6}$$

The error of Air Density is

$$\varepsilon_{\rho_{air}} = \rho_{air} \times \left[ \left( \frac{\varepsilon_{P_{amb}}}{P_{amb}} \right)^2 + \left( \frac{\varepsilon_{T_{amb}}}{T_{amb}} \right)^2 \right]^{1/2}$$

The Vehicle Rolling Resistance can be expressed as:

$$F_{rolling} = m \times g \times C_r \quad \text{A7}$$

$m$	: Vehicle Mass	[kg]
$C_r$	: Coefficient of Rolling	
$g$	: Gravity Acceleration	9.8 [m/s <sup>2</sup> ]

The error of Vehicle Rolling Resistance is

$$\varepsilon_{F_{rolling}} = F_{rolling} \times \left[ \left( \frac{\varepsilon_m}{m} \right)^2 + \left( \frac{\varepsilon_{C_r}}{C_r} \right)^2 \right]^{1/2}$$

$F_{tractive}$  is the driving force, which is related to the engine torque  $T_e$  as

$$F_{tractive} = \frac{2 \times T_e \times \eta_t}{D_w \times N_t} - \frac{4 \times I_{eg} \times a}{D_w^2} \quad \text{A8}$$

$\eta_t$	: Transmission efficiency
$I_{eg}$	: The equivalent moment of inertia of the rotating parts
$D_w$	: Wheel Diameter
$N_t$	: Overall Transmission Ratio

By rearranging and regrouping the Equation A1, A2, A4, A7 and A8,  $T_e$  can be expressed as:

$$T_e = \frac{D_w N_t}{2 \eta_t} \left\{ \left( m + \frac{4 I_{eg}}{D_w^2} \right) \times a + \frac{1}{2} A C_d \rho_{air} (V + V_{wind})^2 + mg(C_r + \sin \theta) \right\} \quad \text{A9}$$

The inertia of the rotating components of the engine and gearbox are generally considered to be negligibly small in the higher gears (i.e. 3<sup>rd</sup>, 4<sup>th</sup>, 5<sup>th</sup>). Moreover, if the vehicle drag is measured by means of a coast down test, the moment of inertia of the wheels is inescapably included in the drag characterization. Hence the model is not seriously compromised if  $I_{eg}$  is ignored. Since the  $T_e = 0$  under the coast down test, and the effects of wind can be dealt with by conducting the test runs in both directions and averaging the results, the force equation can be simplified to

$$\left( -\frac{a(t)}{g} - \sin \theta \right) = AC_d \left( \frac{\rho_{air} V(t)^2}{2mg} \right) + C_r \quad \text{A10}$$

Equation A10 represents the standard form of a straight-line relationship  $y = ax + b$ , and the values of  $AC_d$  and  $C_r$  can be determined from the slope and intercept using a simple regression analysis.

A dedicated Matlab program was composed to process the raw data saved during the coast down tests. The values of  $C_d$  and  $C_r$  are summarized in the Table A-1 for five tested vehicles. From the calculated results, it can be stated that there is less difference for  $C_r$  among the small passenger cars and the light duty trucks. The dominant factor seems to be the vehicle age since the oldest Chevrolet Cavalier has the highest  $C_r$  and the newest Pontiac Vibe has the lowest  $C_r$ . However,  $C_d$  is proportional to the vehicle size and the frontal area which can be verified that Chevy Silverado Pickup with the open bed stands out from the tested vehicles with the highest  $C_d$  value.

Table A-1 The Coefficients of Drag and Rolling For Five Tested Vehicles

Vehicle	Coefficient	Test1	Test2	Test3	Test4	Test5	Test6	Average	STDEV
Audi	$C_d$	0.507	0.423	0.424	0.557	0.404	0.476	0.465	0.059
	$C_r$	0.013	0.018	0.015	0.013	0.016	0.010	0.014	0.003
Vibe	$C_d$	0.372	0.495	0.283	0.364	0.320	N/P	0.367	0.080
	$C_r$	0.012	0.014	0.015	0.011	0.008	N/P	0.012	0.003
Cavalier	$C_d$	0.494	0.302	0.419	0.523	0.215	0.408	0.394	0.117
	$C_r$	0.012	0.022	0.015	0.014	0.014	0.016	0.016	0.003
Silverado	$C_d$	0.618	0.659	0.736	0.740	0.524	0.522	0.633	0.097
	$C_r$	0.013	0.018	0.016	0.011	0.013	0.013	0.014	0.003
Savana	$C_d$	0.544	0.428	0.430	0.653	0.586	0.590	0.539	0.092
	$C_r$	0.016	0.017	0.017	0.012	0.014	0.013	0.015	0.002

Once the  $C_d$  and  $C_r$  were known, the multiple resistance values could be determined using the equations illustrated previously. If the driving route is sufficient flat, the vehicle tractive power is equal to the multiplication between vehicle tractive force and the vehicle speed expressed as the following equation:

$$P = \frac{V \times (F_{inertial} + F_{aero} + F_{rolling})}{1000} \quad A11$$

$P$	: Power of the Vehicle	[kW]
$V$	: Vehicle Velocity	[m/s]
$F_{inertial}$	: Inertial Resistance / Force	[N]
$F_{aero}$	: Aerodynamic Resistance	[N]
$F_{rolling}$	: Rolling Resistance	[N]

Error in Vehicle Power Calculation:

$$\varepsilon_p = P \times \left[ \left( \frac{\varepsilon_v}{V} \right)^2 + \left( \frac{\varepsilon_{F_{aero}}}{\sum F} \right)^2 + \left( \frac{\varepsilon_{F_{rolling}}}{\sum F} \right)^2 + \left( \frac{\varepsilon_{F_{inertial}}}{\sum F} \right)^2 \right]^{1/2}$$

The overall instrument uncertainties in vehicle tractive power calculated from one congested urban experimental test using Chevrolet Silverado are shown in Figure A-1. The tractive power uncertainty is inherently zero at idle where the vehicle tractive power is zero, and increases rapidly as increasing the tractive power. The uncertainty data points are also increasingly scattered when vehicle tractive power increases from zero to 30 kW because of the bad repeatability. However there is not obvious trend after tractive power is over 30 kW due to lack of the data points of high acceleration and high vehicle speed in a typical urban test.

Figure A-2 shows the relative size of the overall instrument uncertainty against vehicle tractive power. It is noticeable that this error ratio decreases with increasing vehicle tractive power and stabilizes at a low value around 4% under high power conditions (i.e. greater than 30 kW). The average relative error is about 6% under typical low power conditions (i.e. less than 30 kW).

The bin values with vehicle tractive power greater than 18 kW and less than 22 kW are also plotted in Figure A-3. The average vehicle tractive power is 20 kW with 0.92 kW average instrument uncertainty indicated by the star mark in the graph. The individual value uncertainty is as high as 25% because of the low repeatability of actual operation.

Comparing with the low uncertainty from instruments in tractive power calculation, poor driving pattern repeatability dominates the overall uncertainty and causes the data scatter.

## CONCLUSION

By estimating the inertial, aerodynamic and rolling resistance, vehicle dynamic model is used to determine vehicle tractive power for any given test vehicle. The real world  $C_d$  and  $C_r$  for five typical vehicles were examined by a series of experimental coast down tests carried out on the same selected road by the same driver. From the experimental results, it is not difficult to find out that  $C_r$  is correlated with the vehicle age and  $C_d$  is correlated with the vehicle size and frontal area. The overall error of the calculated vehicle tractive power is dominated by the uncertainty from bad repeatability because the cumulative instrument error is relatively small.

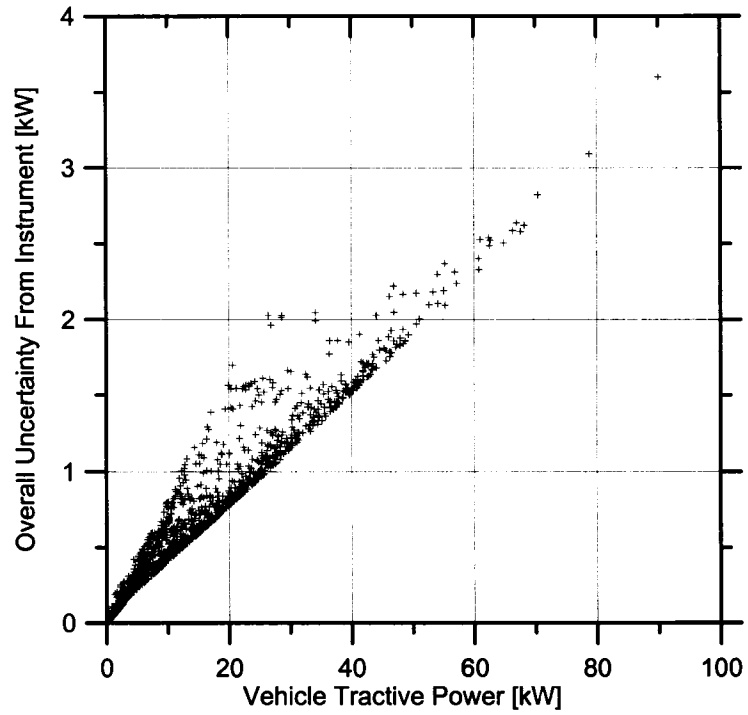


**Figure A-1** Overall Instrument Uncertainty Against Tractive Power

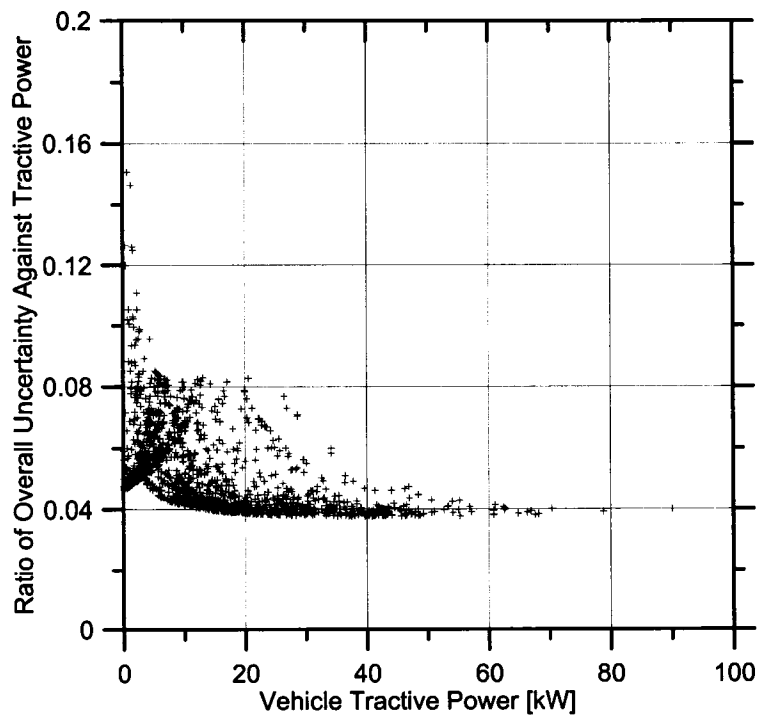


**Figure A-2** Ratio of Uncertainty From Instrument Against Tractive Power ( $\epsilon_p / P$ )

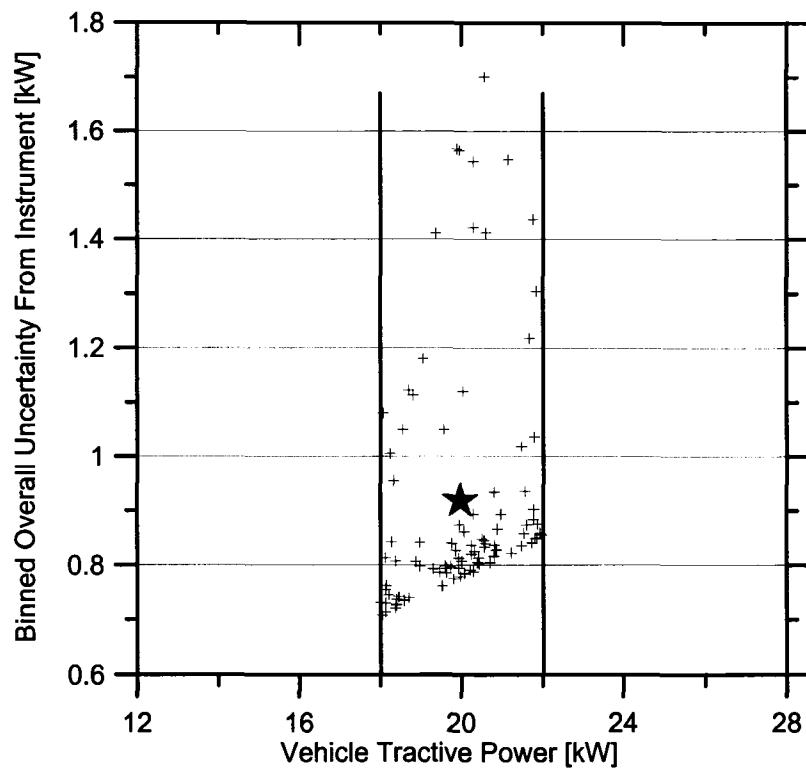


**Figure A-3** Bin Values of Overall Instrument Uncertainty in Tractive Power

## REFERENCE:

1. Yates, A.D.B., Mkwanazi, S. "Methodology for Determining Octane Response at Different Altitudes for Vehicles Equipped with Knock Sensors", SAE Technical paper 2002-01-1663, Society of Automotive Engineers, 2002.
2. J. D. Hawirko. "Modeling Vehicle Emission Factors Determined with an In-Use & Real-Time Emissions Measurement System", Master of Science Thesis, Department of Mechanical Engineering, University of Alberta, 2003.
3. Travis B. Manchur. "Accuracy Of On-Board Vehicle Emission Measurements", Master of Science Thesis, Department of Mechanical Engineering, University of Alberta, 2005.
4. M. D. Checkel, A. Brownlee, L. Doblanko. "Optimizing Vehicle Fuel Consumption and Emissions Through Traffic Optimization Using Vehicle and Traffic Forecasting Models", Combustion Canada 99 Technical Paper H 1.4, 1999.

## **APPENDIX B**

### **Mass Emissions and Fuel Consumption Calculations And Uncertainty Analysis**

*This appendix describes the equations and procedures utilized to determine the instantaneous mass flow rates of fuel and emissions, which can be integrated to give cumulative fuel consumption and emissions for the whole trip. Root Sum Square error formula is used for overall instruments accuracy calculations through combining component errors.*

All calculations were based on the following chemical equation:



Where:

$$B = \text{HC Concentration [ppm]}/1000000 \quad B2$$

$$C = \text{NO}_x \text{ Concentration [ppm]}/1000000 \quad B3$$

$$D = \text{CO Concentration [\%]}/100 \quad B4$$

$$E = \text{CO}_2 \text{ Concentration [\%]}/100 \quad B5$$

$$F = \text{O}_2 \text{ Concentration [\%]}/100 \quad B6$$

$$H = 1 - B - C - D - E - F \quad B7$$

$$A = (C + 2H)/2 \times 3.76 \quad B8$$

$$G = 2A - C - D - 2E - 2F \quad B9$$

$$X = 6B + D + E \quad B10$$

$$Y = 14B + 2G \quad B11$$

The exhaust molar mass:

$$MW_{\text{exh}} = 86.12B + 30.02C + 28.01D + 44.01E + 32.00F + 18.02G + 28.01H \quad B12$$

Error in exhaust molar mass :

$$\varepsilon_{MW_{\text{exh}}} = \left[ \begin{aligned} & (MW_{HC} \times \varepsilon_B)^2 + (MW_{NO} \times \varepsilon_C)^2 + (MW_{CO} \times \varepsilon_D)^2 + (MW_{CO_2} \times \varepsilon_E)^2 \\ & + (MW_{O_2} \times \varepsilon_F)^2 + (MW_{H_2O} \times \varepsilon_G)^2 + (MW_{N_2} \times \varepsilon_H)^2 \end{aligned} \right]^{1/2}$$

The mass based Air to Fuel Ratio can be calculated by the following equation:

$$A/F = 4.76 \times 28.97 \times A / (12.00X + 1.01Y) \quad B13$$

Error in A/F:

$$\varepsilon_{A/F} = \frac{4.76 \times 28.97}{(x \times 12.01) + (y \times 1.01)} \times \varepsilon_A$$

The hydrogen to carbon ration of the fuel is then determined from:

$$H/C = Y/X = (14B+2G)/(6B+D+E) \quad B14$$

Fuel Flow Rate:

$$FF = MAF/(A/F) \quad B15$$

Error in fuel flow rate:

$$\begin{aligned} \varepsilon_{FF} &= \left[ \left( \frac{\partial FF}{\partial MAF} \times \varepsilon_{MAF} \right)^2 + \left( \frac{\partial FF}{\partial A/F} \times \varepsilon_{A/F} \right)^2 \right]^{1/2} \\ &= FF \times \left[ \left( \frac{\varepsilon_{MAF}}{MAF} \right)^2 + \left( \frac{\varepsilon_{A/F}}{A/F} \right)^2 \right]^{1/2} \end{aligned}$$

Emissions in unit of g/s could be calculated from:

$$\text{Emission (g/s)} = Q \times MW_Q \times (MAF + FF) / MW_{exh} \quad B16$$

Where:

$$\begin{aligned} Q &= B, C, D, E \text{ or } F \text{ depending on the associated pollutant} \\ MW_Q &= \text{the molecular weight of the associated pollutant} \end{aligned}$$

Error in instantaneous emission rate:

$$\varepsilon_{Emission} = Emission \times \left[ \left( \frac{\varepsilon_{MW_{exh}}}{MW_{exh}} \right)^2 + \left( \frac{\varepsilon_Q}{Q} \right)^2 + \left( \frac{\varepsilon_{MAF}}{MAF + FF} \right)^2 + \left( \frac{\varepsilon_{FF}}{MAF + FF} \right)^2 \right]^{1/2}$$

The following equation can be used to calculate the emission factor in unit of g/kW.h:

$$\text{Emission Factor (g/kW.h)} = \text{Emission (g/s)} \times 3600 / \text{Power} \quad B17$$

Where:

Emission (g/s) = the associate pollutant mass emission rate  
Power = instantaneous vehicle tractive power

Error in emission factor (g/kW.h):

$$\varepsilon_{EFFPower} = |EFFPower| \times \left[ \left( \frac{\varepsilon_{Emission}}{Emission} \right)^2 + \left( \frac{\varepsilon_{Power}}{Power} \right)^2 \right]^{1/2}$$

The following equation can be used to calculate the emission factor in unit of g/km:

$$\text{Emission Factor (g/km)} = \text{Emission (g/s)} \times 3600 / V \quad \text{B18}$$

Where:

Emission (g/s) = the associate pollutant mass emission rate  
V = instantaneous vehicle speed

Error in emission factor (g/km):

$$\varepsilon_{EFDist} = |EFDist| \times \left[ \left( \frac{\varepsilon_{Emission}}{Emission} \right)^2 + \left( \frac{\varepsilon_V}{V} \right)^2 \right]^{1/2}$$

The following equation can be used to calculate the emission factor in unit of g/kgFuel:

$$\text{Emission Factor (g/kgFuel)} = \text{Emission (g/s)} \times 1000 / FF \quad \text{B19}$$

Where:

Emission (g/s) = the associate pollutant mass emission rate  
FF = instantaneous fuel flow rate

Error in emission factor (g/kgFuel):

$$\varepsilon_{EFFuel} = |EFFuel| \times \left[ \left( \frac{\varepsilon_{Emission}}{Emission} \right)^2 + \left( \frac{\varepsilon_{FF}}{FF} \right)^2 \right]^{1/2}$$

The fuel consumption factor in unit of g/kW.h can be calculated from:

$$\text{Fuel Consumption Factor (g/kW.h)} = \text{FF (g/s)} \times 3600 / \text{Power} \quad \text{B20}$$

Where:

FF = instantaneous fuel flow rate  
Power = instantaneous vehicle tractive power

Error in fuel consumption factor (g/kW.h):

$$\varepsilon_{FPower} = |FPower| \times \left[ \left( \frac{\varepsilon_{FF}}{FF} \right)^2 + \left( \frac{\varepsilon_{Power}}{Power} \right)^2 \right]^{1/2}$$

## **APPENDIX C**

### **Sensor Calibrations**

*To provide accurate fuel consumption and emissions measurement results, a number of sensors need calibrations after a specific time interval required by Equipment Manu. Appendix C details the calibration procedures and results obtained for each sensor.*

## **C.1 Vetronix PXA-1100 5-Gas Analyzer**

A gas calibration is a procedure that ensures the accuracy of the PXA-1100 emissions readings, which is recommended that a gas calibration be performed at least every four weeks. Single Point calibration is the most commonly used procedure because HC, CO, CO<sub>2</sub> and NO<sub>x</sub> are calibrated at the same time by one blend of calibration gas.

### **C.1.1 Choose Calibration Gases**

It is important to use the proper calibration gas when calibrating the PXA-1100. Two things should be considered when selecting a calibration gas: Gas Blend and Gas Concentrations. The Gas Blend indicates the gases contained in the calibration gas and Gas Concentration determines the range of accuracy to which the analyzer is calibrated.

When choosing a calibration gas, the blend of gas should be selected for accurate calibration of a 5-gas analyzer. A Quad-Blend calibration gas is needed to calibrate 5-gas analyzer internal NO<sub>x</sub> transducer along with the infrared bench.

The gas concentration, also referred to as Gas Bottle Values, defines the amount of gas in percent and parts-per-million of each gas contained in the calibration gas blend. Typical gas concentrations are available for specific calibration needs. The calibration gas bottle comes with an external label that lists the concentrations of the calibration gas.

### **C.1.2 Calibration Setup**

This section describes the preparation for calibrating the PXA-1100. Proper preparation and setup will ensure that the analyzer is calibrated accurately.

1. Locate a well ventilated area to perform the calibration because calibration procedure contains Carbon Monoxide, a deadly gas.
2. Supply power to the gas analyzer.
3. Wait for the analyzer to finish its warm-up cycle.

Before starting the calibration procedure, the leak checking is the necessary procedure at the connection among gas pressure regulator, hose assembly and calibration gas bottle. Once the analyzer is ready for calibration, refer to the following sections to perform a Single Point calibration.

### C.1.3 Performing a Single Point Calibration

The PXA-1100 screens will guide the user through the complete Single Point calibration. Once started, simply follow the instructions on the screen. If the user encounters any problems or error messages during the procedure, complete the calibration and then repeat the procedure.

To initiate a Single Point calibration, press 7 to select calibration from the PXA-1100 main menu. Use the following steps to perform a Single Point calibration.

1. Press 1 to select Single Point Calibration from the Calibration menu.
2. Verify the gas bottle values listed on the screen. Press YES if the values match the calibration bottle label. Press NO if the values do not match and enter the correct values. If the user pressed NO to change the concentrations (bottle values), this screen allows the user to enter the correct concentrations. Use the UP ARROW and DOWN ARROW to move the highlight cursor to a field. Use 0-9 to change the numbers. Use the LEFT ARROW to erase the whole field. The RIGHT ARROW erases the last digit entered. Press ENTER button when the correct concentrations are entered. The gas analyzer will automatically purge and zero after the correct bottle values are accepted or entered.
3. Connect the pressure regulator hose to the CAL GAS input port on the front panel of the analyzer. Open the valve on the calibration gas bottle.
4. Adjust the pressure regulator valve on the gas bottle so that the pressure bar gauge on the screen is located in the good range. "Pressure OK" will be displayed when the gas pressure is adjusted properly. If the pressure is either high or low, a pressure control message at the bottom of the screen will be highlighted indicating whether to increase or decrease the pressure to the analyzer. Turn the regulator valve in small 1/8 turn increments and wait 2 seconds for the gauge to read before incrementing again.

5. Let the calibration gas flow for 60 seconds. The analyzer will begin to calibrate the bench and transducers while the gas is flowing.
6. When calibration is complete, close the valve on the calibration gas bottle and disconnect the regulator hose from the CAL GAS port on the analyzer.
7. Press ENTER to return to the Calibration menu.

## C.2 Fast Response Horiba MEXA-720 NO<sub>x</sub> Sensor

The sensor calibration should be carried out every four weeks only in environmental temperatures between 5°C and 45°C and non-condensing relative humidity below 80% with effective ventilation fan on. The gas tank number and pressure are needed to check according to the manufacture's specification.

### C.2.1 Calibration of NO<sub>x</sub> Concentration Output

#### C.2.1.1 Setting the calibration points of NO<sub>x</sub>

1. Connect to the power and wait the equipment to warm up for around three minutes.
2. Press and hold the CAL/SET key for approximately 3 seconds. The mode of the analyzer switches to the setting mode, and a channel number (e.g. ch000) appears on the display.
3. Press the UP or DOWN keys to display "ch000".
4. Press the ENT key to set the channel number.
5. Press the UP or DOWN keys to display the calibration point of NO<sub>x</sub> gas, choose the Four Point Calibration, because the NO<sub>x</sub> emission in the actual vehicle is over 2000 ppm sometimes.
6. Press the ENT key to set the calibration point.
7. Press the M key and return to the measurement mode.

#### C.2.1.2 Setting the concentration of NO<sub>x</sub>

1. Press and hold the CAL/SET key for approximately 3 seconds. The mode of the analyzer switches to the setting mode, and a channel number (e.g. ch000) appears on the display.
2. Press the UP or DOWN keys to display the ch001: Zero Gas.
3. Press the ENT key to set the channel.
4. Press the UP, DOWN or RIGHT keys to display the concentration of calibration gas according to the Excel Spreadsheet.
5. Press the ENT key to set the concentration of calibration gas.
6. Repeat the steps 2 through 5 to setup  
ch002: Middle Gas  
ch003: Span Gas  
ch004: High Concentration NO gas
7. Press the M key and return to the measurement mode.

#### C.2.1.3 Operation of DASIBI flow control meter

1. Turn on the power of DASIBI. It is a flow meter, which can control the different compressed gas flow rate according to the demand. From the combination of different gas at different flow rate, the desired NO<sub>x</sub> concentration can be produced.
2. Open the valves of the four tanks with the compressed gas.
3. Press BACKUP key on the control panel, choose CONTROL, press ENTER, choose MANUAL CONTROL, press ENTER, choose FLOW, press ENTER.
4. Look at the Excel Spreadsheet, choose Gas Tank number on the DASIBI, input the flow rate of that kind of gas.
5. Repeat step 3 and 4 to get different gas concentration.

#### C.2.1.4 Calibration of NO<sub>x</sub> concentration output

1. Fill the bubbler of the calibration unit with water.
2. Connect gas lines to the gas inlet and the exhaust outlet of the calibration unit.
3. Press the M key until the ppm NO<sub>x</sub> LED is lit.

4. Refer to the last section, let DASIBI supply the zero gas to the calibration unit. Hint: the zero gas is pure N<sub>2</sub> at 2 LPM flow rate and NO<sub>x</sub> flow rate is zero.
5. After the indicated value is stabilized, press CAL/SET key. ZERO LED will be lit and the previous setup concentration of the zero gas will be displayed.
6. Confirm that the displayed concentration is proper, and then press the ENT key to perform calibration of the zero point.
7. Repeat the steps 4 through 6 for span gas (press CAL/SET 2 times), the middle gas (press CAL/SET 3 times) and the high concentration NO gas (press CAL/SET 4 times) in this order.

### C.2.2 Calibration of O<sub>2</sub>, A/F and λ output

#### C.2.2.1 Condition Setting

1. Press and hold the CAL/SET key for approximately 3 seconds. The mode of the analyzer switches to the setting mode, and channel number (e.g. ch000) appears on the display.
2. Press the UP or DOWN keys to display the channel number “ch010”.
3. Press the ENT key to set the channel number.
4. Press the UP or DOWN keys to display the Three Point Calibration of A/F and λ. Three Point indicates Zero (stoichiometric) Point, Lean Point and Rich Point.
5. Press the ENT key to set the calibration point.
6. Press the M key to return to the measurement mode.

#### C.2.2.2 Calibration of O<sub>2</sub>, A/F and λ output

1. Press M key until the % O<sub>2</sub> LED is lit.
2. Operate the DASIBI and lead N<sub>2</sub> gas into the calibration unit.

3. After the indicated value is stabilized, press the CAL/SET key once. ZERO LED will be lit and the standard value for calibration (concentration of calibration gas) will be displayed.
4. Check the Excel Spreadsheet. If indicated value is not proper, modify the value with the UP, DOWN and RIGHT key, then press the ENT key. If indicated value is proper, skip to the next step.
5. Press ENT key to calibrate the ZERO point.
6. Repeat the steps 2 through 5 for O<sub>2</sub> span gas (lean point). In this case, however, press the CAL/SET key twice to turn on the SPAN LED.
7. Shut down the Horiba MEXA-720 NO<sub>x</sub> and DASIBI, disconnect the gas inlet line from DASIBI, connect with the rich compressed O<sub>2</sub> tank situated in a portable cart, open the valve of the tank. Turn on MEXA-720 NO<sub>x</sub> again.
8. For 3-point calibration, press M key to turn on the  $\lambda$  LED, and then repeat the steps 2 through 5. For rich point calibration, press the CAL/SET key three times to turn on the RICH LED.
9. Shut down MEXA-720 NO<sub>x</sub>, close the valve of the rich O<sub>2</sub> tank. Disconnect the calibration unit with inlet and exhaust lines. Double check the valves of all gas tanks for safety consideration.

### C.3 Mass Air Flow Sensor

The mass air flow meter used in these experiments was a couple of Siemens HFM 62B automotive mass air flow sensor. The calibration setup of HFM 62B is schematically shown in Figure C-1. This experiment is setup to measure the air pressure differential across the nozzle as well as the output voltage of the sensor. The vacuum or the air pressure differential  $\Delta P$  can be read from the Manometer, then we can derive the Mass Air Flow Rate  $\dot{m}_a$  from air pressure differential  $\Delta P$ . The detail mathematical theory is as follow:

The flow velocity through a nozzle when the initial velocity is very small is calculated from Bernoulli as

$$V = \sqrt{\frac{2\Delta P}{\rho}} \quad [\text{m/s}] \quad \text{C1}$$

Where:

$\Delta P$       pressure differential across nozzle [Pa]  
 $\rho$          density of the flowing fluid    [kg/m<sup>3</sup>]

Mass Flow Rate through the nozzle is:

$$\dot{m}_a = C_d A V \rho_a = C_d A \sqrt{2\rho_a \Delta P} \quad [\text{kg/s}] \quad \text{C2}$$

Where:

$C_d$       coefficient of discharge (~1 for conditions used)  
 $A$          flow area of the nozzle (minimum opening area) [m<sup>2</sup>]  
 $\rho_a$       density of air calculated from local temperature and pressure  
 (ideal gas law) [kg/m<sup>3</sup>]

Volumetric Flow Rate through the nozzle is:

$$\dot{Q} = \frac{\dot{m}_a}{\rho} \quad [\text{m}^3/\text{s}] \quad \text{C3}$$

Where:

$\dot{m}_a$       mass flow rate of air [kg/s]

In order to get the accurate air density, the ambient temperature and pressure should be recorded during the experiments. The flow area of nozzle A can be calculated by measuring the nozzle diameter.

The data acquisition system is used to connect the MAF meter to the laptop computer. The output voltage of the MAF meter can be read from Laptop computer through the Labview program. Two calibration curves are illustrated in Figure C-2 and Figure C-3 respectively.

#### C.4 Ambient Temperature Sensor Calibration

An AD590 temperature sensor is chosen to measure the ambient temperature during the on-board & real-time emissions measurement because of its accuracy, linearity of output, and wide measurable range of temperature. The temperature sensor calibration is normally conducted shortly after the MAF calibration due to the data acquisition system and laptop computer are also used to read the output voltage of the temperature sensor. The sensor is immersed in three different conditions: an ice barrel, ambient air, and the boiling water. The exact temperatures of these three conditions are measured by one thermometer. The result of the ambient temperature calibration is shown in Figure C-4.

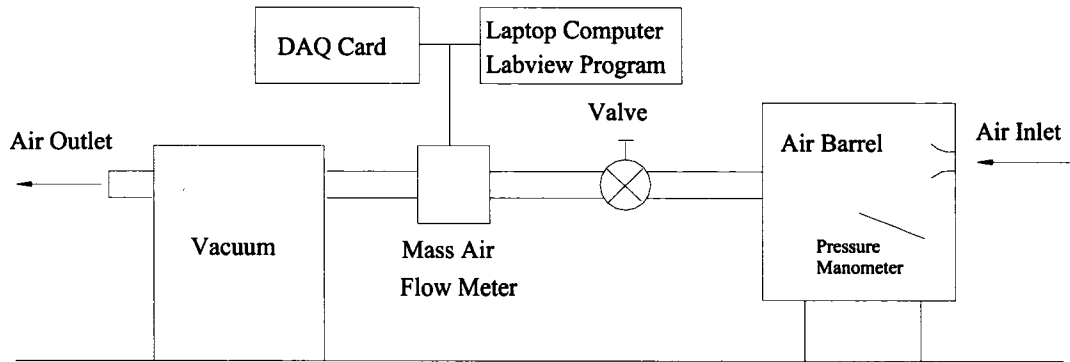


**Figure C-1** Mass Air Flow Meter Calibration Experimental Setup

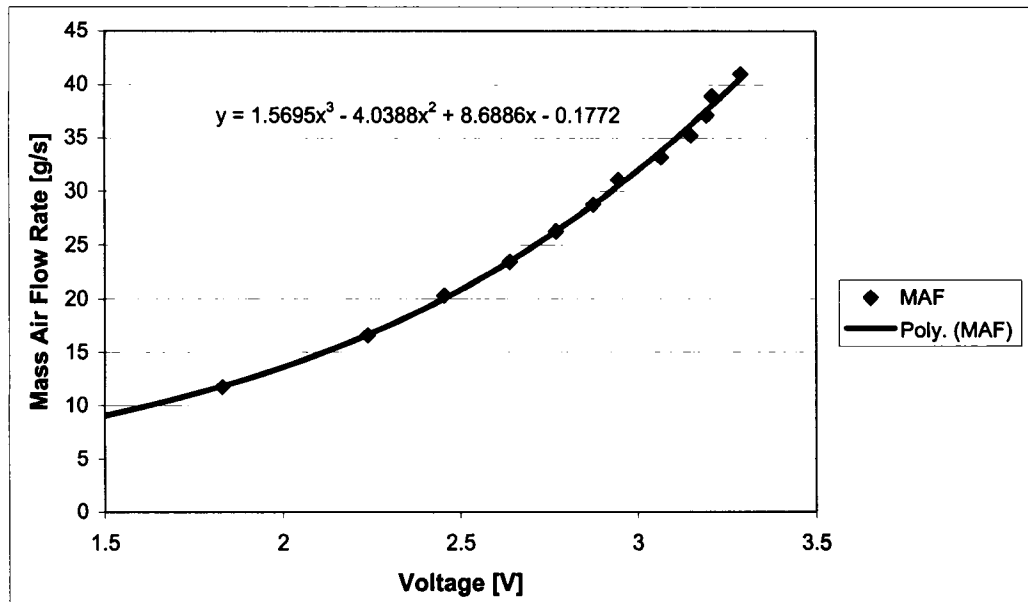


**Figure C-2** Mass Air Flow Meter 1 Calibration Curve

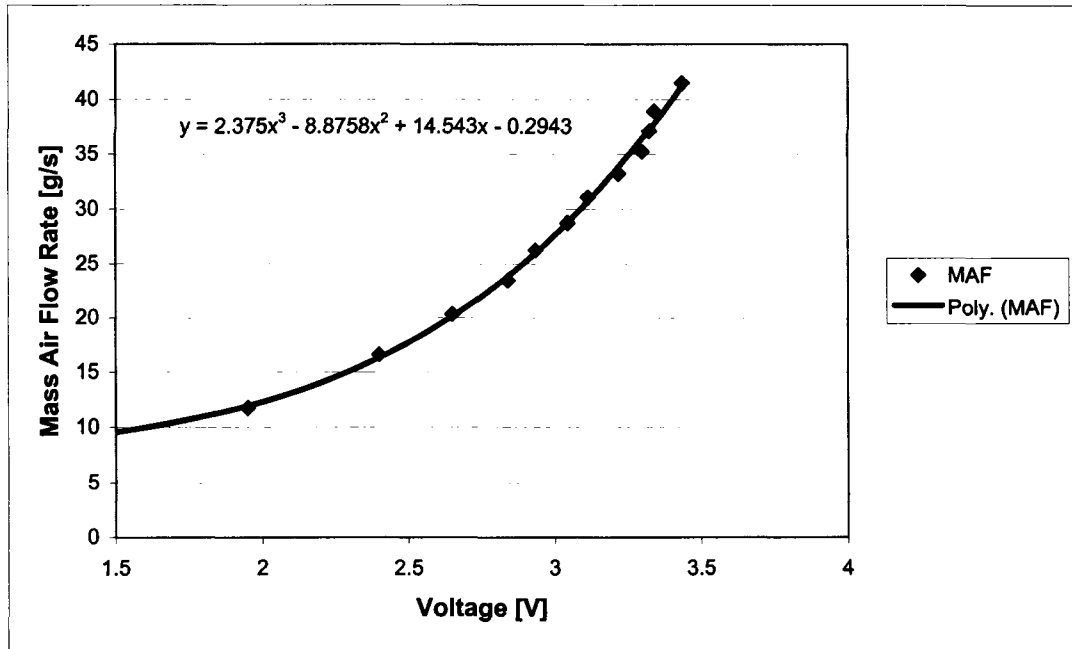


**Figure C-3** Mass Air Flow Meter 2 Calibration Curve

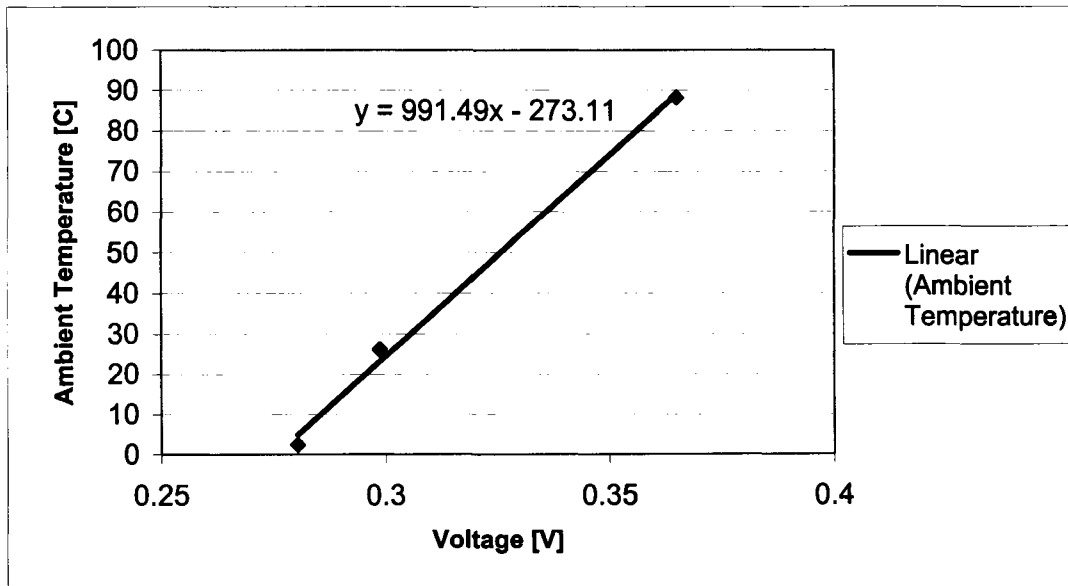


**Figure C-4** Ambient Temperature Sensor Calibration Curve

## **APPENDIX D**

### **Matlab Processing Program**

*The third generation of Matlab Processing Program was composed to read all raw experimental data, calculate the instantaneous mass flow rates of fuel and emissions as well as vehicle tractive power and other desired parameters, create a wide variety of graphs helping user to quantify the data gathered from on-road tests, then output the selected parameters matrix to spread sheet for the later analysis and reference. Special acknowledgement should be mentioned that the previous two generation of data processing program composed by Hawirko and Manchur provided the fundamental outline for this efficient program to be extended to new areas of investigation for all tested vehicles. Appendix D outlines the hierarchy of the program routines and sub-routines and gives short descriptions to clarify their functions in the whole processing procedures.*

## D.1 Program Hierarchical Format

**Emission3.m** --The MAIN Emissions Processing / Analysis Software

**BasicSetup.m**

**VehicleSetup.m**

**GrossData.m**

**NetData.m**

**FilterData.m**

**FirstCombine.m**

**SecondCombine.m**

**TimeAlignment.m**

**Calculation.m**

Statistics.m

**DataError.m**

**CompareData.m**

**Graph.m**

Truncate.m

*DataError.m*

Statistic.m

Export.m

**AveFactors.m**

**SaveData.m**

**CoastDown.m** --Calculates the Cd and Cr constants for a Vehicle based on  
a Coast Down Test

**CoastDownFilter.m**

**BasicSetup.m**

**VehicleSetup.m**

## **D.2 PROGRAM DESCRIPTION**

### **Emission3.m**

LEVEL 1,            Written by: Yutong Gao - May 20, 2005 to Current

Purpose:    To supply every calculation and procedure required to analyze on-road emissions and fuel consumption as the main program

Used in:    (nothing, top level m file)

Uses:      BasicSetup.m, VehicleSetup.m, GrossData.m, NetData.m, FilterData.m, FirstCombine.m, SecondCombine.m, TimeAlignment.m, Calculation.m, DataError.m, CompareData.m, Graph.m, AveFactors.m, SaveData.m

### **BasicSetup.m**

LEVEL 2,            Written by: Yutong Gao - May 20, 2005 to Current

Purpose:    To setup the column numbers for all parameters based on where they are stored in the original data matrix and to set the emission data time delay constants

Used in:    Emissions3.m, CoastDown.m

Uses:      (nothing)

### **VehicleSetup.m**

LEVEL 2,            Written by: Yutong Gao - May 22, 2005 to Current

Purpose:    To setup the specifications of all vehicles required to calculate tractive power, etc.

Used in:    Emissions3.m, CoastDown.m

Uses:      (nothing)

## **GrossData.m**

LEVEL 2,            Written by: Yutong Gao - May 24, 2005 to Current

Purpose:    To store all the data from the raw .csv data files and converts them to matrices oMgasHoriba,oMgasVetronix and oMecm

Used in:    Emissions3.m

Uses:        (nothing)

## **NetData.m**

LEVEL 2,            Written by: Yutong Gao - May 25, 2005 to Current

Purpose:    To eliminate initial non-running time for three original data matrices

Used in:    Emissions3.m

Uses:        (nothing)

## **FilterData.m**

LEVEL 2,            Written by: Yutong Gao - May 25, 2005 to Current

Purpose:    To filter out erroneous data readings ("spikes" and "dips") and smooth out the data values collected.

Used in:    Emissions3.m

Uses:        (nothing)

## **FirstCombine.m**

LEVEL 2,            Written by: Yutong Gao - May 30, 2005 to Current

Purpose:    To combine filtered ECM data matrices and Vetronix Analyzer matrices into one matrix using Analyzer Time as the Base Time

Used in:    Emissions3.m

Uses: (nothing)

### **SecondCombine.m**

LEVEL 2, Written by: Yutong Gao - June 20, 2005 to Current

Purpose: To combine filtered Horiba matrices with first combined matrices into one matrix using Vetronix Analyzer Time as the Base Time

Used in: Emissions3.m

Uses: (nothing)

### **TimeAlignment.m**

LEVEL 2, Written by: Yutong Gao - June 20, 2005 to Current

Purpose: To shift the emissions data gathered by the gas analyzer to line up with the vehicle data due to transport time from the engine through the exhaust pipe and the sample hose to the analyzer

Used in: Emissions3.m

Uses: (nothing)

### **Calculation.m**

LEVEL 2, Written by: Yutong Gao - June 21, 2005 to Current

Purpose: To calculate instantaneous mass fuel consumption rate, emissions rates, vehicle power, driving distance, acceleration, emission factors and other interested values from the gathered data

Used in: Emissions3.m

Uses: Statistics.m

## **Statistics.m**

LEVEL 3,                      Written by: Yutong Gao - June 22, 2005 to Current

Purpose:    To produce various statistics tables showing the values of interested parameters within the specific duration of speed and power, etc

Used in:    Calculation.m

Uses:        (nothing)

## **DataError.m**

LEVEL 2 and 4,              Written by: Yutong Gao - June 25, 2005 to Current

Purpose:    To list equipment measurement accuracy/error, then calculate the quantitative error at each time stamp

Used in:    Emissions3.m

Uses:        (nothing)

## **CompareData.m**

LEVEL 2,                      Written by: Yutong Gao - June 24, 2005 to Current

Purpose:    To compare the difference in readings for MAF, NOx, AFR, etc

Used in:    Emissions3.m

Uses:        (nothing)

## **Graph.m**

LEVEL 2,                      Written by: Yutong Gao - June 26, 2005 to Current

Purpose:    To produce Graphs/Charts/Trends/Summary Tables/Export Options among any parameters chosen by user

Used in:    Emissions3.m

Uses: Truncate.m, Statistics.m, Export.m

### **Truncate.m**

LEVEL 3, Written by: Yutong Gao - June 1, 2005 to Current

Purpose: To allow user to select an analysis range of interest (Truncate Data) and subsequently view the graphical results in Graph.m

Used in: Graph.m

Uses: DataError.m

### **Export.m**

LEVEL 3, Written by: Yutong Gao - June 26, 2005 to Current

Purpose: To allow the user to export the data summary to a text file

Used in: Graph.m

Uses: (nothing)

### **AveFactors.m**

LEVEL 2, Written by: Yutong Gao - Jan10, 2005 to Current

Purpose: To average the instantaneous emissions and fuel consumption factors (g/km, g/kgfuel, g/kW.h) along with vehicle speed or tractive power

Used in: Emissions3.m

Uses: (nothing)

### **SaveData.m**

LEVEL 2, Written by: Yutong Gao - Sept20, 2005 to Current

Purpose: To save the calculated matrices selected by user into excel programs for

later use in graphing/plotting

Used in: Emissions3.m

Uses: (nothing)

### **CoastDown.m**

LEVEL 1,            Written by: Yutong Gao - June28, 2005 to Current

Purpose: To calculate the vehicle specific drag and rolling coefficients as well as the vehicle tractive power through calculations from Coast Down Test data illustrated in Appendix A

Used in: (nothing)

Uses: CoastDownFilter.m, VehicleSetup.m, BasicSetup.m

### **CoastDownFilter.m**

LEVEL 2,            Written by: Yutong Gao - June29, 2005 to Current

Purpose: To filter out erroneous data readings and smooth out the data values collected.

Used in: CoastDown.m

Uses: (nothing)